Durham E-Theses

A torque magnetometer using strain gauges as transducers

Warnock, R.F.

How to cite:

Warnock, R.F. (1975) *A torque magnetometer using strain gauges as transducers*, Durham theses, Durham University. Available at Durham E-Theses Online: http://etheses.dur.ac.uk/8949/

A Torque Magnetometer Using Strain Gauges As Transducers

By

R.F. Warnock,   B.Sc.

Presented in candidature for the degree

of

Master of Science

June 1975

ABSTRACT.

A short critical history of magnetometers suitable for the measurement of magnetocrystalline anisotropy constants, is presented as an introduction for the necessity of having a new type of magnetometer capable of measuring the large anisotropies associated with the heavy rare earth elements, and particularly for work on the gadolinium - terbium binary alloy system.

An instrument has been developed which is compact and rugged with good stability and sensitivity, and is able to make measurements of anisotropy constants (using crystals of a convenient size) having values in the range 10^5 to 10^9 erg cm^{-3} .

A modification is indicated which will extend this range to 10^3 to 10^9 erg cm $^{-3}$.

ACKNOWLEDGEMENTS.

CONTENTS.

CHAPTER I.

Magnetocrystalline Anisotropy and the Anisotropy Constants.

1. Historical Introduction.

Before single magnetic crystals were available, experiments on magnetization produced magnetization curves similar to fig.1.1.The precise shape of the curves depended on the material, but the same materials showed very small differences between similarly prepared specimens: the magnetizations generally rose rapidly in low fields and soon reached a plateau of slight inclination.
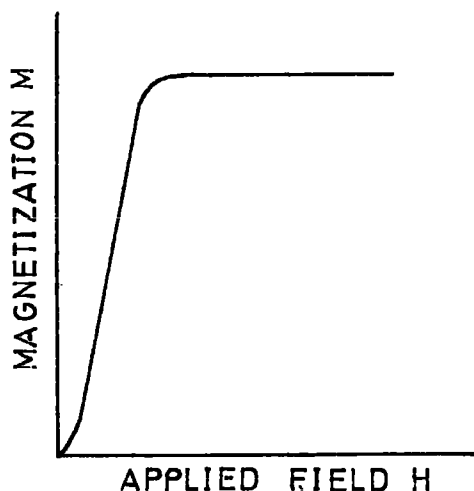
Fig. 1.1 Magnetization curve for polycrystalline material.

The theories which apparently described this effect involved separate, non-interacting atomic dipoles which were generally randomly aligned, but could rotate at various angles to the increasing field until saturation - complete alignment of all dipoles - occurred.

In 1904 and 1905 Weiss (ref.6,9,10,11) published his account of magnetization experiments which he performed on large single natural crystals of magnetite and pyrrhotite. He found that pyrrhotite could be easily saturated in the plane of the hexagonal base of the crystal structure (it is rhombohedral) but saturation was difficult to achieve perpendicular to this plane. Uncertainties about the constancy of composition delayed interpretation but in 1907, Weiss announced his ideas. (ref.4).

He suggested that the atomic dipoles could influence one another sufficiently to align themselves parallel to their neighbours in a small

region. These "domains" would be magnetically saturated in various directions, and the vector sum of the domain moments would give the total moment of the specimen.

Preparation of artificial single magnetic crystals and the advent of X ray techniques, which made possible their accurate alignment with respect to a magnetic field, confirmed Weiss's results. Beck (ref.7), Honda & Kaya (ref.3) and Sucksmith, Potter & Broadway (ref.8), showed that the magnetization curve would rise more slowly when certain crystallographic directions were aligned parallel to the magnetic field. These were called hard directions, and the directions in which magnetization rose quickly in low fields were easy magnetic directions. The crystals magnetized in easy directions contained less magnetic energy when saturated than did those which were magnetized in the hard directions.

These ideas were assimilated with Weiss's theory, and it was recognised (Webster ref.13, and Heisenberg ref.14) that unmagnetized materials would have many domains of saturation, each with its magnetization in an easy direction.

If the entire crystal were saturated in an easy direction, and then rotated until it was saturated in a hard direction, an amount of work would be required which would equal the energy difference between magnetizing the crystal in the two directions, i.e. to the difference in free energy between the two states. This is equivalent to the area between the magnetization curves of the two directions and is called the anisotropy energy for that particular hard direction.

In any crystallographic plane the anisotropy energy is either roughly constant or varies in an oscillatory manner, with angular distance θ from any easy direction. The evaluation of anisotropy energy in terms of polar co-ordinates referred to the principal axes of cubic crystals was first achieved by Akulov (ref.5), who found that the torque T_θ per unit volume when the magnetization of the crystal was at angle θ to the [100] direction was described by

$$T_\theta = T_{100} + \tfrac{1}{4} K \left(1\tfrac{3}{4} - \cos 2\theta - \tfrac{3}{4} \cos 4\theta\right)$$

when measured in the (100) plane. T_{100} is the torque when the magnetization

lies along the [100] direction, and the numerical factor K is the anisotropy constant. The torque arises when the magnetization is not in an easy direction, and is due to the extra magnetic energy which the crystal then has. Accurate experiments now require several anisotropy constants for most crystals.

(2) Anisotropy Constants.

It is assumed possible to describe the anisotropy energy in terms of constants multiplied by trigonometric functions of the angle between the magnetization vector and arbitrary standard directions. The standard directions are chosen for convenience with respect to the particular principal crystallographic directions and the easy directions of magnetization. If the magnetization is in a direction with direction cosines $\alpha_1, \alpha_2, \alpha_3$, with respect to the axes of the crystal we write the anisotropy energy as follows:

$$f_K = K_0 + K_1 (\alpha_1^2 \alpha_2^2 + \alpha_2^2 \alpha_3^2 + \alpha_3^2 \alpha_1^2) + K_2 (\alpha_1^2 \alpha_2^2 \alpha_3^2) + \cdots \qquad \text{Equation 1.1}$$

The magnitudes and signs of the anisotropy constants K_0, K_1, K_2 etc, describe the positions of the hard and easy directions, and are written in terms of energy per unit volume. Their values depend on the temperature.

(a) Uniaxial Crystals.

The term uniaxial implies that there is only one easy axis of magnetization, and that magnetization perpendicular to this axis is uniformly difficult. Cobalt at room temperature is a typical example. It has a hexagonal structure with easy direction along the hexagonal axis. If the direction cosines are referred to two axes at 120° in the basal plane and to the c axis, equation 1.1 can be transformed into

$$f_K = K_0 + K_1 \sin^2 \Theta + K_2 \sin^4 \Theta \qquad \text{Equation 1.2}$$

where Θ is the angle between the c axis and the direction of magnetization. The values of these constants are not those of equation 1.1 . For cobalt they are positive and about 10^6 erg cm^{-3} (ref.49). The zero value of anisotropy energy is often fixed by putting $K_0 = 0$.

(b) <u>Cubic Crystals.</u>

Cubic crystals may have more than one easy direction; e.g. in iron the $\langle 100 \rangle$ directions are easy, and the body diagonals hard. K_1 and K_2 are both positive and are a little over 10^5 erg cm^{-3} at room temperature (ref.38). In nickel K_1 is less than zero and the $\langle 111 \rangle$ directions are easy. K_2 is positive and K_1 and K_2 are an order of magnitude smaller than for iron, (ref.39).

(c) <u>Hexagonal Crystals - The Rare Earths.</u>

The heavy rare earths have complicated magnetic dipole arrangements in various hexagonal crystal structures, and the difficulty of magnetization varies in the basal plane. Their anisotropy constants are large, and two extra terms are required to describe anisotropy compared to cobalt:

$$f_K = K_0 + K_1 \sin^2\theta + K_2 \sin^4\theta + K_3 \sin^6\theta + K_4 \sin^6\theta \cos 6\phi . \quad \text{Equation 1.3}$$

The K_4 term describes the basal plane anisotropy which shows six-fold symmetry in its dependence on the azimuthal angle ϕ .

For gadolinium $K_1 \doteqdot K_2 \doteqdot K_3 \doteqdot 10^6$ erg cm^{-3} and

$$K_4 \doteqdot 10^3 \text{ erg cm}^{-3}.$$

At room temperature and a little below, the c axis is the easy direction, but K_1 decreases rapidly with decreasing temperature and becomes negative at about 240K so that the easy direction moves toward the basal plane without, however, entering the basal plane, (ref.40,41,42,43,44).

Terbium and dysprosium (ref.45,46) have c axis components of order 10^8 erg cm^{-3} at 0 K (their Curie points are below room temperature). For them $K_4 \doteqdot 10^6$ erg cm^{-3}

and is negative for dysprosium. Holmium, erbium and thulium (ref.47,48) have similar very large K values.

(d) <u>Tetragonal Crystals.</u>

A suitable expression for the anisotropy energy of a tetragonal crystal is $$f_K = K_0 + K_1 \sin^2\theta + K_2 \sin^4\theta + K_3 \cos^2\alpha \cos^2\beta$$

which was used by Guillaud (ref.12) on $Mn_2 Sb$. θ is the angle between

the magnetization and the tetragonal axis [001] and α, β are the angles with respect to the other axes. For Mn_2 Sb, $K_1 = 10^5$ erg cm^{-3} at room temperature, and the [001] axis is the easy direction. There is some asymmetry in the (001) plane.

(3) **The Techniques of Determining Anisotropy Constants.**

(a) **Magnetization Measurements.**

By determining the increasing magnetization of a crystal orientated in a particular direction in a magnetic field, the magnetization curve for that direction can be drawn. This can produce the anisotropy constants in two ways.

(i) The work to magnetize the specimen to saturation M in a direction [hkl] is

$$W_{hkl} = \int_0^M H dM_H$$

where M_H is the magnetization component in the direction [hkl] and at the value H of applied field. The anisotropy energy difference $f_{hkl} - f_{mnp}$ between the directions [hkl] and [mnp] is the area between the magnetization curves for those directions, so

$$W_{hkl} - W_{mnp} = f_{hkl} - f_{mnp} .$$

For example consider a cubic crystal with magnetization measured in the [100] , [110] and [111] directions. The corresponding direction cosines are $(1,0,0)$, $\left(\frac{1}{\sqrt{2}}, \frac{1}{\sqrt{2}}, 0\right)$, $\left(\frac{1}{\sqrt{3}}, \frac{1}{\sqrt{3}}, \frac{1}{\sqrt{3}}\right)$ so equation 1.1 reduces to

$$f_{100} = K_0$$
$$f_{110} = K_0 + \tfrac{1}{4} K_1$$
$$f_{111} = K_0 + \tfrac{1}{3} K_1 + \tfrac{1}{27} K_2$$

so
$$K_1 = 4 (f_{110} - f_{100}) \equiv 4 (W_{110} - W_{100})$$

and
$$K_2 = 27(W_{111} - W_{100}) - 36(W_{110} - W_{100})$$

determine K_1 and K_2.

If several types of anisotropy influence the magnetization curve, it is difficult to judge the separate effect of each on the magnetization curve. Further, the irreversible magnetization process introduces hysteresis into

the magnetization curve, and in some materials the hysteres$_\wedge^{is}$can be as large as the magnetic anisotropy, so that this method could not be used in such cases.

(ii) A theoretical magnetization curve can be predicted and made to agree with the experimental curve by substituting appropriate values of the anisotropy constants. Suppose we apply a field H to the [110] direction of an iron specimen (see fig.l.3 & l.4), which we presume to have no shape anisotropy. Any domain vectors parallel to [001] or to [00$\bar{1}$] directions, (i.e. at 90° to H) would produce a magnetostatic energy of $(M_sH - \tfrac{1}{\hbar}M_sH)$ per unit volume in excess of the energy of domains in the [100] and [010] directions (which are at 45° to H). M_s is the saturation magnetization per unit volume and it is the same magnitude for all domains. Domains in the [$\bar{1}$00] and [0$\bar{1}$0] directions would have excess magneto-static energy of $(M_sH + \tfrac{1}{\hbar}M_sH)$ per unit volume. Hence as H increases these two sets of domains decrease in volume in favour of the [100] and [010] aligned domains and in such a way as to balance out the total magnetostatic energy HM_H of the resultant magnetization M_H of the specimen. At even very low fields the domains will all have turned to either of the [100] or [010] directions. As H increases further the magnetization of these domains begins to rotate toward the [110] direction.

Consider (fig.1.4) a domain at an angle $(\psi - \theta)$ to H. Its magneto-static and anisotropic energies balance for equilibrium and the direction cosines of M_s are $\alpha_1 = \cos\theta$, $\alpha_2 = \sin\theta$ and $\alpha_3 = 0$ with respect to the [100] direction.

From equation 1.1

$$f_K = K_0 + K_1 \cos^2\theta \sin^2\theta$$

or

$$f_K = K_0 + K_1\left[\cos^2\left(\tfrac{\pi}{4} - \theta\right) - \tfrac{1}{2}\right]^2$$

since the angle ψ between H and the easy direction [100] is $\tfrac{\pi}{4}$ in this case. The magnetostatic energy contribution is

$$f_H = -M_sH\cos\left(\tfrac{\pi}{4} - \theta\right)$$

and f_K and f_H combine to give the minimum energy, so

$$\frac{\partial}{\partial\theta}(f_H + f_K) = 0 \ .$$
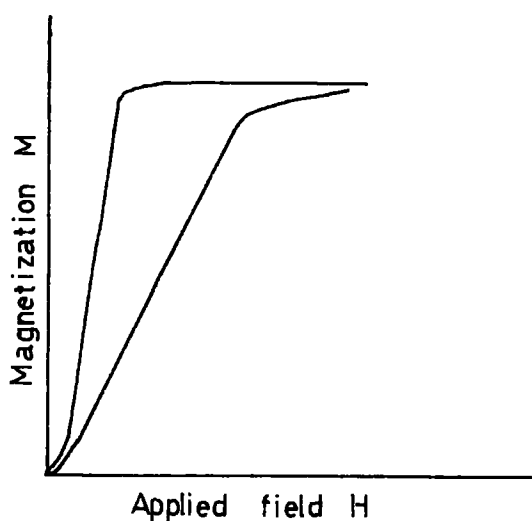
Fig.1.2

Two magnetization curves for a single crystal aligned in two non-equivalent directions.

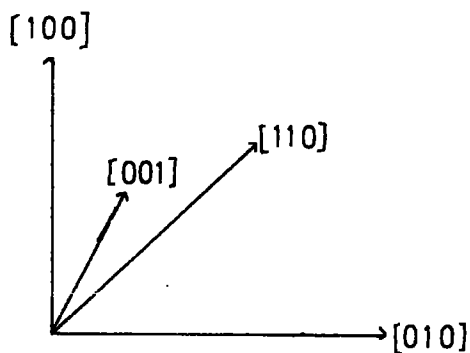Fig.1.3. The directions [100], [010] and [110] lie in the (001) plane. [100] and [010] are at right angles and [110] bisects them.
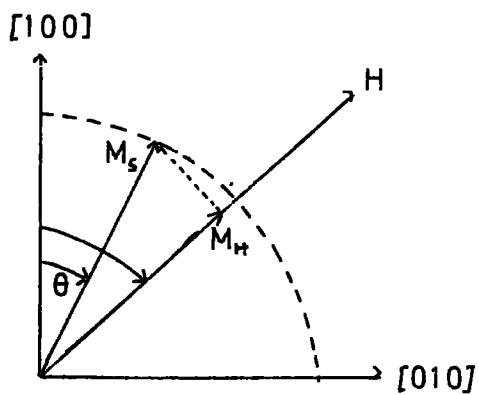

Fig.1.4 The field H is applied along the [110] direction and draws the magnetization vector M_s of some domain out of the easy direction [100] so that M moves from 45° from H to θ from H.

From this $\qquad M_s H = 4 K_1 \left[\cos^2 \left(\frac{\pi}{4} - \theta \right) - \frac{1}{2} \right] \cos \left(\frac{\pi}{4} - \theta \right)$

or $\qquad \dfrac{M_s H}{4K_1} = \left(\dfrac{M_H}{M_s} \right)^3 - \dfrac{M_H}{2M_s}$ $\qquad$ Equation 1.4

which describes the magnetization curve of the component of M_s along

H $(M_H = M_s \cos \left(\frac{\pi}{4} - \theta \right))$, for experimentally we measure M_H. M_s is

determined from the asymptotic values of M_H , and values of M_H , H , and

of M_s are readily substitued in equation 1.4 to find K_1 . If saturation

cannot be achieved, two values of M_H corresponding to different values of

H will give two simultaneous equations in M_s and K_1 .

Equation 1.4 fits the magnetization curves of many materials very

well, but it is not the most convenient, nor the most accurate way of

finding K_1 .

(b) Torque Measurements.

If $f = f_H + f_K$ is the total free magnetic energy of a crystal

saturated in a magnetic field, then the torque on the magnetization

is $L = -\dfrac{\partial f}{\partial(\psi - \theta)}$ by definition (not $L = -\dfrac{\partial f}{\partial \psi}$ as used in ref.50) where

θ and ψ are the angles that M_s and H respectively make with the easy

axis, (fig.1.4) . Again $\dfrac{\partial f}{\partial \theta} = 0$ since the magnetization vector always

rotates so that f is a minimum, and $\dfrac{\partial f_H}{\partial \theta} + \dfrac{\partial f_K}{\partial \theta} = 0$. Now f_K is a

function of θ only, and θ and ψ are not explicitly related so that

$\dfrac{\partial f_K}{\partial \psi} = 0$. Therefore

$$L = -\dfrac{\partial f}{\partial(\psi-\theta)} = - \left[\dfrac{\partial f}{\partial \psi} \dfrac{\partial \psi}{\partial(\psi-\theta)} + \dfrac{\partial f}{\partial \theta} \dfrac{\partial \theta}{\partial(\psi-\theta)} \right]$$

$$= - \dfrac{\partial f}{\partial \psi} \dfrac{\partial \psi}{\partial(\psi-\theta)}$$

$$= - \dfrac{\partial f_H}{\partial \psi} - \dfrac{\partial f_K}{\partial \psi}$$

$$= - \dfrac{\partial f_H}{\partial \psi} .$$

Now $\qquad f_H = - M_s H \cos (\psi - \theta)$

so $\qquad \dfrac{\partial f_H}{\partial \psi} = M_s H \sin (\psi - \theta) = - \dfrac{\partial f_H}{\partial \theta}$

$$= - \left(- \dfrac{\partial f_K}{\partial \theta} \right) .$$

Therefore $\quad L = - \dfrac{\partial f_K}{\partial \theta}$, and this is the justification that torque

measurements can produce anisotropy constants. A typical torque curve

might look like fig. 1.5 .
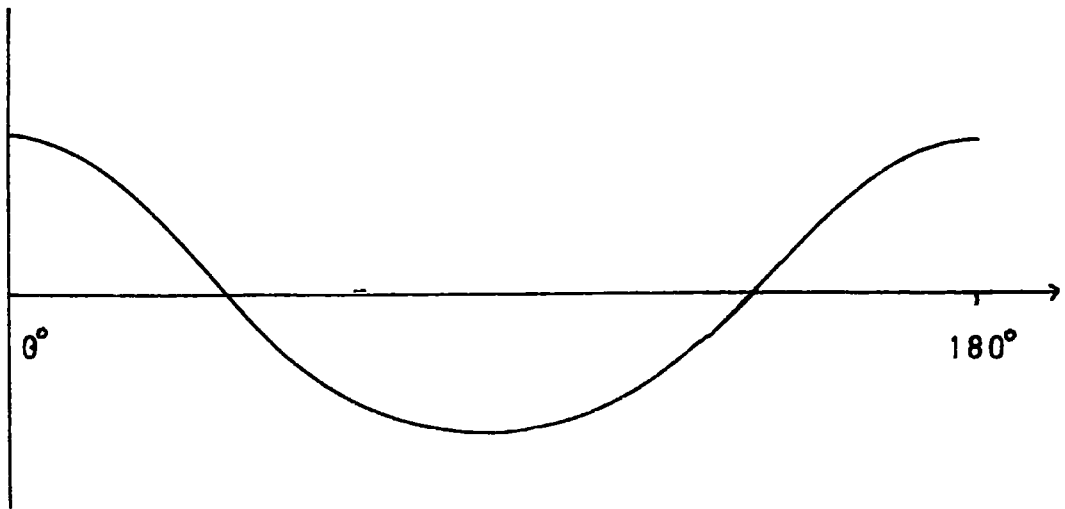
FIG. 1.5   A TYPICAL 180° TORQUE CURVE.

In the case of hexagonal crystals K_4 can be determined by the maximum or minimum points of the torque measured in the basal plane. Then the value of Θ in equation 1 . 3 is 90° and the maximum torque is

$$L_{max} = \frac{\partial f_K}{\partial \phi}\Big|_{max} = 6K_4 \sin 6\phi \Big|_{max}$$

or

$$L_{max} = \pm 6K_4$$

depending on the sign of K_4.

Finding K_1 , K_2 , and K_3 requires a more elaborate analysis. Equation 1.3 may be written

$$f_K = \left[K_0 + \tfrac{1}{2} K_1 + \tfrac{3}{8} K_2 + \tfrac{5}{16} (K_3 + K_4 \cos 6\phi) \right]$$
$$+ \left[- \tfrac{1}{2}K_1 - \tfrac{1}{2}K_2 - \tfrac{15}{32} (K_3 + K_4 \cos 6\phi) \right] \cos 2\Theta$$
$$+ \left[\tfrac{1}{8} K_2 + \tfrac{3}{16} (K_3 + K_4 \cos 6\phi) \right] \cos 4\Theta$$
$$+ \left[- \tfrac{1}{32} (K_3 + K_4 \cos 6\phi) \right] \cos 6\Theta \; ,$$

or conveniently as

$$f_K = A + B \cos 2\Theta + C \cos 4\Theta + D \cos 6\Theta .$$

For measurements not made in the basal plane but at some constant ϕ value,

the torque is

$$L = -2B \sin 2\theta - 4C \sin 4\theta - 6D \sin 6\theta .$$

A Fourier analysis of this curve will provide values of B, C and D, from which, since

$$B = \frac{1}{2} K_1 - \frac{1}{2} K_2 - \frac{15}{32}(K_3 + K_4 \cos 6\phi)$$

$$C = \frac{1}{8} K_2 + \frac{3}{16}(K_3 + K_4 \cos 6\phi)$$

$$D = -\frac{1}{32}(K_3 + K_4 \cos 6\phi)$$

we find the following values of

$$K_1 = -2B - 8C - 18D$$

$$K_2 = 8 (D + C)$$

$$K_3 = -32D - K_4 \cos 6\phi .$$

Expressions for the torque in various planes in cubic crystals have been derived by Bozorth (ref.15), Tarasov & Bitter (ref.16) and Schlechtweg (ref.17). Their results are summarised by Bozorth (ref.18).

(c) <u>Ferromagnetic Resonance.</u>

The angular momentum vectors of electrons in a magnetic field precess at a rate depending on the field strength. If a second field is made to oscillate at various frequencies, the electrons are found to absorb energy at the specific frequencies at which their angular momentum vector can resonate with the secondary field. If an anisotropic cubic crystal is in an applied field H then its anisotropy constant K_1 is equivalent to an "anisotropy field" $H_{100} = \dfrac{2K_1}{M_s}$ for the $\langle 100 \rangle$ directions (ref.19).

For a thin cubic crystal, parallel to the (100) plane the resonant frequency is

$$\omega_o = \alpha \left[\left(B + \frac{2K_1}{M_s} \right) \left(H - \frac{2K_1}{M_s} \sin 4\theta \right) \right]^{\frac{1}{2}} \qquad \text{Equation 1.5}$$

where B is the induction in the crystal and

$$\alpha = \frac{ge}{2mc}$$

is a constant from wave mechanics, g is Lande's splitting factor, and c, m and e are the velocity of light and the electronic mass and charge

respectively. ϕ is the angle between H and the [001] direction in the crystal.

If the specimen is not saturated, further terms are introduced into equation 1.5 , and if the anisotropy constants K_2 and K_3 are large, they may modify the resonance curve and make it difficult to interpret. Equation 1.5 also applies to uniaxial crystals.

The oscillating field is generally applied by microwave techniques, and the anisotropy constant found from the shift of the resonance field between two directions. For example, the anisotropy field in cubic $\langle 111 \rangle$ directions is $H_{111} = - \dfrac{4K_1}{3M_s}$ so that the shift in resonance fields between the [100] and [111] directions corresponds to the difference in anisotropy fields and is

$$\Delta H = H_{100} - H_{111} = \frac{10 \ K_1}{3M_s} \ .$$

Δ H may be determined quite accurately so that small anisotropies and small crystals may be easily investigated (Bickford, ref.51) .

CHAPTER 2 .

Measurement of Anisotropy Constants.

1. ## Introduction.

The three principal techniques are, in order of historical development:

(i) Measurement of the magnetic moment of a sample as an applied field is increased from zero until it produces saturation magnetization.

(ii) Measurement of the torque on a magnetically saturated sample as it is made to rotate through 180° in the applied field.

(iii) The examination of the resonance curve of a saturated specimen in an oscillating field.

In each case, single-crystal specimens must be used. They must be cut into a convenient shape, generally ellipsoidal, spherical or disc, and the crystallographic directions must be accurately known.

Consider a cross section of the specimen, fig. 2.1. M_s and H represent the directions of the applied field H and saturation magnetization M_s which are not necessarily parallel. Induced on the specimen is a magnetic polarity which opposes the field H and creates an internal demagnetizing field. For specimens whose surfaces are described by equations of the second degree, Maxwell (ref.19) has shown that the internal field, the induction and the magnetization are always uniform, so that the demagnetizing field is uniform for the above mentioned shapes. Then the demagnetizing field is written $- NM_s$ and is parallel to the magnetization, and in the opposite direction. The factor N is the demagnetizing factor and $0 \leqslant N\mu_0 \leqslant 1$ in MKSA units. N depends on the shape of the specimen and has been calculated by Osborne, (ref.20) for many cases. (Thin discs may be regarded as approximately prolate spheroids and their demagnetizing factors are deduced from the same formula. This is especially useful for torque magnetometry).
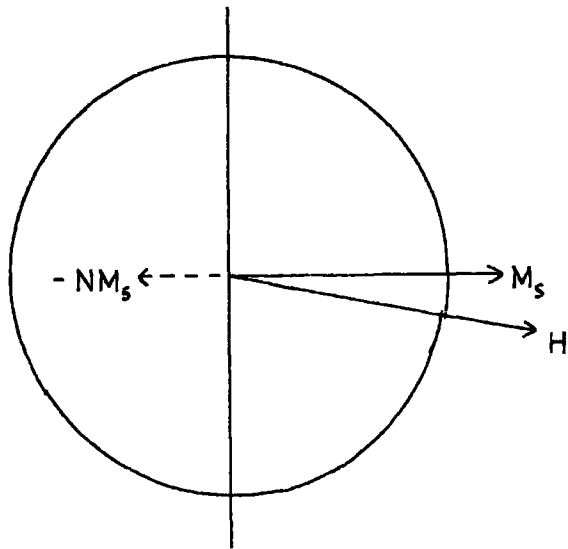
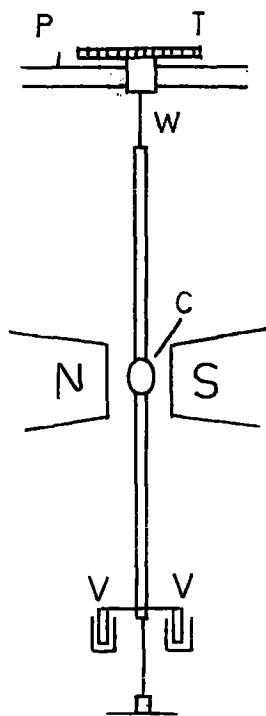FIG. 2.1 A CROSS SECTION OF A CRYSTAL SATURATED BY A MAGNETIC FIELD H, SHOWING THE DEMAGNETIZING FACTOR $-NM_s$.

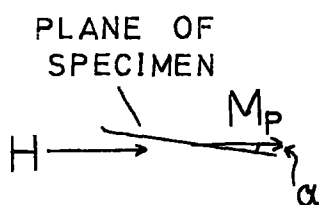FIG. 2.2 THE TORSION BALANCE MAGNETOMETER OF WEISS (REF. 10, 11) AND BECK (REF. 22).

FIG. 2.3 VERTICAL VIEW OF THE SPECIMEN. IN FIG. 2.2.

(2) Magnetization Measurements.

(a) Many modern methods are elaborations of the techniques used by Weiss, (ref.10,11) , who in his work on Pyrrhotite used a torsional method and a ballistic method. The torsion method is more sensitive and may be used on smaller specimens, but is subject to more possible errors, and some measurements require that crystals have a large magnetic anisotropy.

His apparatus is depicted in fig.2.2 . A torsion wire W suspends the crystal C between the poles N.S. of a magnet. The crystal is held in a non-magnetic stirrup, the lower section of which suspends a long wire with damping vanes V attached; these are immersed in oil, and the bottom of the wire fixed to avoid azimuthal motion. The torsion wire is suspended from a rotatable torsion head T which has a linear scale which may be read by telescope as it passes the needle P.

A magnetic field H will exert a couple $H M_s \sin \Theta = H M_N$ per unit volume when the magnetization is at an angle Θ to H. M_N is the intensity of magnetization normal to the field and may be plotted for various field directions as the magnetic field is rotated in small amounts. M_N is found by counter rotating the torsion head by angle $\emptyset$ until the torsion wire balances the torque and the crystal resumes its original direction. If C is the torsion constant of the wire

$$H M_N = C \emptyset \quad .$$

This formula enables M_N to be plotted at constant H as H is rotated, or M_N may be plotted against increasing H while the direction of the crystal is constant in the field.

If the specimen is disc shaped, then M_N is found with the disc horizontal, and the component M_P of magnetization parallel to the field is found by suspending the disc sideways at a small angle α to the field (fig.2.3).

The couple on the disc at this angle is countered by rotating the torsion head by ψ and

$$H M_P \sin \alpha = C \psi .$$

M_p is now studied by rotating the disc in the vertical plane. In this mode the lines of force are not quite parallel to the plane of the disc and so it is not strictly M_p which is measured. However, for a highly anisotropic material the difference is negligible. Sucksmith et al criticise this method (ref.21).

Beck (ref.22), in his pioneering work on iron, and Webster (ref.23) used similar apparatus. The small crystals available to Beck, meant that his discs had large demagnetizing factors, and to keep M_S and H in the same plane, he cut especially thin discs, 0.06 m.m. to 0.1 m.m. thick. Even so, M_p had to be found by an induction measurement in three separate planes.

Webster's apparatus had slight modifications, fig.2.4 . His torsion head was threaded and adjustable to any height to facilitate the centring of the crystal in the field. He suspended a heavy weight from the lower torsion wire and constrained it to prevent lateral movement. The angle of the torsion head was determined by viewing a meter scale reflected in a mirror which was attached to the head; and with a telescope the rotation could be determined to better than 1 arc. The system was unstable when the suspension had nearly returned to zero, because M_p decreases suddenly so the magnetization couple disappears. Its effect was reduced with thicker torsion fibres, but then the sensitivity was also much less. He was able to use larger specimens, (4.74 m.m. diameter by 0.369 m.m. thick) but required second order demagnetizing corrections.

In Weiss' second method, he had a large magnetizing solenoid containing a smaller detecting solenoid concentric with it and slightly removed from the middle, fig.2.5 .

His crystal was placed at the end of a rod along the axis of the solenoids and could be rapidly inserted into the detecting solenoid. The deflection registered on a ballistic galvanometer in series with the latter solenoid, would be proportional to the magnetization along the axis, so that M_p could be measured. This equipment was easy to construct and operate, and the results were satisfactory in spite of the reduction in sensitivity compared to the torsional balance.
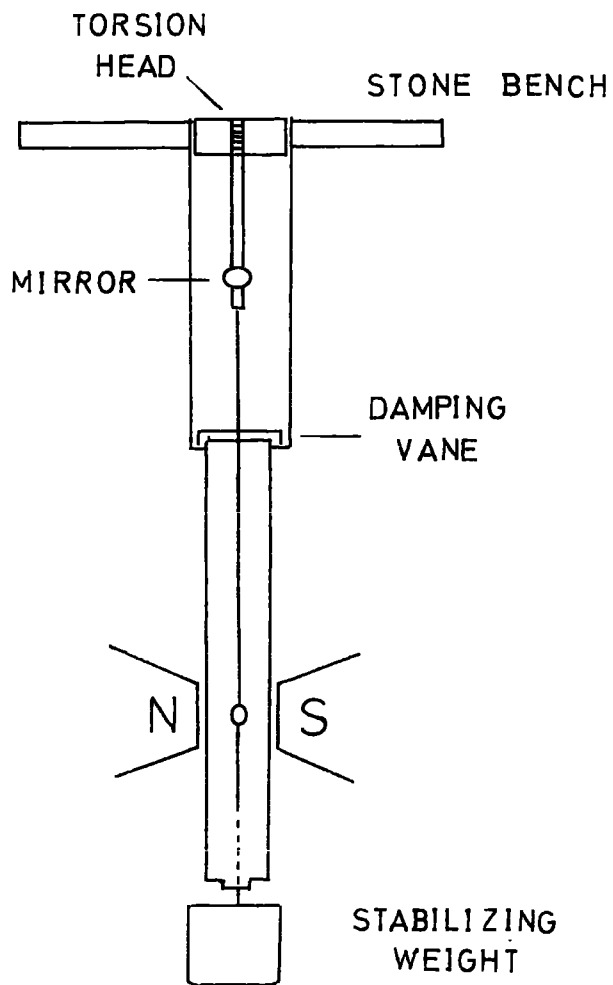
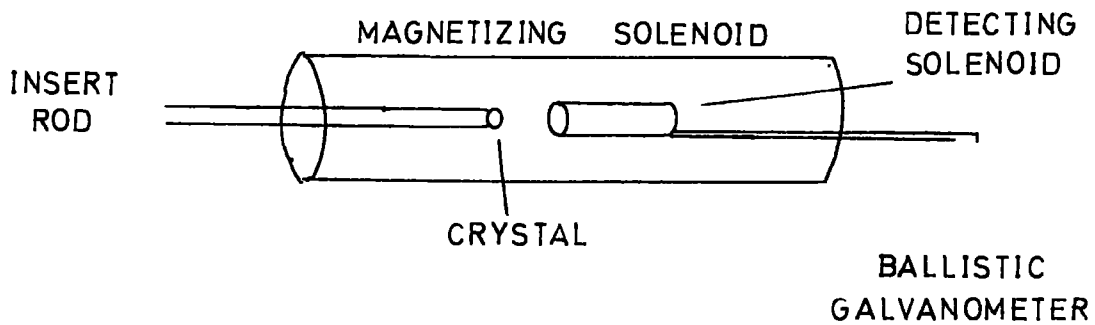Fig.2.4   The magnetometer of Webster, ref.23.

Fig.2.5   The ballistic magnetometer of Weiss, ref.10,11.

(b)   The experiments of Honda and Kaya (ref.24), marked a great advance

in technique, both of experiment and of specimen preparation. Their

apparatus is outlined in fig. 2.6 . Two rotatable discs were mounted

on a long brass plate and connected by a pulley belt. One was mounted

with a small disc to which the specimen could be cemented, and the other

could be rotated manually so that the specimen would be rotated remotely

by designated amounts. Small sensing coils, not attached to the pulley

system but capable of being swivelled in a horizontal plane, were mounted

close together on either side of the crystal table so that the crystal

was at their centre. A large magnetizing solenoid was placed so that the

crystal on the pulley system could be inserted at the centre of this

solenoid.

The specimen was rotated to some chosen angle with respect to the

field of the solenoid, and any deflection on the galvanometer allowed to

return to zero. The specimen was then swiftly rotated until one of the

principal crystallographic axes coincided with the direction of the applied

field. A flux change corresponding to the magnetization along the chosen

direction of the crystal would pass through the sensing coils, and the

signal from a ballistic galvanometer attached to the sensing coils gave

a measure of this magnetization, and a magnetization curve can be plotted

for the chosen angle. By rotating the sensing coils either parallel or

perpendicular to the solenoid axis M_N and M_P are readily found.

(c)   Because of edge effects, the precise value of the demagnetizing factor

of a disc is impossible to calculate, and Williams (ref.25), avoided much

of this uncertainty by cutting some specimens of silicon-iron in the shape

of a picture frame (see fig. 2.7). Each side of the specimen was parallel

to a principal crystallographic direction, i.e. parallel to one of the sets

$\langle 100 \rangle$, $\langle 110 \rangle$ or $\langle 111 \rangle$.

For samples in the shapes of discs or ellipsoids the effective field

is small and is the difference between the two larger quantities the applied

field and the demagnetitizing field. Thus small effective fields cannot

be determined accurately and the initial part of the magnetization curve
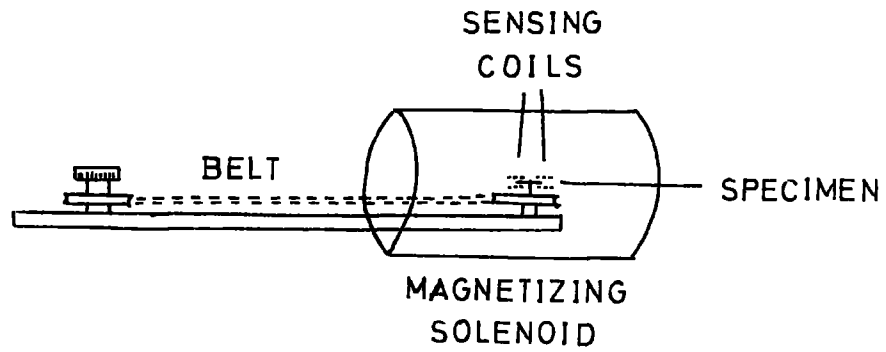
Fig.2.6 The apparatus of Honda and Kaya, ref.24.

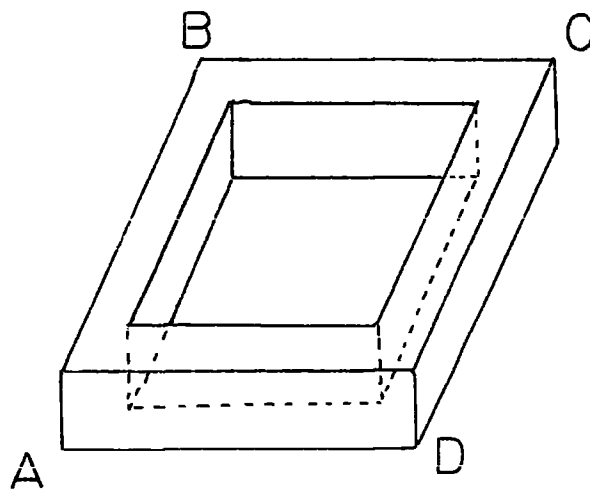Fig.2.7. The 'Picture frame' specimen of H.J. Williams. For the case

of parallelogram sides cut parallel to [100] and [110]

directions the corners A B C D are right angles for a

cubic crystal. For parallelogram sides cut parallel to

[111] directions the angles at A and C are $2 \sin^{-1}\frac{1}{\sqrt{3}} = 70^{\circ}. 53$

and at B and D, are $2 \cos^{-1}\frac{1}{\sqrt{3}} = 109^{\circ}. 47$.

suffers from considerable error. The parallelogram specimens offered a
continuous flux path so their demagnetizing field is considered negligible,
but the flux at corners may not be parallel to either parallelogram edge.

The magnetic properties were investigated by winding each specimen
with primary and secondary coils and testing with a fluxmeter. This
provided reliable, accurate results, but the shape in which the specimens
must be cut depends on magnetically equivalent directions and demands a
prior knowledge of the anisotropy, and their preparation is more than
usually tedious.

In materials where the magnetic easy directions change with temperature,
this method could not determine how anisotropy constants vary with tempera-
ture. Okamura and Hirone (ref.30) used this method to find the temperature
variation of magnetization of nickel, but their results appear to have been
slightly anomalous and little interest has been shown in the technique since
then.

The Oscillating Sample Magnetometer.

This is a refined device for the measurement of the magnetization of
crystals. Although Plotkin (ref.60) originally designed such an instrument,
it was the work of Van Oosterhout (ref.53) and Foner (ref.54) which pointed
to the qualities and possibilities of the instrument. It has proved so
sensitive and adaptable that it has been widely used and developed (refs.
55,56,57,58,59,64). The principle of this type of magnetometer is that the
specimen is made to perform small regular oscillations within a uniform
magnetic field so that the resulting flux changes around the region of
oscillation may be measured from the signals received from detecting coils
placed near this region, and the magnetization evaluated through prior
calibration with a specimen having an otherwise determined magnetization.
If the specimen vibrates between two identical sensing coils connected in
series opposition, it will induce an alternating voltage E between them
which will be proportional to the rate of change of local field. This is
in turn proportional to the rate of change of magnetization $\frac{\partial M}{\partial t}$ within

their sensitive volume, so

$$E \propto \frac{\partial M}{\partial \mathfrak{z}} \frac{d\mathfrak{z}}{dt}$$

where $\mathfrak{z}$ is a measure of the position of the specimen.

Plotkin's design was specifically for use in a magnetizing solenoid, and a similar idea was used by Van Oosterhout, whose method is shown in fig.2.8 and fig.2.9 . The sample vibrates between the two central pickup coils, and induces an alternating voltage between them. It is impossible to prevent some vibration of the pickup coils and this will cause a spurious signal if the second derivative of H, $\frac{\partial^2 H}{\partial \mathfrak{z}^2}$, is appreciable.

Two compensating coils, coaxial with and at either side of the pickup coils and connected in opposition as shown in fig.2.8 will counterbalance this spurious signal. They may be sufficiently far away from the specimen to fail to detect its oscillations.

A loudspeaker excited by an oscillator is a convenient vibrator and a reference signal is taken from two coils around a standard magnet which is attached to the vibrator. The reference signal is attenuated to balance the signal from the sample and any subsequent change in sample magnetization may be determined by amplifying the difference between these signals as shown. This makes the method extremely sensitive (down to moments of 10^{-13} Wbm) and eliminates any effects due to changes in vibration amplitude, driver wave form or amplifier gain.

Foner's design (ref.55) had the advantage of being useable with an electromagnet. This he achieved by using detecting coils with effective area-turns non-symmetrically distributed about the axis of specimen vibration. The design is shown in fig.2.10 . A conical paper cup is attached to the cone of a loudspeaker, and holds the specimen support vertically. Near the top of the specimen support is a small permanent magnet which generates a reference signal in two coils placed at either side of it. The specimen is at the bottom of the holder and it oscillates perpendicularly to the axis of two coaxial detecting coils which are connected in series opposition; the axes of the detecting coils are parallel to the magnetic field.

Part of the reference signal is phased to balance the sample signal,

PICK UP
COILS

SPECIMEN

DIRECTION OF
OSCILLATION

MAGNETIC
FIELD

COMPENSATION
COIL
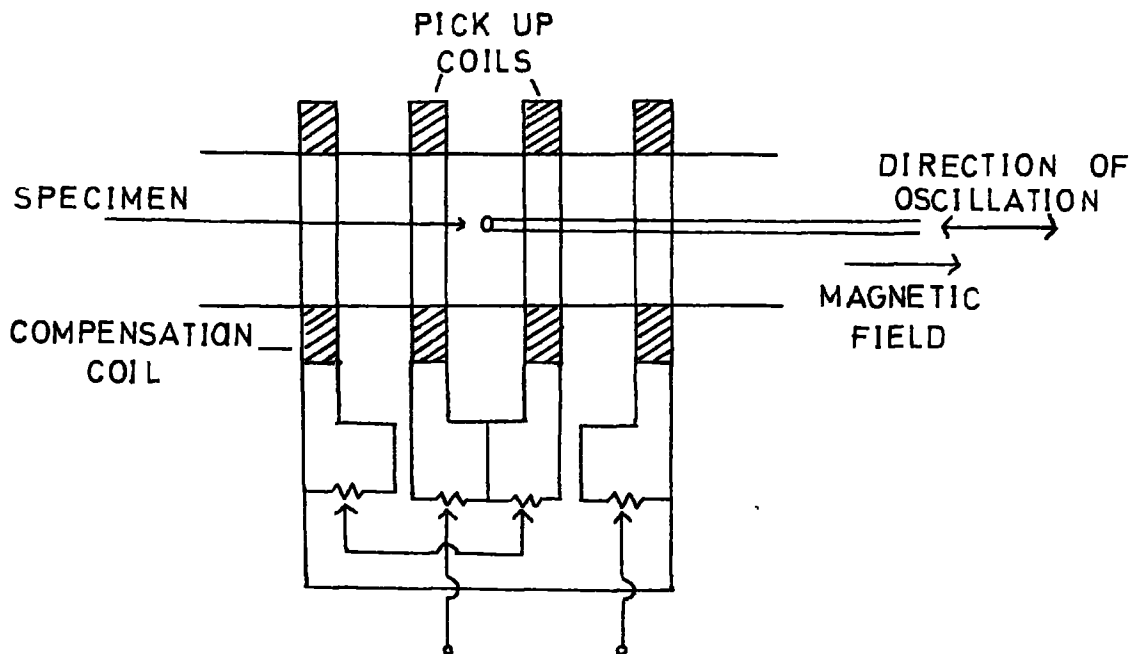
Fig.2.8   The region around the specimen in the vibrating sample

magnetometer of Van Oosterhout. ref.53.

LOUDSPEAKER

COILS

STANDARD
MAGNET

AMPLIFIER

AUDIO
OSCILLATOR

PHASE
SHIFTER

AMPLIFIER

PHASE
SENSITIVE
DETECTOR

MAGNETIZING
SOLENOID

INDICATOR

Fig.2.9   The Instrumental layout required to measure the magnetization

by the vibrating sample method.
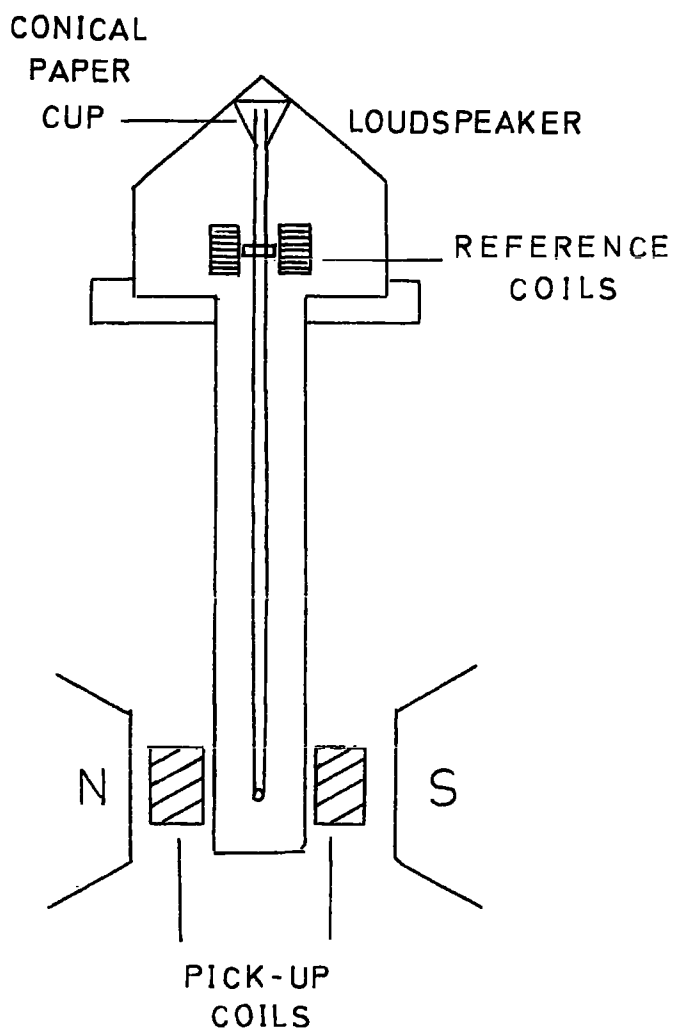
Fig.2.10. An outline of S.Foner's vibrating sample magnetometer. ref.55.

and the difference signal is sent through a tuned amplifier to an oscillo-
scope which is used as a null detector. Instability of the magnetic field
has a minimum effect because the coils are in opposition.

The apparatus is simple, versatile, and highly accurate (Foner obtained
a magnetization curve for nickel to better than 1% accuracy).

The entire unit may be evacuated or pressurised so that magnetization
may be determined as a function of applied field or temperature or pressure,
(however, the low temperature usefulness is not good because of the electro-
mechanical vibrator). Further, the vibrating system and specimen may be
readily rotated to observe the directional properties of the specimen. The
one complication which cannot be eliminated automatically through instru-
mental modification is the magnetic image of the specimen in the electro-
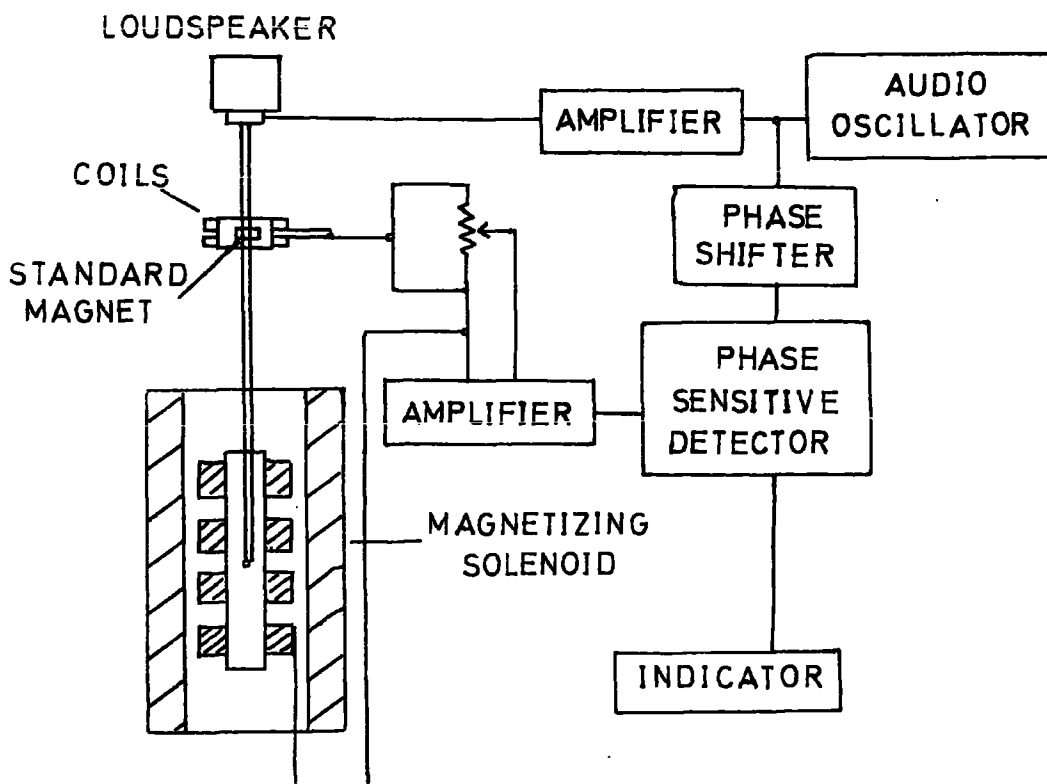magnet: the effect must be calculated and depends principally on the spacing
of the pole pieces and the total moment of the specimen.

Dwight, Menyuk and Smith (ref.70) continued the development of Smith's
magnetometer (ref.61) and improved the sensitivity by a factor of 100. They
chose carefully matched electromagnet pole faces to increase the homogeneity
of the field (this is the most limiting factor on sensitivity), and they
attached a monitoring coil to the sample drive system and compared the
oscillating voltage from it with a standard frequency.

By feeding the difference between standard and monitor frequencies
through a power amplifier to the driving system they maintained the uniform-
ity of specimen vibration.

Among the adaptations of the basic design, the possibilities for the
magnetometer of Foner and McNiff (ref.57) seem particularly important for
the high field experiments desired for anisotropy measurements of the heavy
rare earths. They used flux integration techniques on a sample which was
vibrated slowly ($\frac{1}{10}$ Hz to 3 Hz) over a region extending beyond the pickup
coil centres; fig.2.11 .

The instrument was intended for use in superconducting magnets. The
sample rod was driven by a rock and pinion gear drive, and held the sample
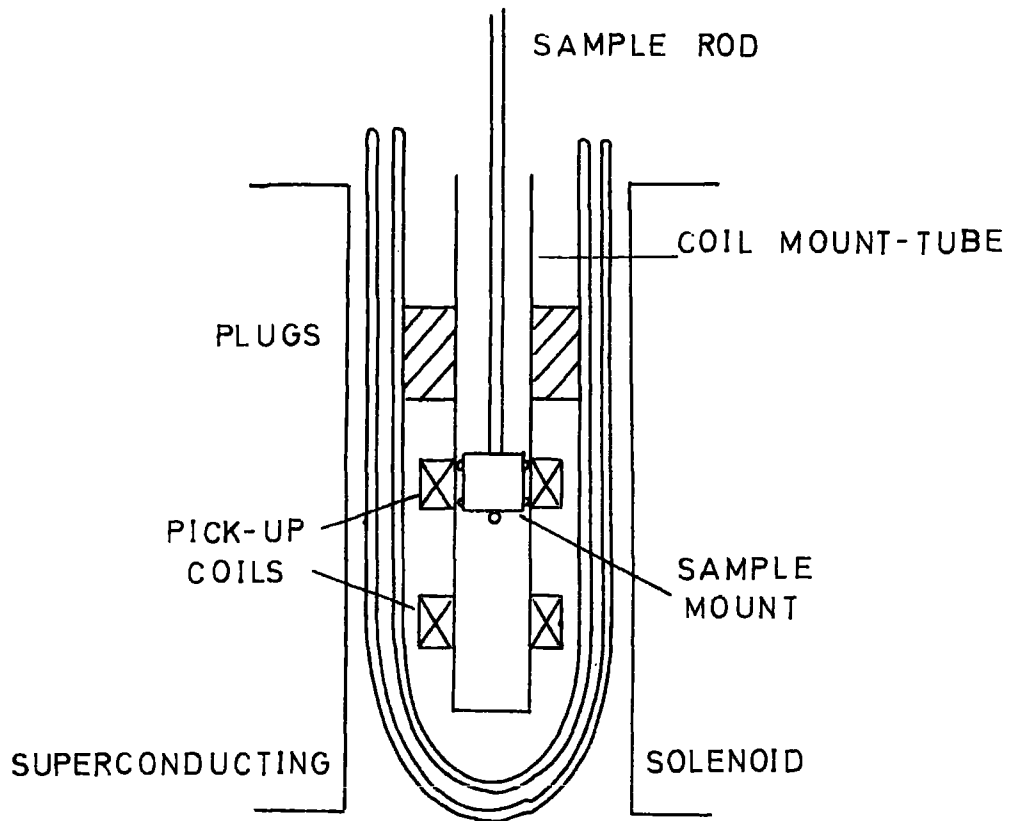mount which was kept accurately centred by Teflon guides within a tube on

Fig.2.11. The field region of Foner and McNiff's magnetometer. ref.57.
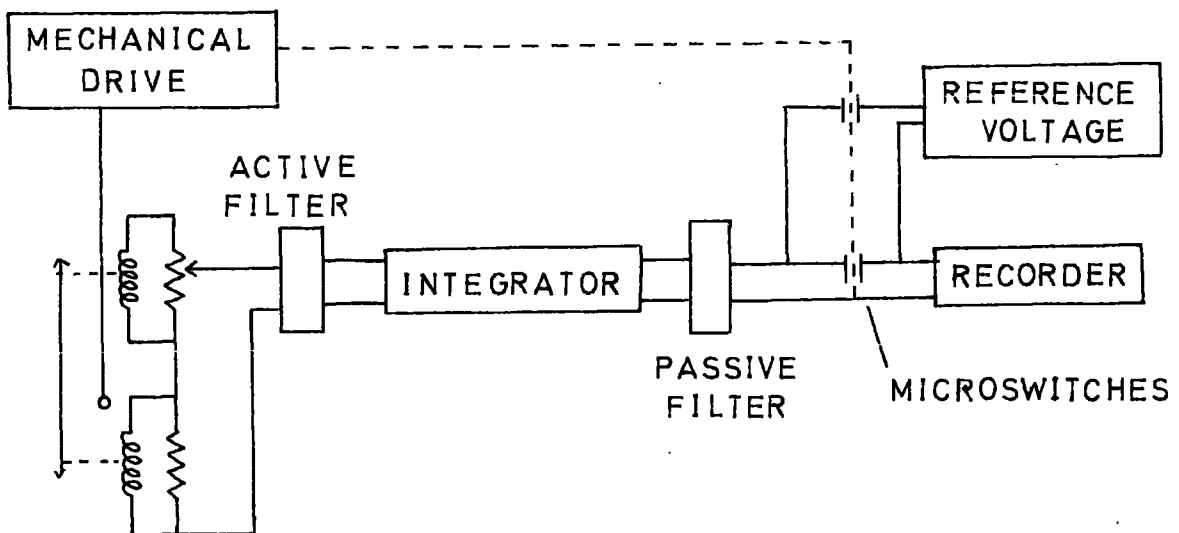

Fig.2.12. A block diagram of Foner and McNiff's magnetometer.

which the detecting coils were mounted. The coil mount tube was in turn
centred by a plug in the inner dewar. The rigid coil mounting avoided
background field pickup, and the centring guides reduced radial positioning
errors.

Precision in these details was important for the kind of work intended
for the magnetometer. In a high magnetic field a strongly magnetized sample
will suffer a significant and unwanted force in even a small field gradient,
and such errors are impossible to calculate or eliminate electronically.

Variations in the differential permeability (between the specimen and
its surrounding medium) were recorded as a function of time (possible because
the sample moved beyond the coil centres) and used to further minimise
positioning errors.

Fig.2.12 shows a block diagram of the magnetometer. The specimen moved
past the centres of the detecting coils on each vibration. These coils were
initially well balanced in order to minimise the effect of fluctuations in
the applied field, and their output was fed to a high stability electronic
flux-integrator. Each vibration was recorded as the difference from a
reference voltage source, and they could then time-average the field fluct-
uations and measure small differences of the output as a function of applied
field or of temperature.

Other low temperature - high field magnetometers have been built by
Strnat and Bartimay (ref.56) and by McGuire (ref.58). Strnat (ref.65,66)
has proved the usefulness of his magnetometer for anisotropy measurements
on intermetallic - rare earth compounds, and it is shown in outline in fig.2.13
The sample was mounted on a rod which was rigidly clamped to a small platform.
The platform could freely slide vertically and was attached by a short moving
arm to an eccentric cam driven by a synchronous motor. The flux signal from
the detecting coils was put through an integrating digital voltmeter which
converted the voltage input into a sequence of pulses, the number of pulses
being proportional to the input. Counting over a fixed time, the number of
pulses was proportional to the magnetization of the specimen, and a digital-
analogue converter D.A.C. passed this signal to an X - Y recorder.

INTEGRATING
DIGITAL
VOLTMETER

DAC

X-Y
RECORDER

POWER
SUPPLY

LIQUID
NITROGEN
DEWAR

SPECIMEN

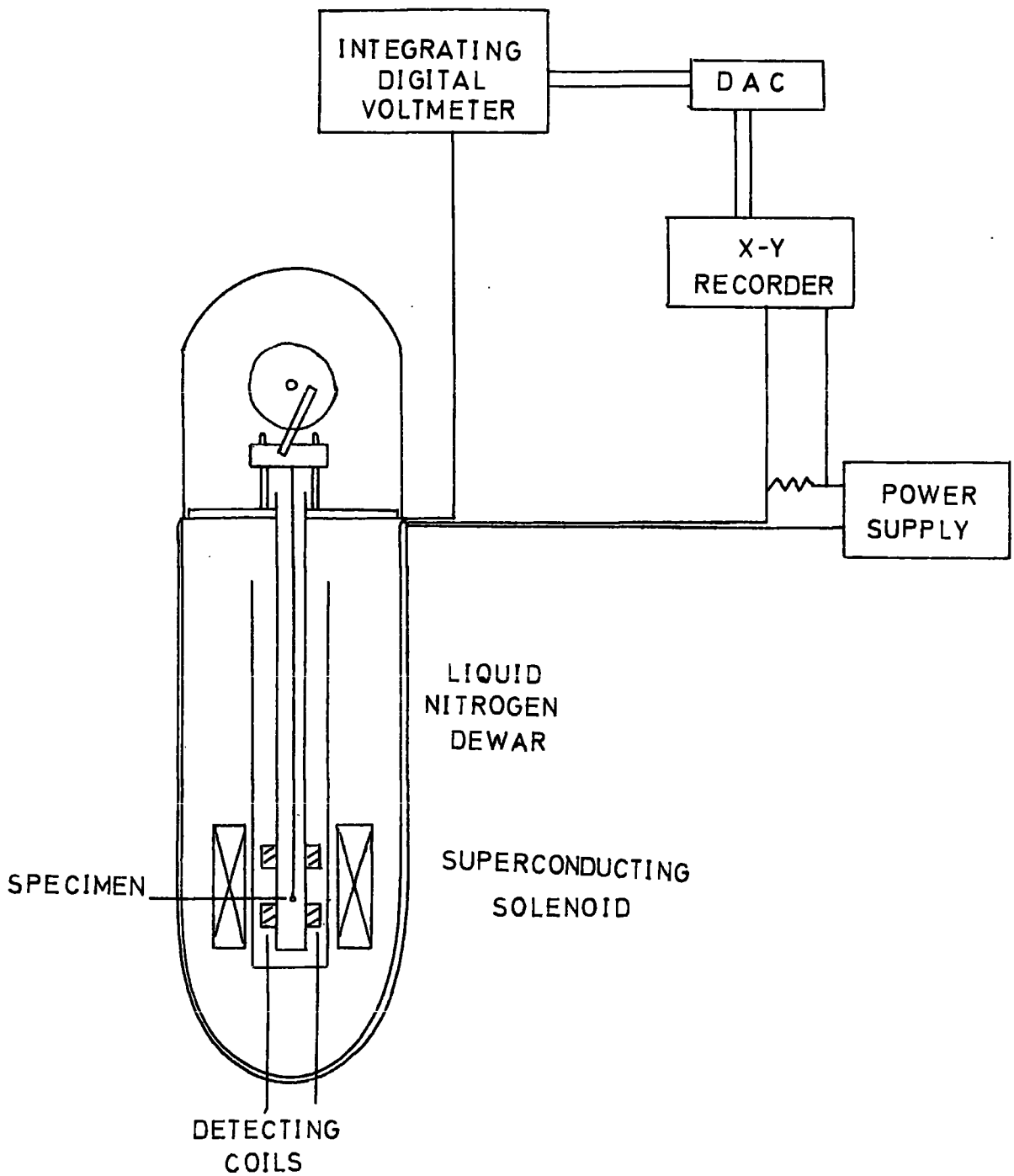SUPERCONDUCTING
SOLENOID

DETECTING
COILS

Fig.2.13. The high field oscillating specimen magnetometer of Strnat
and Bartimay, ref.56.

The field signal for the magnetization curve was taken from the voltage across a small resistance in the circuit of the solenoid and its power supply.

Further improvements of pickup coil design have been explained by Noakes, Arrott, and Haakana (ref.68), who used a six-coil system to eliminate the sensitivity to field noise and microphonics, and a six cycle chopper attached to the drive of the specimen in such a way as to eliminate all even harmonics and the third harmonic.

Because very low temperatures require some vacuum system to isolate the experimental region, any device which relies on an even transmission of mechanical motion to the specimen is at a grave disadvantage. Gubser and Mapother (ref.62) used a remotely controlled piezoelectric vibrator in their compact vibrating sample magnetometer, and their idea was borrowed by Mangum and Thornton (ref.63) , for adaptation to a vibrating sample magnetometer, outlined in fig.2.14 .

A Bimorph (the trade name belonging to the Clevite Corporation, for a flexing piezoelectric element) consisting of two flexible piezoelectric strips, oppositely oriented and fixed one on either side of a thin sheet of brass, was used as a vibrator. If the two strips have suitable piezoelectric compliances $C_{D,\sigma}$ an oscillating voltage applied across them will alter their lengths so that they will flex from side to side. When one end of the bimorph is clamped it behaves like a vibrating cantilever.

One end of a Bimorph was clamped to the magnetometer support, and it had a specimen holder attached to its free end. The specimen holder passed between the coaxial centres of the two pickup coils which were clamped in the magnetometer support, while a reference signal was obtained by a similar arrangement lower down the bimorph from an yttrium iron garnet sphere.

Bimorphs have several mechanical resonances but troublesome modes may be avoided by using the fundamental resonance. Below 10K the magnetization of YIG is nearly independent of temperature so in this range the reference signal can be used with a servosystem to vary the voltage applied to the Bimorph in order to maintain a constant amplitude of vibration.
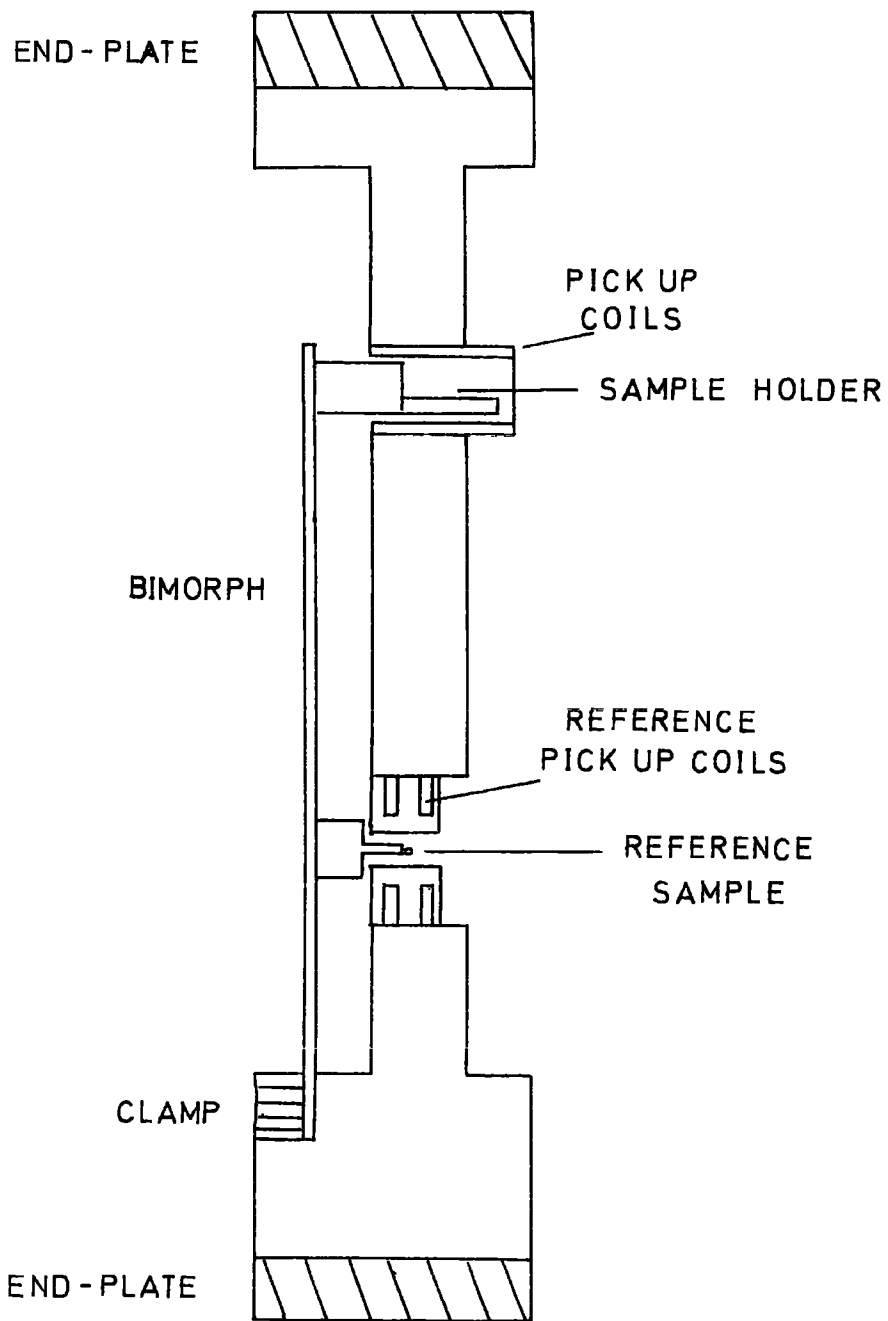
Fig.2.14. A cross section of the Magnetometer of Mangum and
Thornton, ref.63.

This is a very compact magnetometer and could be constructed with a maximum dimension of 10 m.m. according to Mangum and Thornton. The noise levels in the detecting coils was unchanged in fields of 2.2 T so that the sensitivity and accuracy would be excellent in the small temperature range, 0.3 K to 5 K, over which they used it, but this would limit its applicability.

Over a higher temperature range some other source of reference signal would be required, and very elaborate calibration would be needed to allow for the voltage adjustment necessary to keep the Bimorph vibrating with its fundamental frequency which changes by 25% between 300 K and 0.3 K.

The Vibrating Coil Magnetometer.

The Vibrating Coil Magnetometer has many similarities with the vibrating sample magnetometer as regards instrumentation, versatility and accuracy, and it was developed at around the same time by D.O. Smith (ref.61).

A small detecting coil is made to vibrate near the magnetized sample and because the field is non-uniform a measureable e.m.f. will be generated across the coil. The coil system is generally vibrated along a direction parallel to the applied field H ; the apparatus involved, is indicated in fig.2.15 .

Very uniform fields are necessary with this type of magnetometer. Any non-uniformity may be difficult to correct for, especially as non-uniformities may be functions of the applied field. The second derivative of H , $\frac{\partial^2 H}{\partial \zeta^2}$ has been compensated for by taking two concentric, coaxial coil pairs, each with a region of uniform sensitivity, as a detecting system. The inner coil is the sampling coil and the outer, the compensating coil (fig.2.16) and the area-turns configuation is designed to give the coil system zero quadrupole moment. The input circuit of fig.2.15 is an amplifier which introduces a negative scale factor to adjust the detector signal, depending on the relative sizes of the detecting and bucking coils which are connected in opposition.

Especially when the magnetometer is used with an electromagnet (as shown) it is even then hard to reduce the sensitivity to the external field to a negligible quantity and this is the main limitation to the measuring

BALL BEARINGS

VIBRATING COIL

SPECIMEN

POLE PIECE

VIBRATOR

POWER AMPLIFIER

MICRO VOLTER

INPUT CIRCUIT

40 HZ OSCILLATOR

AMPLIFIER

PHASE SENSITIVE DETECTOR

APPLIED FIELD

X-Y RECORDER
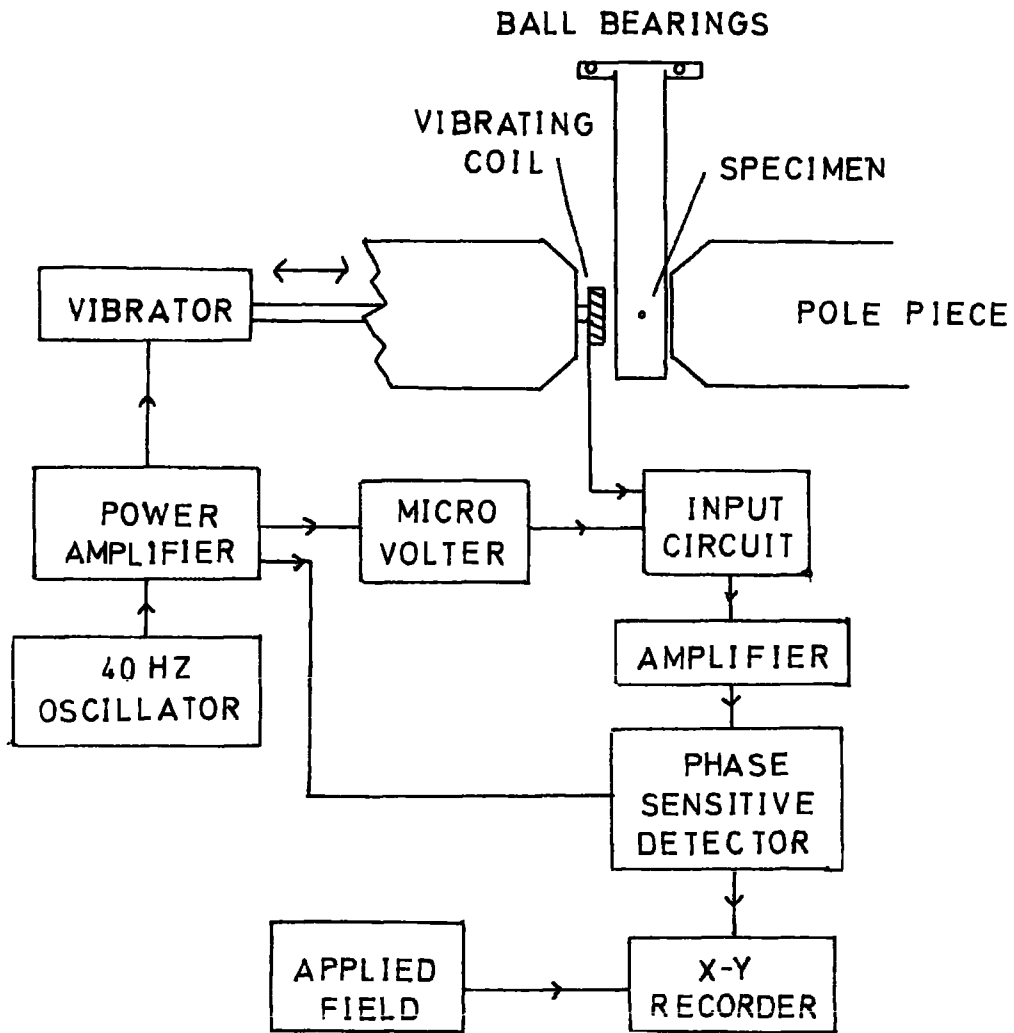
Fig.2.15   The Apparatus of D.O.Smith's Vibrating Coil Magnetometer
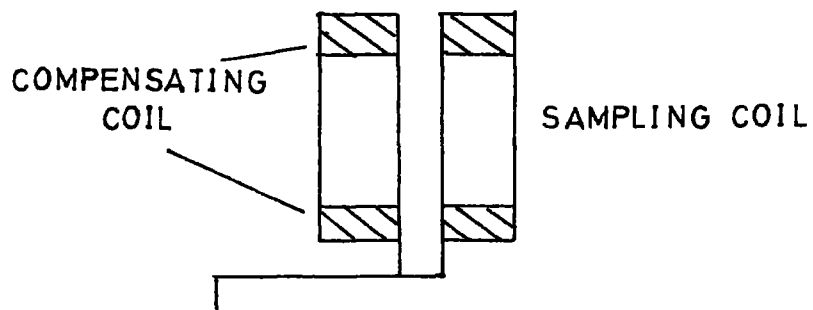
ref.61.

COMPENSATING COIL

SAMPLING COIL

Fig.2.16   The Apparatus of D.O.Smith's Vibrating Coil Magnetometer

included this compensating coil arrangement.

sensitivity. However, the magnetometer can perform measurements over a wide range of physical conditions, and it may be advantageous compared to the vibrating sample magnetometer in work involving a wide range of temperature or application of hydrostatic pressure.

Specialised requirements have been met by a number of ingenious modifications. Kaeser, Ambler and Schooley (ref.67) desired to make magnetization measurements in the milliKelvin temperature range, in which even a single vibration reaching a small specimen could alter its temperature significantly, and a vibrating specimen magnetometer seemed out of the question. They made the vibrating pickup coils small enough to fit inside the dewar, and suspended them from thin stainless steel tubes which were guided by a loudspeaker spider.

Farrell (ref.69) used a similar detector coil suspension and drive system for low temperature work on superconductors, and obtained accuracies claimed to be 1%, which were of the same order as uncertainties of temperature.

Gubser and Mapother (ref.62) designed a vibrating coil magnetometer using a Bimorph as vibrator which they used below 1 K.

(3) Torque Magnetometry.

   (a) Early Experiments.

The principles behind the torque curve method of determining anisotropy constants, were first enunciated by Akulov, (ref.31) and Gans (ref.32).

As experimental technique and accuracy improved, elaborations of the theory were made by Bozorth (ref.15), Schlechtweg (ref.17), Tarasov and Bitter (ref.16), and Bozorth and Williams (ref.33). Williams (ref.26), and Dahl and Pfaffenberger (ref.27), were the first to use this method successfully, although Akulov (ref.34), had made some attempts previously. This method removed doubts about hysteresis in the magnetization curve, but the torques on nickel and iron crystals were small, and to improve the sensitivity, Williams used disc specimens of order 1 inch in diameter. Besides the fact that such large single crystals are hard to make, it is difficult to arrange for large magnetic fields to be uniform over such an area. More sensitive techniques have made torque magnetometry the most important

technique in the measurement of ferromagnetic anisotropy.

The principle of the method is identical to that of the torsional apparatus of Weiss: a disc is suspended from a torsion wire and a saturating magnetic field is rotated about the plane of the disc. The torque is determined every 10° or so and a complete curve of torque against direction of magnetization is produced. This is interpreted as explained in section 3 (b) of chapter 1. The maximum torque increases as the field is increased and it is the limiting torque curve as the applied field approaches infinity which precisely determines the anisotropy constants.

Dahl and Pfaffenberger had an iron yoke mounted on a turntable, and wound with copper coils which could be excited by an array of batteries, (fig.2.17). The turntable could be adjusted horizontally and vertically so that the specimen would be precisely in the centre of the pole-pieces as they rotated. Two reversed conical pole pieces produced a field which was reasonably uniform over the region around the specimen. The electromagnet was small and this contributed further to reducing the maximum field to only 500 Gauss. The underside of the specimen had a small dimple drilled in its centre, and it rested on a conical pivot to prevent it from swinging toward either pole piece, but this introduced errors in the torque through friction, and the dimple must have altered the demagnetizing field in a small but unpredictable way. The specimen was suspended from a torsion fibre which had been calibrated from a mechanical torque. Their fibres had large torsion constants and large samples were needed to produce measureable torques, so only the first order anisotropy constant K_1 could be measured.

Williams (ref.52) in a modification of his earlief apparatus (ref.26) used two torsion wires in his experiment. A short rod attached a small mirror to the upper surface of his disc specimens, and the mirror was suspended by the upper torsion wire. The second fibre was attached to the bottom of his specimen and passed through a hole drilled through the electromagnet's yoke and the bench, and it suspended a large calibrated
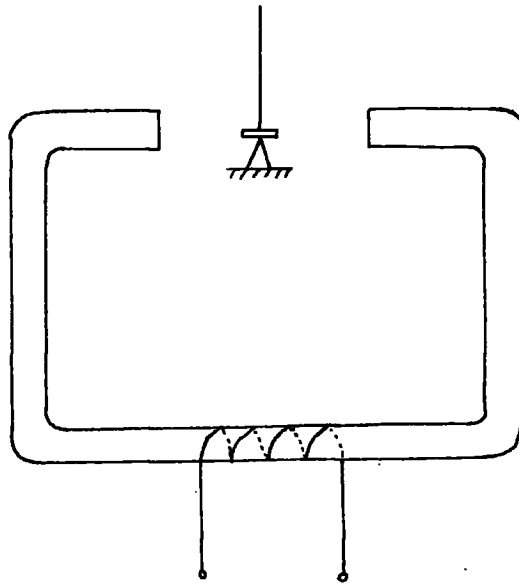
FIG. 2.17   THE PRINCIPLE OF THE APPARATUS OF
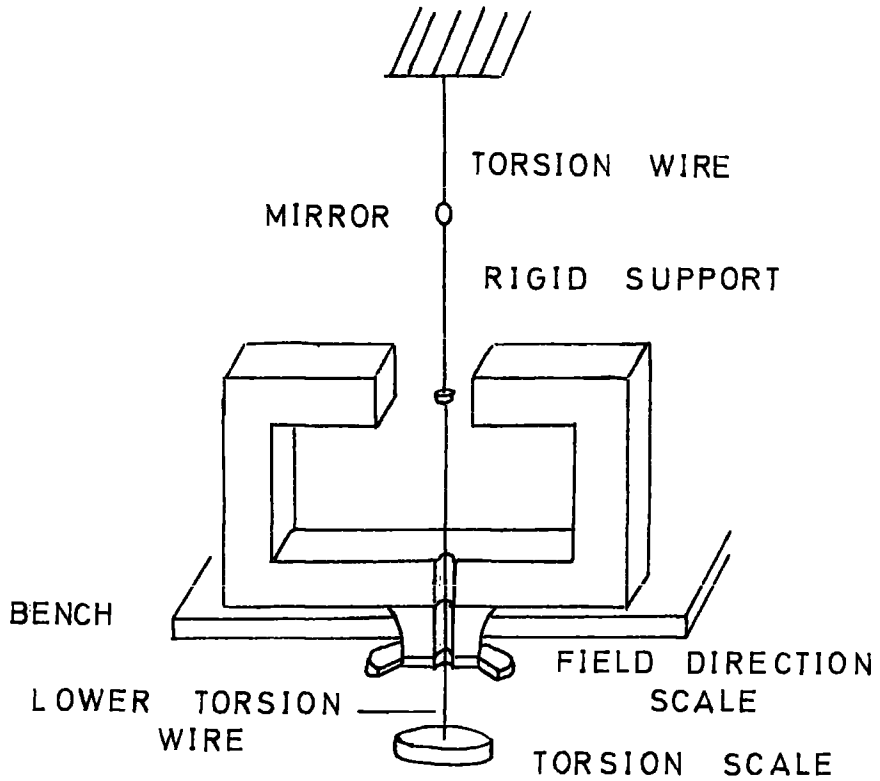DAHL AND PFAFFENBERGER.

FIG. 2.18   THE APPARATUS OF WILLIAMS (REF. 52).

disc which gave a measure of the torque on the specimen. The magnet
could be rotated by an amount measured on a scale attached to it. This
altered the torque on the crystal which rotated slightly, taking the mirror
with it, and deflecting a light beam reflected by the mirror. The torsion
disc was rotated in a contrary direction so that the light beam returned to
its original position; the angle through which the torsion scale rotated
determined the torque. This instrument was used in room temperature
experiments.

Brailsford (ref.28), improved the torsion apparatus in many respects,
(see fig. 2.19). His torsion fibre T was suspended through a large calibrated
brass disc A and attached to a spindle S_1 which held the upper of two discs
between which the specimen was clamped. Both the upper and the lower spindle
S_2 rested on journal jewel bearings which substantially reduced friction.
A protective tube D around the torsion wire, had a long pointer P attached
to its lower end, and a collar C on it, rested on the apparatus support. The
electromagnet was fixed and was more powerful than those used previously in
this experiment, producing fields up to 2.8 kGauss. A pointer not shown in
fig.2.19 attached to the electromagnet, gave the rotation of A with respect
to the field. The tube D could be rotated by hand, and the specimen would
rotate with A so that the position of the pointer Q gave the angular dis-
placement of the specimen. The torque on the wire was calculated from the
small advance that P had made over the disc A_1 and this should equal the
torque on the specimen.

This instrument was built to investigate materials suitable for
transformers and though providing results rapidly and conveniently at
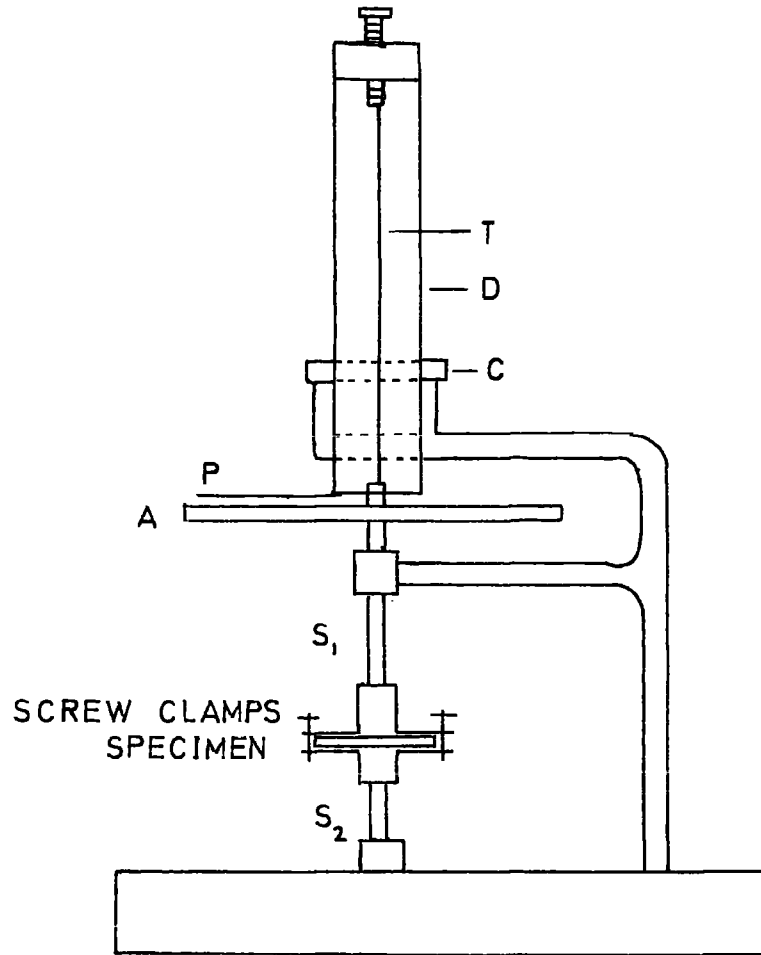room temperature, could not be adapted for low temperature work.

FIG. 2.19   THE MAGNETOMETER OF BRAILSFORD (REF. 29).

(b) <u>Automatic Balancing Torque Magnetometers.</u>

There are seven main difficulties with torque measurements by torsion fibre;

(i)   They are time consuming;

(ii)   Measurements are not continuous;

(iii)   A preliminary knowledge of the anisotropy constants must be available so that a suitable torsion fibre may be chosen to match the range of torque to be measured. The fibre must be capable of measuring the largest torque expected, and remain within its elastic limit, and it must provide a reasonably large deflection in order to minimise reading errors;

(iv)   The need for an enclosure in which a constant and predetermined temperature may be maintained, makes design for a support to stabilize the specimen difficult;

(v)   For low temperature work, the specimen must be in an evacuated enslosure. If the torsion wire is outside the evacuated system, it will require a vacuum seal joint which could involve friction greater than any torque to be measured: thus the torsion wire must necessarily be included in the vacuum system;

(vi)   At low and (especially) at high temperatures, a temperature gradient exists along the torsion wire; this effects the torsion constant and hence the calibration;

(vii)   The torque produced by the fibre must always be in stable equilibrium with the magnetic torque on the specimen. Suppose that E is the total rotational potential energy of the specimen. It is due to the anisotropy energy f_K and the torsional energy $\frac{1}{2} C\theta^2$, where C is the torque constant of the fibre and θ its angle of twist. Then

$$E = f_K + \tfrac{1}{2} C\theta^2 .$$

For stable equilibrium $\dfrac{\partial E}{\partial \theta} = 0$ and $\dfrac{\partial^2 E}{\partial \theta^2} > 0$,   so

$$C > \left| \frac{\partial^2 f_K}{\partial \theta^2} \right|$$ at all times.

Penoyer had a system which attempted to eliminate these problems, (ref.29). His specimen was held in a rigid suspension which could rotate in a horizontal plane (fig.2.10) . The specimen was centred between the poles of an electromagnet which could rotate in a horizontal plane, in a manner controlled by a d.c. motor. The shaft of the motor also rotated a potentiometer in a linear voltage source, and this provided an output which could be used to indicate the rotation of the magnetic field direction.

To counterbalance the torque on the specimen, a small coil was attached to the other end of the specimen suspension and placed between the poles of a small permanent magnet. A small plane mirror was attached to the suspension system. A collimated light source shone onto the mirror, and the light was reflected onto the edge of a triangular prism at either side of which were two photocells positioned so as to receive equal amounts of the light reflected at the prism. The photocell signals were passed to a d.c. amplifier which controlled the current in the balancing coils and passed a corresponding signal to the X - Y recorder.

When the torque on the specimen rotated the mirror slightly, there was a reduction in the amount of light incident on one of the photocells and an increase of light incident on the other.

The difference between the photocell signals was amplified and passed on to the balancing coil so as to give the coil and the specimen another torque equal to and opposing the torque on the magnetization of the specimen and thereby keeping the specimen fixed, at least to within $\pm 0°.5$. As the electromagnet is rotated, the inputs to the X - Y recorder produce a contin- uous signal which is traced out as a torque curve. The torque curve is produced very rapidly and simply and in such a short time that the tempera- ture can obviously be assumed constant.

Manually operated magnetometers, in which the torque is recorded when the specimen is at various orientations in the magnetic field, and the instrument readjusted after each measurement, suffered from their lack of speed when it came to analysing many specimens.
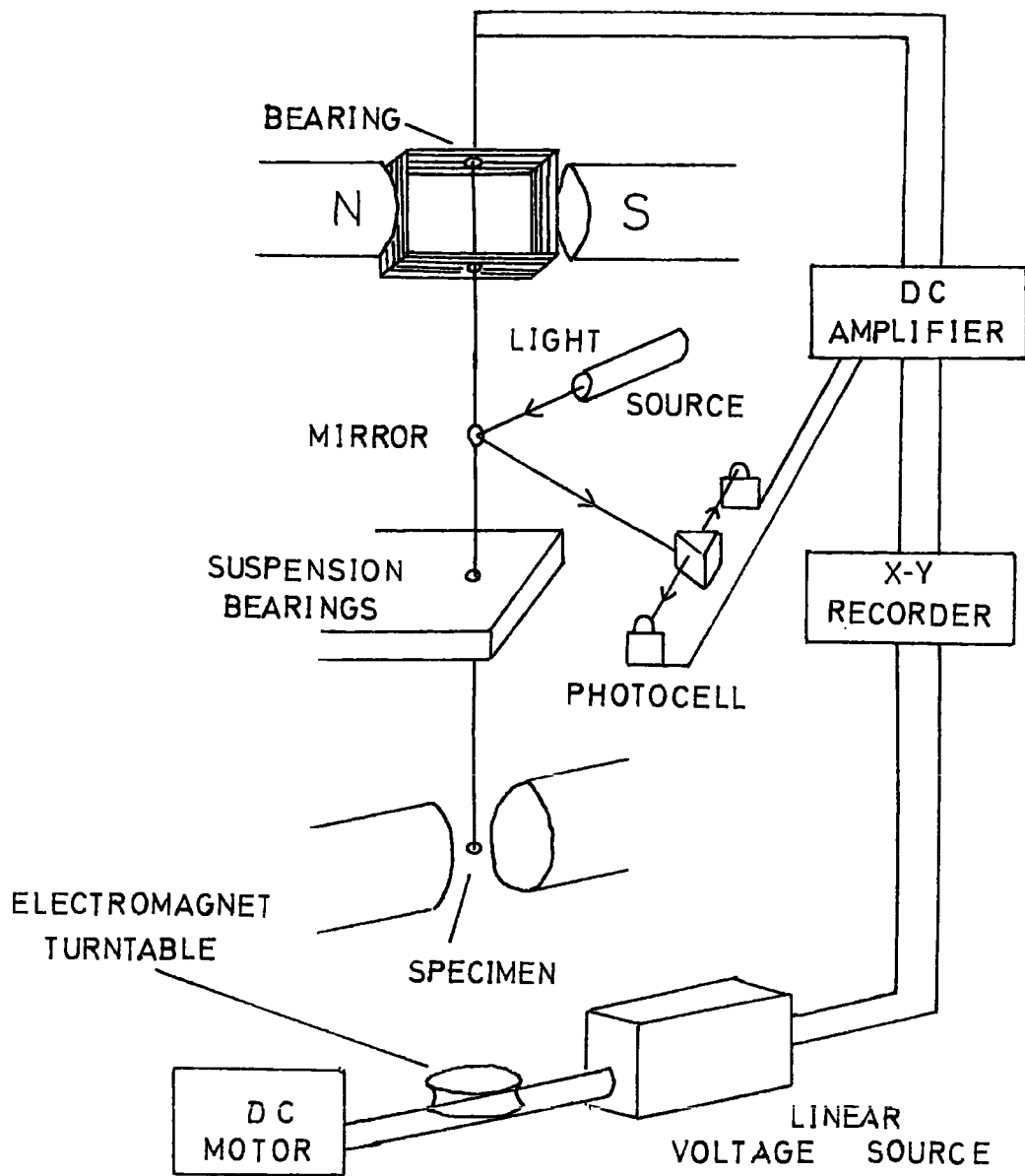
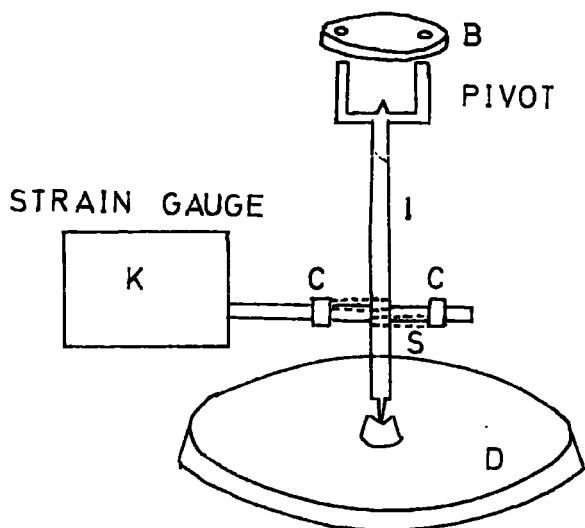Fig.2.20. Penoyer's torque magnetometer, ref.29.

Fig.2.21 The magnetometer of D.S.Miller, ref.36.

Ingerson and Beck (ref.35) designed a continuously recording magnetometer in which the torque curve was displayed on a cathode ray oscilloscope. This was much more efficient in producing results, but still the record of the torque curve had to be indirectly produced by photography.

D.S. Miller (ref. 36) adapted the latter system by recording on an X - Y recorder (actually a modified X - T recorder was used originally). His disc specimens were rigidly held by spring jaws on the holder B (fig.21) . The holder could be inserted onto the two arms of a pivoted shaft I which was held in a frame on a calibrated disc D. An electro-mechanical strain gauge K was also mounted on D, and a thin phosphor-bronze strip S was wound once around the shaft I and tightly fixed by two locking collars C to the shaft of the gauge. The whole structure could be rotated with the specimen in a magnetic field. The torque on the specimen is easily transmitted through the shaft I and phosphor-bronze strip to the gauge shaft. The output terminals of the gauge were connected to the recorder, and the synchronous motor driving the structure also moved the chart paper of the recorder.

This was successful in applications where small torques were involved, butsome error was unavoidable in the measurement of angles because of the small rotation ($\doteq 1^{o}$) permitted by the bronze strip.

Byrnes and Crawford (ref.53) adopted many of Miller's ideas, but they used a torque shaft which was suspended from a lucite platform and required no bearings at the bottom. This enabled them to put the specimen holder at the lower end and surround it with a cryostat so that low temperature work could be undertaken, at least to liquid nitrogen temperature. They used a thin beryllium-copper strip, shaped like a fork with two prongs so that the grip end would fit between the prongs, to connect the shaft to the gauge transducer; this was less likely to slip on the shaft.

A 360° torque curve could be produced in 4 minutes. The machine was rugged and could be manhandled without significantly altering the calibration, so specimens could easily and quickly be attached to the holder and their torque curves rapidly produced.

The magnetometer of Tajima and Chikazumi (ref.37) had no bearings, and the error in the angular position of the specimen was entirely negligible. The specimen holder was at the bottom of a long metal shaft suspended from a cylinder of phosphor-bronze, fig.2.22. The cylinder was hollow, 10 m.m. outer diameter and 1 m.m. thick, and had twelve slits, each 20 m.m. long and 1 m.m. wide. The slits increased the susceptibility of the cylinder to twist, but retained enough rigidity in it to hold the specimen in any field. Two paper strain gauges of the cross-wire type to determine torque, were bonded on opposite sides of the phosphor-bronze cylinder.

In order to measure the large torques involved in work on the heavy rare earth elements, more specialised techniques must be used.

Rhyne and Clark (ref.45) fixed their samples in the centre of a small solenoid and balanced the moment from each in the applied field (fig.2.23)The solenoid was pivoted and as the magnetic field was increased a larger current was required by the solenoid to keep it in the same position. The accuracy with which the solenoid could be kept stationary was the main limiting factor in the experiment, and since this accuracy was equivalent to the difference between the torques of the specimen and solenoid and was a small quantity compared to the torques, the method has a much better sensitivity compared to the direct measurement of torque.

They used their data to find the second anisotropy constants of dysprosium and terbium to an accuracy which they considered to be $\pm$ 25%, very good considering that the elements were not saturated in their hard directions.
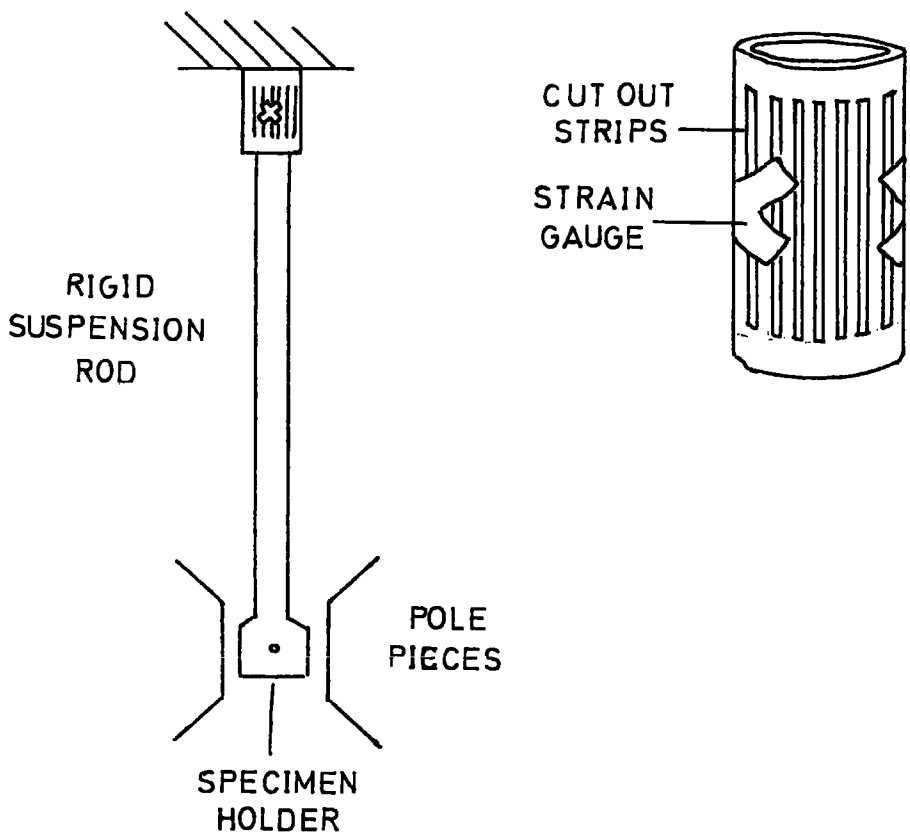
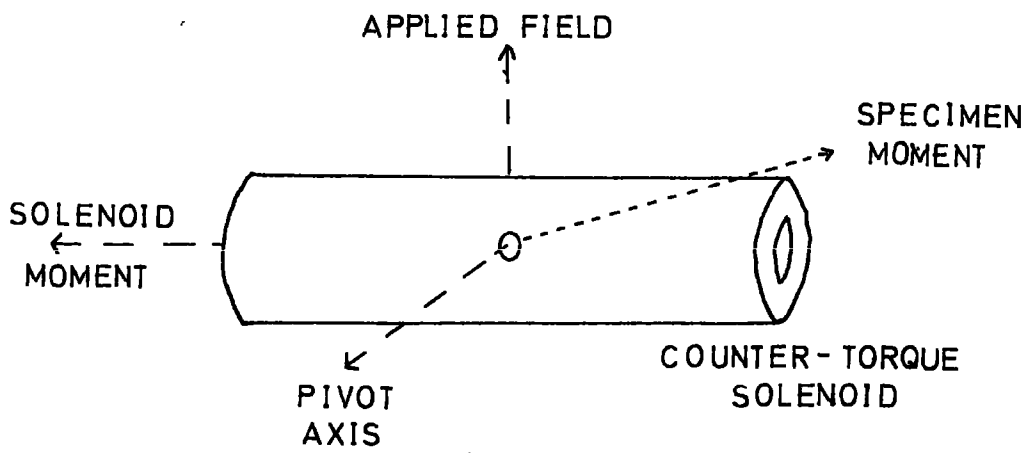Fig.2.22. The apparatus of Tajima and Chikazumi, ref.37.

Fig.2.23. A specimen at the centre of the torsion solenoid of Rhyne
and Clark, ref.45.

The Rotating Sample Magnetometer.

In this device the sample is rotated rapidly in a steady magnetic field. Generally the applied field is made large enough to restrain the total moment of the specimen from deviating by more than a few degrees from the direction of the field H. The moment oscillates up to some angle α to either side of the field direction and produces a small component M_1 of the total magnetization normal to the field.

A pair of solenoids monitor the variation in M_1 and produce a signal which can be interpreted to provide measurements of magnetic moment, hysteresis, magnetocrystalline ansiotropy and anisotropic susceptibility. There appears to be no intrinsic upper limit to the range of moments measureable, but most of the published data relates to work on ferromagnetic thin films.

Ingerson and Beck (ref.71) first designed and built such an instrument, which they used to measure the magnetocrystalline anisotropy of rolled silicon-iron sheet. Their apparatus was basically as shown in fig.2.24, with a motor rotating a disc-shaped sample which was placed at the centre of a small stationary pick-up coil. The signal from the coil was integrated electronically and displayed on an oscilloscope as a torque curve. This was possible because the time base of the oscillⁱscoⁱpe was triggered by, and synchronous with the rotation of the sample.

Because of the low number of components necessary for the experiment, the apparatus is cheap and easily constructed, but it produces only a small signal with a high noise level. Some modifications to the principle were made by Hagedorn (ref.72), who rotated the field about a stationary sample. Unfortunately this imposed severe limits to the magnitude of the field which could be applied so that only small anisotropies could be measured; this was not an important consideration for him as he was interested in thin films, but his methods of noise elimination were used by Gessinger, Kronmuller and Bundschuh (ref.77), and by Flanders (ref.74,75,76).

The principles of Flander s'experiment are outlined in fig.2.25, in block form. The diagram also suggests the simplicity and ease of construction of the apparatus. The sample is rotated by a small synchronous motor at a
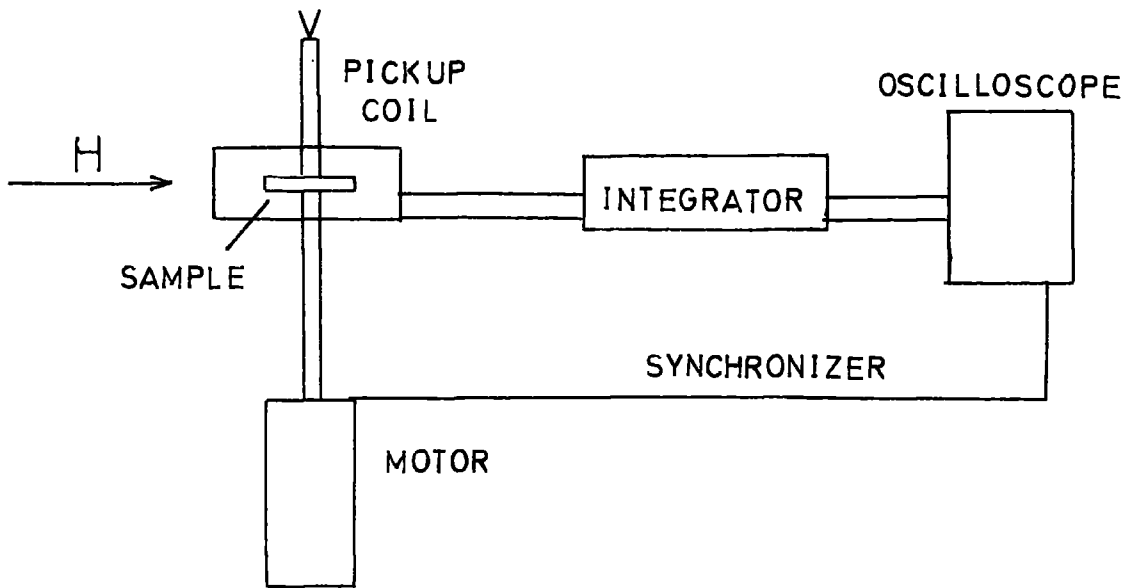
Fig.2.24. The original rotating sample magnetometer of Beck and
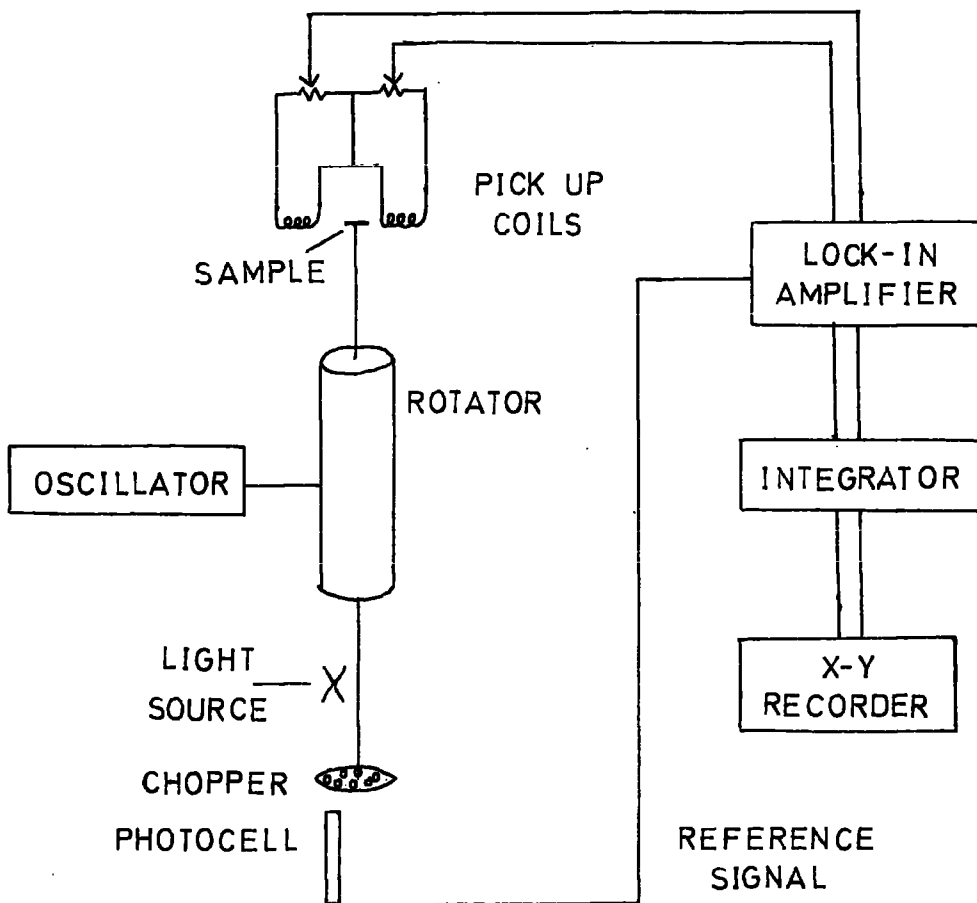
Ingerson, ref.71.

Fig.2.25. A block diagram of a rotating sample magnetometer used to

measure anisotropy (after Flanders, ref.74,75,76).

rate between 30 Hz and 100 Hz, the lower rate being governed by the response of the lock-in amplifier, and the upper rate limited by the bearings and gears of the drive system, as well as by the mechanical lead through necessary with any vacuum system.

Flanders used a light chopper attached to the rotating shaft of the motor, in conjunction with a photocell to give a reference frequency-signal required to modulate the lock-in amplifier. Two similar detection coils connected in series opposition, produced a signal which was proportional to the magnetization of the sample, the angular velocity of the sample and the angle between the magnetization and an easy direction of the sample.

For measurements of magnetocrystalline anisotropy, the rotation axis of the sample is best put perpendicular to the applied field, and the sample should have an axis of symmetry coinciding with the rotation axis. Optimum sensitivity is achieved by having the pick-up coils arranged axially at right angles to the field, so that they generate a signal proportional to $M_\perp$ - the component of magnetization perpendicular to the field. Connecting identical coils in series opposition eliminates (to the first order) noise sources such as spurious sample or coil vibration, or field variation, providing that the coils are symmetric with respect to the field. It is not necessary that the coils be symmetric with respect to the sample, and they may be positioned so that the magnetization signals add, or one coil may be at such a distance that it does not augment the signal of the other significantly.

A lock-in amplifier can generate an alternating reference voltage of various frequencies and amplitudes and the chopper is needed to provide a governor for the reference frequency. The L.I.A. then averages out the noise from the input, and gives an output proportional to the signal created by the magnetization alone.

Because the signal from the pick-up coils depends only on the dimensions and shape of the coils and the configuration of the coils and sample, for a given sample these factors can be represented mathematically by a coupling constant C. Apart from noise, the output from the coils is then a voltage

V such that

$$V = v C \frac{dM_\perp}{dt}$$

depending on the volume v of the sample and the time t. This formula

contains an implicit variation of V with angle ψ between the total magnet-

ization and the easy direction, because

$$\frac{dM_\perp}{dt} = \frac{d\psi}{dt} \frac{dM_\perp}{d\psi} = \omega \frac{dM_\perp}{d\psi} \quad .$$

If the anisotropy of the sample is relatively small for the field used

(i.e. if $H \gg \frac{K}{M_s}$ where K is the principal anisotropy constant and $\frac{K}{M_s}$ is

approximately the anisotropy field) then the angle α between M_s and the field

will always be small. Consequently ω may be regarded as being constant so

that

$$V(\psi) = - \frac{v C \omega}{H} \frac{d^2 f_K}{d\psi^2}$$

defines a direct proportionality between the induced voltage and the rate of

change of torque, the torque being

$$H M_\perp = - \frac{d f_K}{d\psi} \quad .$$

Hence the signal from the pickup coils, detected and aplifiedᵐ by the L.I.A.,

can be integrated to produce a signal directly proportional to the torque.

When the output signal is not integrated it may be expressed (ref.76) as

a power series in $\left(\frac{K}{M_s H}\right)$, each term being multiplied by Fourier components

$(\cos n\omega t)$. For uniaxial anisotropy the first three terms are shown in

$$V = -v C \omega M_s \left[2\left(\frac{K}{M_s H}\right) \cos 2\omega t - 4\left(\frac{K}{M_s H}\right)^2 \cos 4\omega t + 9\left(\frac{K}{M_s H}\right)^3 \cos 6\omega t \right] .$$

Each component may be separately identified and measured by the L.I.A.,and

the ratio of the magnitudes of any two terms will determine K.

Cubic and hexagonal anisotropies naturally require a more cumbersome

analysis but in principle may be determined by this method. The ability of

the L.I.A. to separate signals of any frequency, enables it to measure other

anisotropic influences such as variation of saturation magnetization with

angle, field induced anisotropy and strain induced anisotropy. Providing

some mathematical analysis predicts all the anisotropic components, it is

in principle possible for the L.I.A. to separate a sufficient number of terms

to form a non-degenerate set of simultaneous equations. This applies even to

cases in which $H \ngtr H_K$ but a satisfactory general analysis for this case

has not yet been published.

CHAPTER 3.

The Need for a New Magnetometer.

The Gadolinium - Terbium Alloy System.

The project for which the magnetometer was required involved the investigation of the anisotropy constants of the gadolinium - terbium binary alloy system. Properties of several rare earth - rare earth binary systems have been examined previously (e.g. ref.84,85,86) but experiments on this particular system have been curiously lacking, apart from the efforts of Tajima and Chikazumi (ref.37,78) to determine the anisotropy constants of terbium by alloying a very small quantity of terbium (about 1% by weight) with gadolinium; they allowed for the effect of pure gadolinium on their torque curves, and assumed that the results were indicative of the magneto-crystalline anisotropy of pure terbium.

Perhaps people have been put off by the differing easy magnetic direction of gadolinium and terbium, and their different directional behaviour which may make results awkward to interpret, or the systematic variation of magnetic properties with increasing atomic number may have led people to feel that there would be no unusual features in the system, and that no profound advance of understanding could be gained from examining it. However, since the atomic and ionic dimensions of gadolinium and terbium are so similar (3+ ionic radius ratio = 1.016 ; 4 f electron radius ratio = 1.021 ; $'\frac{c}{a}'$ value ratio = 1.006 ; 'a' spacing ratio = 1.008) it should be possible to observe precisely the change in properties effected by the gradual alteration in mean sphericity of the ionic ground state from gadolinium (^8S) to terbium (^7F) .

This systematic change in magnetic properties is most radical near the middle of the series, and gadolinium is the first to have a ferromagnetic phase. Its Curie temperature is 293 K (ref.79) and it has no antiferromag-netic phase. (Doubts exist over the interpretation of results by Salamon and Simons (ref.80) who found a small 'a' axis resistivity anomaly, and a small step change in specific heat at 226 K indicating a phase change . Similarly, the work of Belov, Levitin, Nikitin and Ped'Ko (ref.87,88) is now disregarded.

In very low fields (about 1.5 Oe or less) they found small peaks in the specific magnetization - temperature curve at 210 K. Small anomalies in the coercive force and the remanence were also found by these people, but were not observed elsewhere.)

Terbium occurs next in the series, and it has an antiferromagnetic phase between T_N = 229 K and T_C = 221 K, and is ferromagnetic below this temperature.

Heavier rare earths have systematically lower Curie T_C and N éel T_N temperatures, T_C being nearly proportional to the de Gennes factor G $(G = (g - 1)^2 J (J + 1)$, where g is Landé's 'g'factor' of the total angular momentum vector J of the metallic ion) and T_N is proportional to $G^{\frac{2}{3}}$.

Features Required of the Magnetometer.

(i)   The magnetometer should be adaptable for use with both an electro-magnet and a solenoid magnet.

Durham University Solid State Laboratory possesses a large electro-magnet which may give fields of up to 3 T when its conical pole pieces are attached. This is too small to make much progress into the terbium end of the Gd - Tb system, since Tb has not yet been saturated in a hard direction although magnetized at 15 T, and it was anticipated that work could be carried out at the high field facility at R.R.E., Malvern.

(ii)   Consequent to the latter point, the magnetometer must be compact, rugged, and rigid.

(iii)   Alterations to the calibration should not occur through frequent demounting.

(iv)   Accuracy and reproduceability were demanded for measuring anisotropy constants in the range 10^6 erg cm^{-3} to 5 x 10^8 erg cm^{-3} e.g. for a torsion system this would imply that torques in the range 10^4 dyn-cm to 5 x 10^5 dyn-cm could be measured with precision.

The Elimination of other Designs.

(i)   Normal ballistic magnetization experiments are slow and cumbersome, and open to much numerical error in the final result, because of hysteresis

effects. Further, these devices generally lack the compactness and high rigidity necessary for work involving solenoids having axial access and encumbranced with a double dewar system.

(ii) Vibrating coil and vibrating sample magnetometers are basically built around a particular magnet, and are insufficiently adaptable, although accurate and reliable at high fields and low temperatures. They need calibrating each time they are reconstructed because their output is susceptible to small changes in the configuration of the surroundings.

(iii) Resonance experiment and inelastic neutron scattering require much more specialised detection techniques and are expensive to set up from scratch.

Neutron diffraction would not be continuously available, transport would be a problem, and results can only be interpreted in the light of a very extensive analysis.

(iv) Rotating Sample Magnetometers are extremely promising and are under considerable development effort in other laboratories because of the wide variety of information which can be easily extracted from them once an experiment is under way. However, the large anisotropies anticipated for the Gd-Tb system suggest that the magnetization vector of the rotating specimen would not stay close to the field direction with the fields presently available. This factor would introduce many extra frequency terms into equation 2.5, and a suitable mathematical analysis to delineate each effect, appears daunting at present.

(v) Torque magnetometers are the type most universally used for determination of magnetocrystalline anisotropy, producing the anisotropy constants most directly, but the usual torsion fibre techniques seemed inadequate :

(a) the torsion fibre suspension may become unstable at high fields unless the sensitivity is reduced. Harrison (ref.81) has shown that, for instance, for a cubic structure crystal of volume v suspended by a fibre of torsion constant K, the sensitivity is limited by the condition that $k > 2K_1 v$ if a complete torque curve is to be measured. (K_1 is the first anisotropy constant and the (100) plane of the crystal is parallel to the field direction).

(b) automatically balancing torque systems (29,45,82,83) take much
     time to set up, and are cumbersome to operate (especially if an
     electromagnet has to be rotated).

(c) torsion suspension systems are incompatible with solenoids having
     axial access only, because the field must be applied perpendicular
     to the suspension.

Consequently an original design of torque magnetometer was embarked
upon.

CHAPTER 4

The Magnetometer.

Principle.

The design of the magnetometer is based on the wheel, fig.4.1 . The specimen is to be attached to the axle of the wheel. In a magnetic field the torque on the specimen acts on the axle, and attempts to rotate the wheel. The rim is fixed, and the torque results in a slight distortion of the spokes. The spokes are rectangular and have strain gauges attached longitudinally, and these measure the bending of the spokes and produce a signal proportional to the torque.

Design.

Fig. 4.2 represents a mechanical beam of length l, width w, thickness t, which is rigidly fixed to a wall (equivalent to the rim of the wheel). The beam suffers a strain when a force F (the force exerted through the axle) is applied normally to its free end. A strain gauge is shown in outline, attached to the beam (spoke) with its centre a distance b from the free end of the beam.

According to Timoshenko (ref.1) the strain at b is

$$\varepsilon_b = \frac{6Fb}{Ewt^2} \qquad \text{Equation 4.1}$$

and the deflection at the free end is

$$y = \frac{6Fl^3}{Ewt^3} \qquad \text{Equation 4.2}$$

where E is Young's modulus for the beam.

To make the magnetometer symmetric and rigid, it was built with four spokes. The axle had radius a so that a torque T on the axle exerts a force P on the end of the spokes where

$$T = 4Pa \qquad \text{Equation 4.3}$$

so

$$P = \frac{T}{4a} \quad .$$

The volume of a typical disc specimen is $\doteq 10^{-2}$ cm^3 so the maximum torque will be $\doteq 10^7$ erg for the heavy rare earths, and the maximum force on each spoke $\doteq 10^7$ dyne. For the proposed dimensions of the spokes, l = 6 m.m. W = 5 m.m. t = 2 m.m. equation 4.2 gives y = 4 x 10^{-1} m.m. (E $\doteq$ 5 x 10^{10} dyn cm^{-2} for the material chosen), and the maximum angle through which the axle

Fig.4.1. A vertical view of the magnetometer showing the position of the strain gauges on the sides of the spokes.
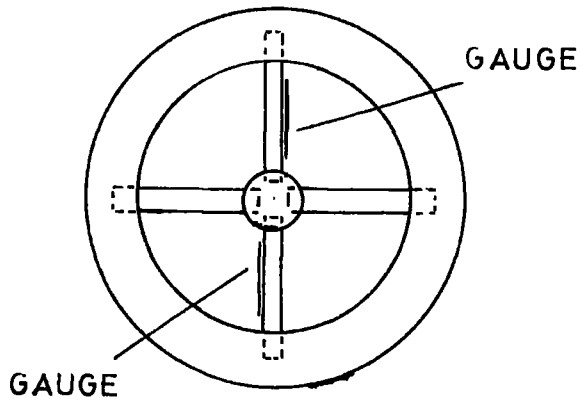

Fig.4.2 The dimensions of a beam fixed rigidly to a wall and showing the outline of a strain gauge attached to the upper surface.
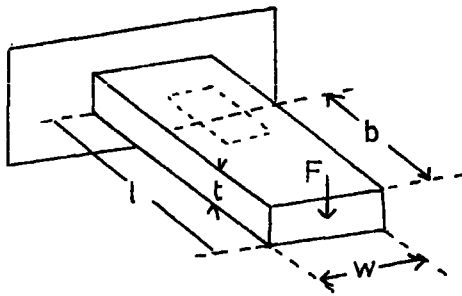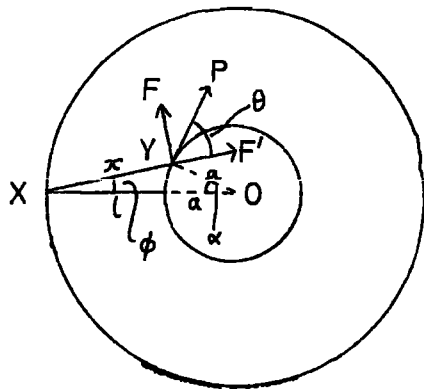

Fig.4.3. The components of force on the spoke X Y which has been rotated by ϕ from its unstrained position X Z while the axle has rotated α rad.

would turn is $\propto = 10^{-1}$ rad.

The force P on each spoke has a component F perpendicular to the spoke X Y (see fig 4.3), and a component F' parallel to the spoke. The angles are sufficiently small to regard the spoke as having rotated rigidly by $\emptyset$ from its unstrained position X Z . P is at angle Θ to X Y and

$$\sin \Theta \doteq \cos \doteq 1$$
$$\cos \Theta \doteq \sin \doteq 0$$

so $\qquad$ F = P and F' = 0 .

The strain gauges of the magnetometer, form an arm of the usual Wheatstone Bridge arrangement, which is used to determine the resistance changes in the gauges. Between the limits imposed by the sensitivity of the bridge and the maximum strain acceptable to the gauges, a digital voltmeter or X - Y recorder across the bridge can measure strain from 10^{-2} to 10^{-5} . This is equivalent to torques of 5×10^{3} erg to 5×10^{6} erg and in specimens of volumes ranging from $10^{-1} cm^{3}$ to $10^{-3} cm^{3}$ it would be possible to measure anisotropy constants of 5×10^{4} erg cm^{-3} to 10^{9} erg cm^{-3}.

Construction.

The magnetometer was cut from strips of a special plastic, 'Nylon 6', prepared by Mr.L.J.Maisey, of the Rubber and Plastics Research Association (R.A.P.R.A.). The use of metals in the construction of the spokes, was eliminated because their high Young's Modulus (10^{2} x higher than for plastics) would have necessitated a proportional reduction in the size of the spokes to obtain the same strain range. The brittleness of metals at low temperatures would have made such use dubious, and the accurate cutting of the spokes and axle to such dimensions would be very difficult.

Unfortunately, most plastics become extremely brittle (more so than metals) at low temperatures, and recycling distorts them and alters their mechanical properties radically. However, the Nylon 6 developed by R.A.P.R.A. seems to be free of these difficulties. The only doubt was that the expansion coefficient, characteristically very high in plastics, might be too great for the strain gauges to bear comfortably. The behaviour

was tested by measuring the expansion coefficient of the plastic by a strain gauge method as described in the appendix. Nylon 6 does not approach Teflon in the extravagance of its expansion, and the gauges behaved consistently well throughout a number of experimental runs.

The rim, the spokes and the axle were cut separately from a 5 m.m. thick strip. It would have been more satisfactory to mould them, or cut them as a single piece, but that would have made it impossible to apply the pressure to bond the gauges correctly.

The spokes were cut and filed into rectangular blocks 9 m.m. x 5 m.m. x 2 m.m. cleaned thoroughly with a degreaser and dried. A thin layer of Micro Measurements M-Bond 610 adhesive was applied to the spokes and gauges. The gauge was placed carefully parallel to the long side of the spoke, covered with Mylar (which does not adhere to M-Bond 610), clamped at about 25 lb in^{-2} and cured for 2 hours at 150° C. The gauges were Micro Measurements type WK -15-031 CF-350; 350Ω wire resistance gauges made from a Karma alloy of very low magnetoresistance, and having a self temperature compensation of 31 p.p.m.

After curing, the gauges were cooled slowly, coated with a protective layer of 610 adhesive, and cured again.

The slots in the disc which was to form the rim, the ends of the spokes and the slots in the axle, were degreased, cleaned, dried and coated with a thin layer of Araldite A Y 105 mixed with YF 953 hardener, they were placed together in a small jig which gave rigidity to the structure while it was heated in an oven for 1½ hours at 120° C.

The specimen holder, a small cylinder of Nylon 6, 2 m.m. radius and 5 m.m. long, was attached by 8 B A brass screw, and cemented with Araldite Y F 105 to the lower side of the axle. A short aluminium rod, 80 m.m. long and 10 m.m. diameter, was bonded with M-Bond 610 to the centre of a 15 m.m. wide section of Nylon 6 cut from a 25 m.m. diameter disc, and was cured for 2 hours at 150° under 50 lbs in^{-2}. This was to support the magnetometer, and two 5 m.m. thick segments of Nylon 6 were placed as spacers between the support and the magnetometer. On the base of the support, two pieces of

plastic, identical to the spokes and mounted similarly with strain gauges, were bonded with Araldite. They were placed so as to be parallel to the spokes with gauges, so that the dummy gauges being connected to the second arm of the bridge circuit, would balance out effects of thermal expansion, magnetoresistance and lead-wire connections.

To facilitate electrical connections, two small strips of Vero board were glued to opposite sides of the aluminium rod and close to the bottom. The 4 - leads from each gauge, were soldered to the Vero board, and once constructed, no part of the magnetometer need be disturbed.

The support rod could be inserted into a stainless steel tube of length appropriate to magnet and cryostat dimensions, and the other end of the steel tube was attached to an Edwards Rotary Vacuum shaft. Two aluminium discs were slotted over the tube. Their diameter was slightly less than the glass cryostat into which the system was to be fitted, and they provided the extra rigidity to the steel tube which was necessary to keep the magnetometer in a fixed position in the magnetic field.

The rotary shaft was sealed into the top of the brass cryostat head (fig. 4.5) and had a linear helipot inverted over it. A small emf was put across the helipot, and the output from the helipot tap, being proportional to the rotation of the shaft, would give a signal depending on the angle through which the magnetometer was turned. The helipot casing was rigidly attached to the cryostat head.
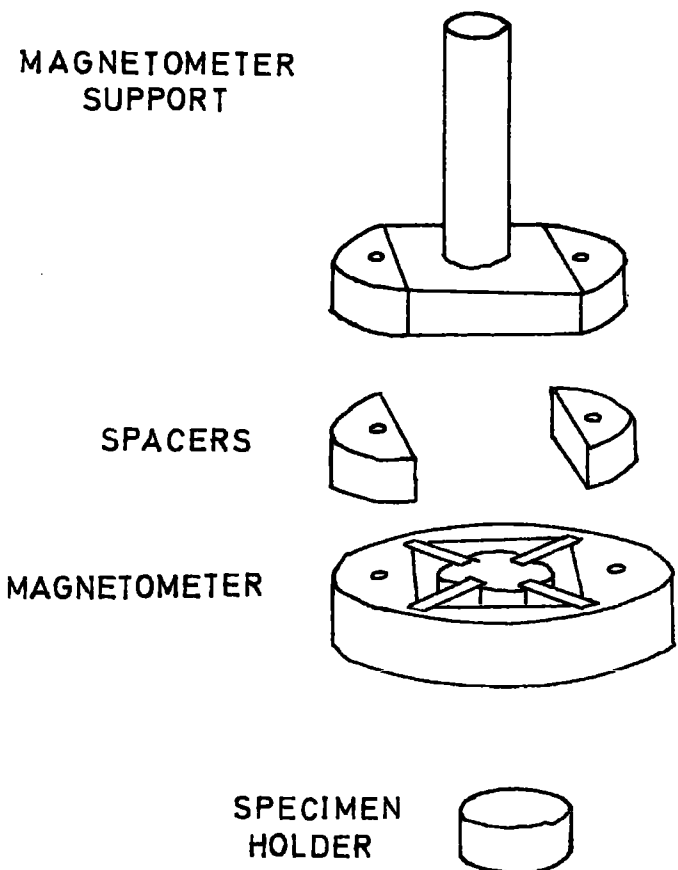
MAGNETOMETER
SUPPORT

SPACERS

MAGNETOMETER

SPECIMEN
HOLDER

FIG 4.4   THE CONSTRUCTION OF THE MAGNETOMETER.

HELIPOT

ROTARY SHAFT
VACUUM SEAL

ELECTRICAL
LEAD THROUGH
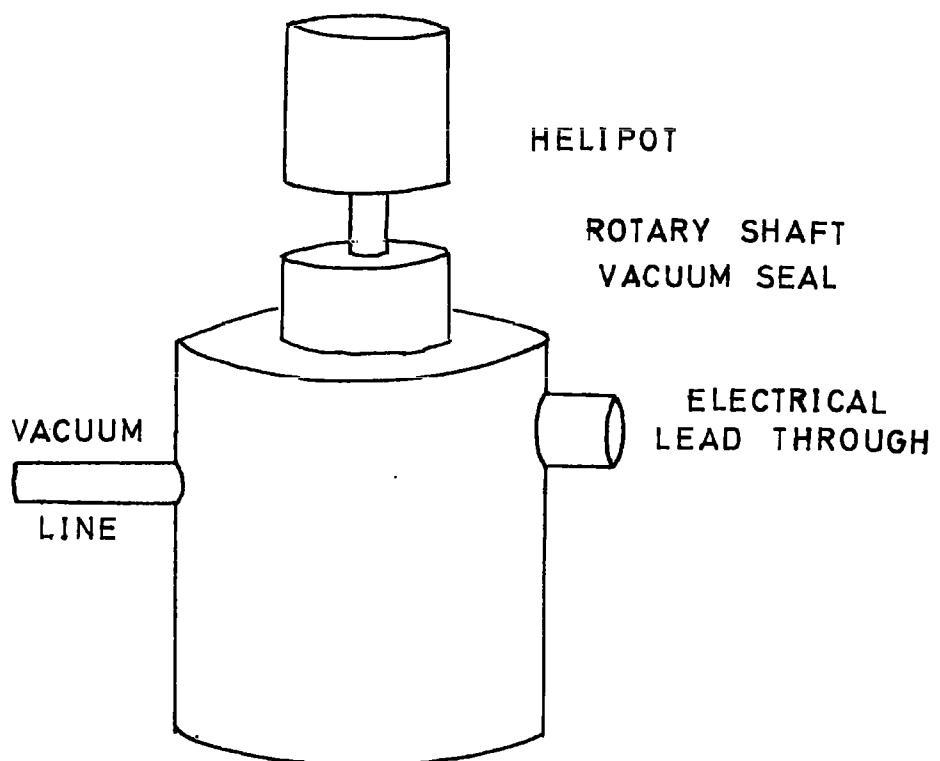
VACUUM

LINE

FIG. 4.5   THE HEAD OF THE MAGNETOMETER.

Calibration of the Magnetometer.

For the magnetometer to provide a satisfactory measurement of torque, three characteristics must be observed in it:

(i)   the output of the bridge must vary linearly with the torque imposed;

(ii)   after the initial calibration, all results should be accurately reproduceable;

(iii) for a given torque, the output of the bridge must be calibrated for the various temperatures at which measurements are anticipated to be required.

(i) Calibration of Linearity.

Calculations with the formulae introduced earlier in this chapter showed that the measured torque could be expecfed to be linear with produced torque for values ranging up to somewhat more than one hundred times the greatest torque contemplated in actual experiments. (This means that a graph of produced torque against measured torque should be a straight line). The limits were imposed by the deviation from linearity in bridge output with respect to small changes in arm resistance after the bridge became unbalanced by a certain amount, and by the bending of the magnetometer's spokes becoming non linear with respect to applied force after a certain level of strain is introduced. It will be seen that these expectations were slightly confounded by experience although later experiments show how these difficulties may be overcome.

The linearity of the magnetometer was calibrated using a small solenoid consisting of 230 turns of 26 SWG wire. This could carry a current which was great enough to produce a torque ten times that expected from crystals. The test solenoid was rotated until it was perpendicular to the applied field. When a current of I amp passed through the solenoid, a field of H tesla put a torque

$$L = 1.074 \ H \ I \ \times \ 10^{-2} \ N \ m$$

onto the solenoid (a figure deduced from the mean area-turns of the solenoid). If H is in oersted then

$$L = 10.74 \ H \ I \ \text{dyn cm} \ . \qquad \text{Equation 4.4}$$

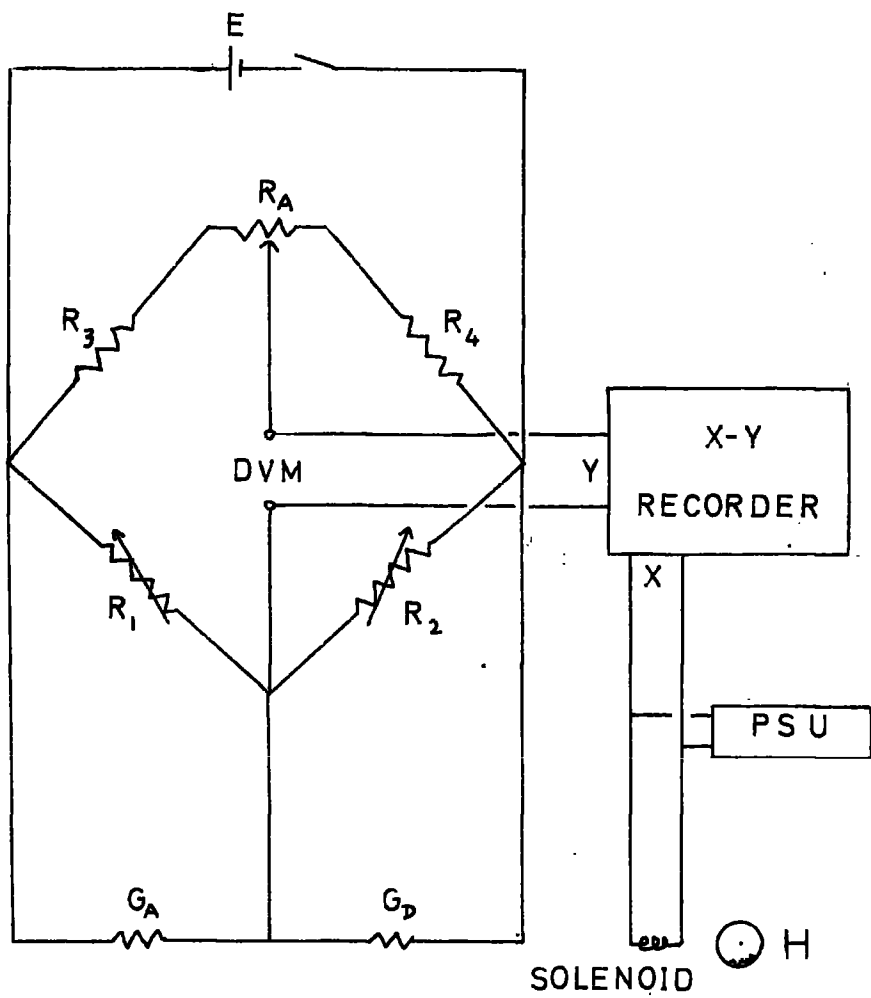Fig.4.6 shows the circuit diagram of the experiment. A voltage of a little

Fig.4.6. A circuit - and block - diagram showing the apparatus used to calibrate the magnetometer.

over 1.2Vwas supplied by a power supply unit E to excite the bridge consist-
ing of the active and dummy strain gauges G_A and G_D. Two 100 k Ω helipots
R_1 and R_2 shunt G_A and G_D and the other arms of the bridge are completed by
two fixed resistances R_3 and R_4 whose values are close to the nominal 350 Ω
of the strain gauges, and a small resistance R_A is used as a potentiometer
to balance any differences between R_3 and R_4 or between R_1 and R_2 . A digital
voltmeter DVM determined the balance point of the bridge to better than
$\pm$ 0.5μV. The helipots were not necessary for this experiment, but provided
the delicate adjustment necessary to find the null point of the bridge; two
were used to make the wiring identical in each half of the bridge.

Besides being monitored by the digital voltmeter, the output of the
bridge was passed to an X - Y recorder. The X terminals of the recorder
were connected to the output of the power supply unit PSU which supplied the
current to the torque producing solenoid. This solenoid was glued to the
crystal holder of the magnetometer. A given field was applied to the solenoid
and the current through it was gradually increased from zero. The increasing
moment of the coil produced an increasing torque which correspondingly unbal-
anced the Wheatstone bridge by an amount described by the Y movement of the
chart recorder whose Y sensitivity was set at 0.05 mV per cm. X movement of
the recorder depends on the voltage applied to the solenoid, and by Ohm's law
and equation 4.4 this should be proportional to the produced moment. With a
maximum solenoid current of two amps, the original results for various fields
are shown in fig.4.7. Each graph took about 20 secs. to form.

    (a)   Noise on the curve appeared to be due entirely to the amplifier
            or servo-system of the X - Y recorder and has not been included
            in the figure. The gain of the Y amplifier was set at its highest
            value and gave a Y sensitivity of 0.05mV cm^{-1} . Although it is
            probably five times more sensitive, the DVM gave no such indication
            of noise, which appeared as an intermittent vibration of the recorder
            pen in the Y direction. The sampling rate of the DVM was set at
            10 Hz and the response time could easily have coped with the noise
            indicated on the X - Y recorder, the rate of this being about 2 Hz
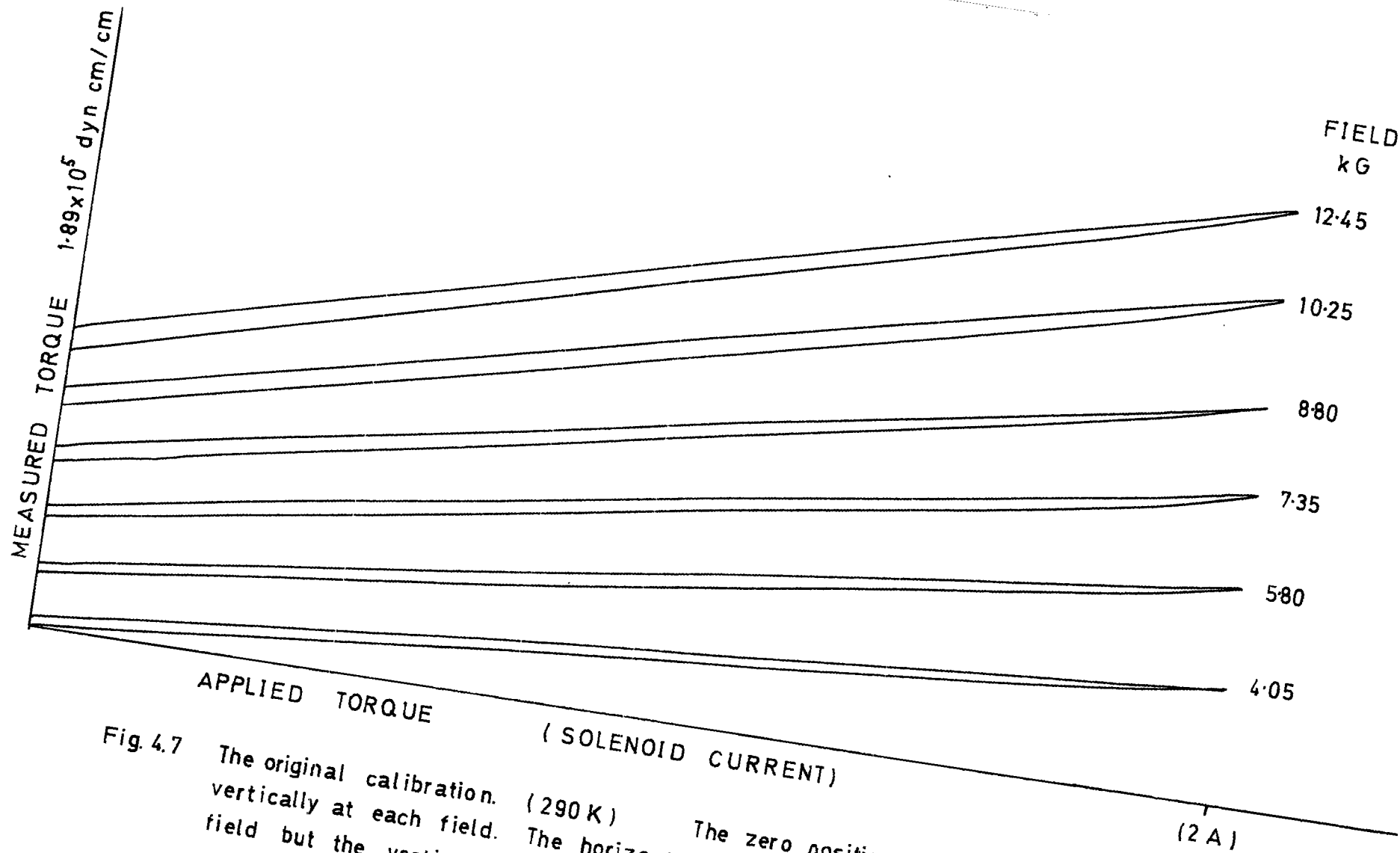   and the amplitude 15 μV.

Fig. 4.7   The original calibration. (290 K)   The zero position is shifted vertically at each field. The horizontal scale depends on the field but the vertical scale is constant.

(b) Hysteresis is considerable, being about 9% of the maximum torque in each case.

(c) There is a slight departure from linearity especially on the lower (increasing current) part of the curve. Here, it is about 0.6% over the full length of the curve in the largest fields. Plainly most of this departure occurs at the extreme right hand side of the lines and later it was discovered that some of this effect was due to the solenoid voltage being taken higher than the recorder servomechanism could cope with, but the strain on the servomechanism was not noticed at first.

(d) Deviations from linearity of the decreasing current part of the curve are too small to be measured over the lower 70% of the curve. Hence, the initial objective was to eliminate all hysteresis. By experience it was found that the amount of hysteresis depended on the time rate of change of torque, and it was possible to reduce the hysteresis by increasing and decreasing the torque very slowly. Fig.4.8 shows how effective this was.

In this instance the rise to maximum torque took about two minutes for each field. Except at the highest fields (and torques) hysteresis is now negligible, and the non-linearity has decreased to 0.5% of the full torque line. Finally a torque line was produced in which the maximum torque was 5×10^4 dyn cm. Hysteresis was entirely negligible (up to fields of 1 T) and non-linearity was too small to be determined even when the full curve was produced in less than 10 seconds. Thus it became clear that the magnetometer would work very satisfactorily if the torques were kept below 10^4 dyn cm. However for this to be effective the signal to the X - Y recorder must be pre-amplified in order that the pen produce a reasonable deflection. It seems that this will be feasible without introducing too much noise and further investigations are now under way.
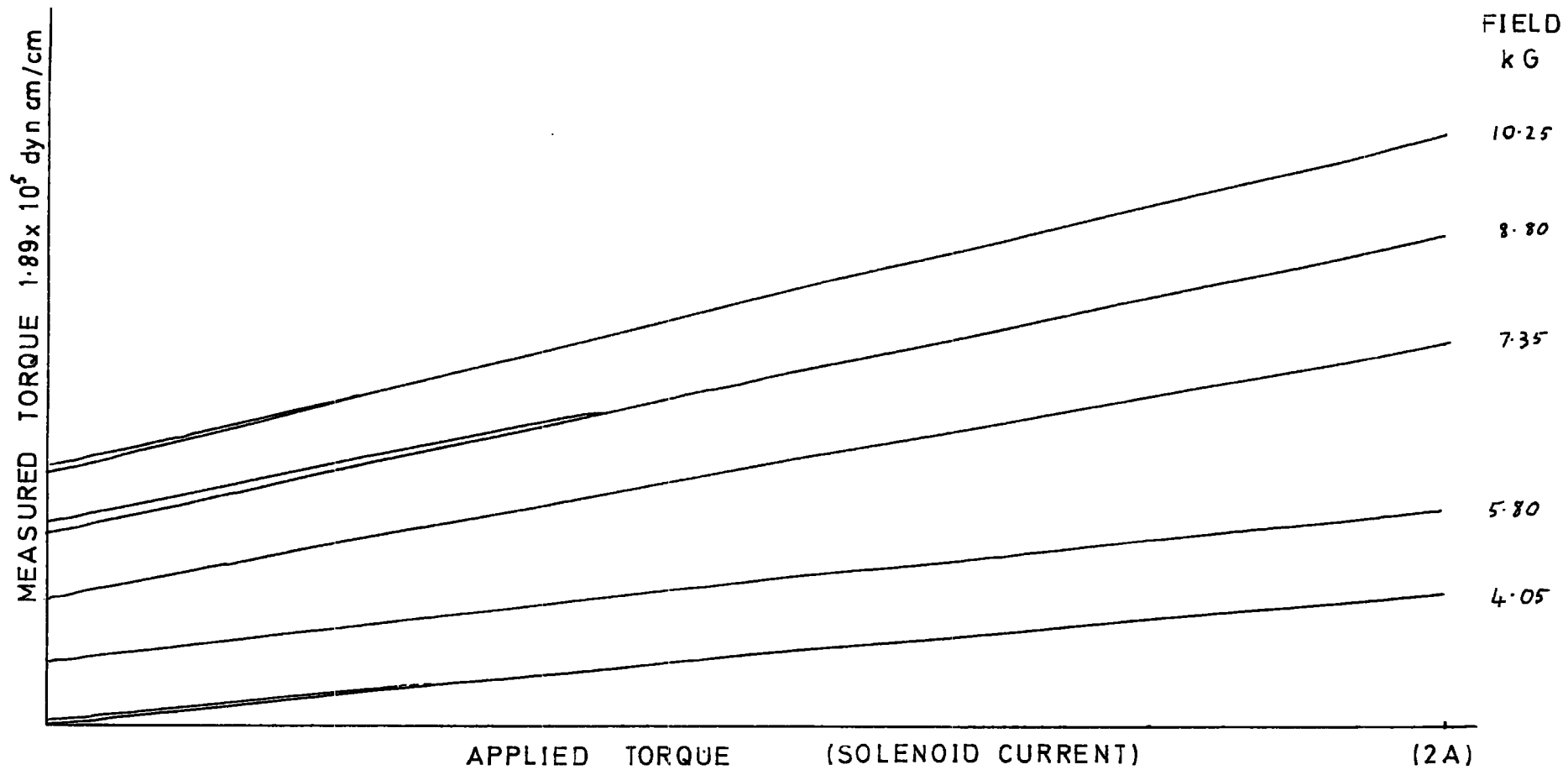
Fig.4.8. Torque lines for a much slower rate of torque increase, again at room temperature.

(ii) Reproduceability.

Initially the reproduceability was no better than to within 5% ,
but the later results from the low magnitude torque lines seem to give
results agreeing to better than 1% at all temperatures and torques.

(iii) Temperature Calibration.

A given torque will produce a signal which varies with temperature
because of the following effects.

(a) Principally, the variation of Young's modulus of Nylon 6, which
affects the results as a reciprocal in equation 4.1 . Judging by
the results obtained mechanically and by ultrasonics for similar
plastics and nylon, the Young's modulus of Nylon 6 could be expected
to increase by upwards of 100% as the temperature decreases from
290 K to 4 K. (Some efforts were made to determine the elastic
constants through ultrasonic means but reflections were too weak
with the transducers which were available). Thus the response to a
given torque may be halved between these temperatures.

(b) A relatively minor variation in the gauge factor k of the strain
gauges. The alteration ΔR of gauge resistance R is proportional
to the strain ε imposed according to the relation
$$\frac{\Delta R}{R} = k\varepsilon .$$
k is practically constant over a fifty degree Kelvin temperature
range around 290K, but between 4K and 300K its value reduces by
4% according to the manufacturer's specifications, and a strain
will produce a slightly different bridge output e according to
$$e = \frac{G_A G_D E k\varepsilon}{(G_A + G_D)^2} , \qquad \text{Equation 4.5}$$
where G_A and G_D are the active and dummy gauge resistances respect-
ively, and E is the input voltage of the Wheatstone bridge.

(c) A very small effect is caused by the linear contraction of the
spokes, amounting to < 2% over a 300 degree Kelvin temperature
range. According to equation 4.5 this should produce a change in
strain output of a similar magnitude, but it is effectively counter-
balanced by the dummy gauge, which, being bonded to similar but

unstrained material, suffers a similar thermal contraction.

(d)   An alteration in the null point of the bridge amounting to $300\,\mu V$

was observed in cooling from 290 K to 80 K.   This appeared to be

due to resistance effects on the soldered electrical connections,

but whatever its cause, the amount seems to be too small to alter

the response characteristics of the bridge.   The effect could

easily be allowed for without disturbing the bridge resistance by

altering the zero setting of the X - Y recorder.   ($300\,\mu V$ is

equivalent to altering the resistance of one arm of the bridge by

$0.05\,\Omega$, or 0.01% .)

For the process of calibration at various temperatures, the proceedure

was adopted as in section (i) .   Some results are displayed in figures 4.9,

4.10, 4.11, 4.12, and 4.13.   Generally the linearity of the lines improves

greatly with decreasing temperatures, and deviations from linearity are too

small to determine below 200 K, but there is a certain amount of hysteresis

which it was impossible to eliminate.   The graph of results taken at 125 K

shows how the hysteresis increased with rate of increase of torque.   Similar

graphs were taken at the other temperatures but are not included here, because

the results were similar and non quantifiable.   The calibration deduced from

each graph is shown at the top of the graph and they are collected in table

4.1 , which shows the amount of torque required to produce a $50\,\mu V$ shift in

the null point of the bridge at a given temperature.

A graph of the calibration is shown in fig. 4.14.   From what was said

earlier, this graph should follow very closely the graph of Young's modulus

E_6 for Nylon 6, and it is hoped to obtain measurements by ultrasonic testing

which will enable us to verify this shortly.   As a rough comparison fig. 4.14

indicates that E_6 increases 2.1 times between 290 K and 77 K whereas McClintock

and Kropschot (ref.89) found a corresponding figure of 2.6 times for 'Nylon'

(and 12.3 times for 'Teflon').

Fig. 4.15 is the calibration of measured torque against applied torque at

80 K.   The upper section is for calibration lines with the solenoid current

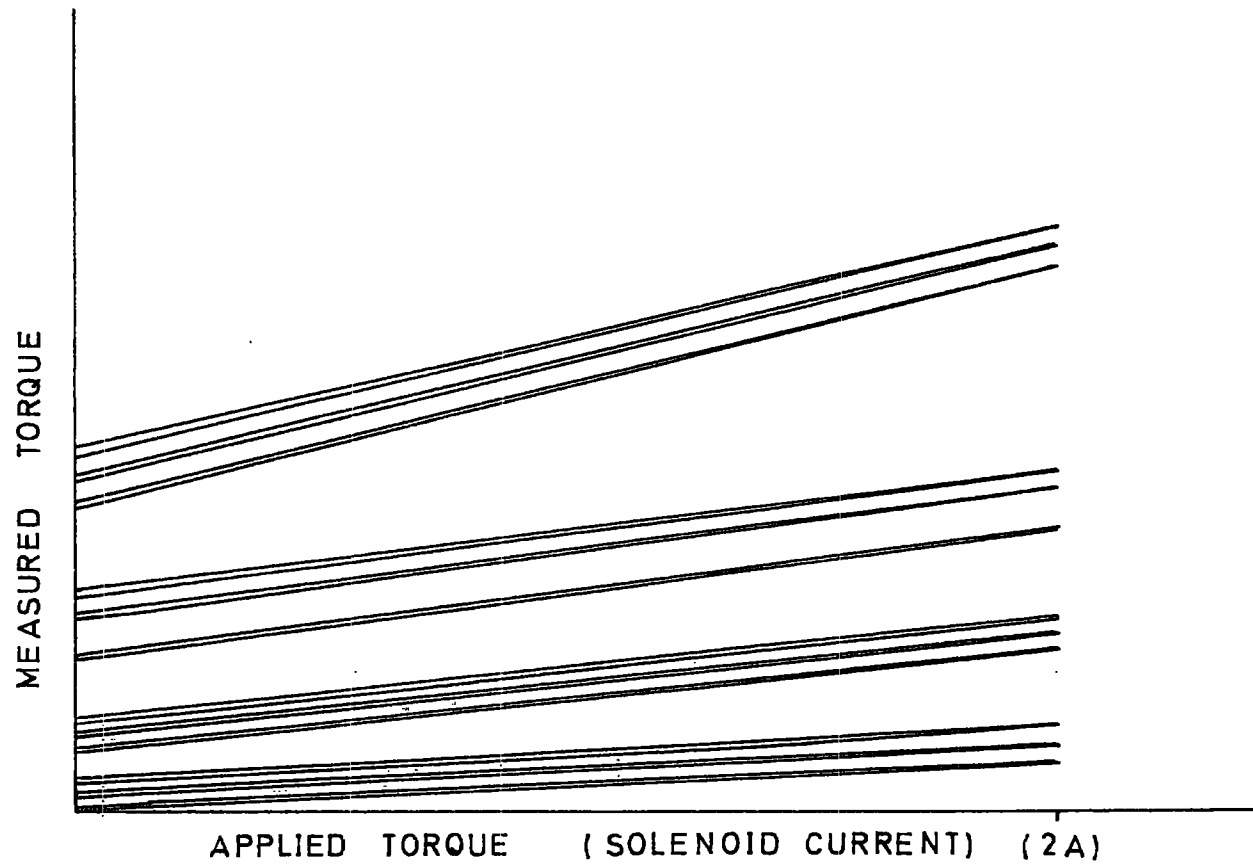reversed.   This means that the torque is in the reverse direction, and the

Fig.4.9. Graph of applied torque plotted against measured torque at 125 K. For each field three graphs are shown; the lower one produced in 4 minutes, the middle one in 40 seconds, and the upper one in 5 seconds.
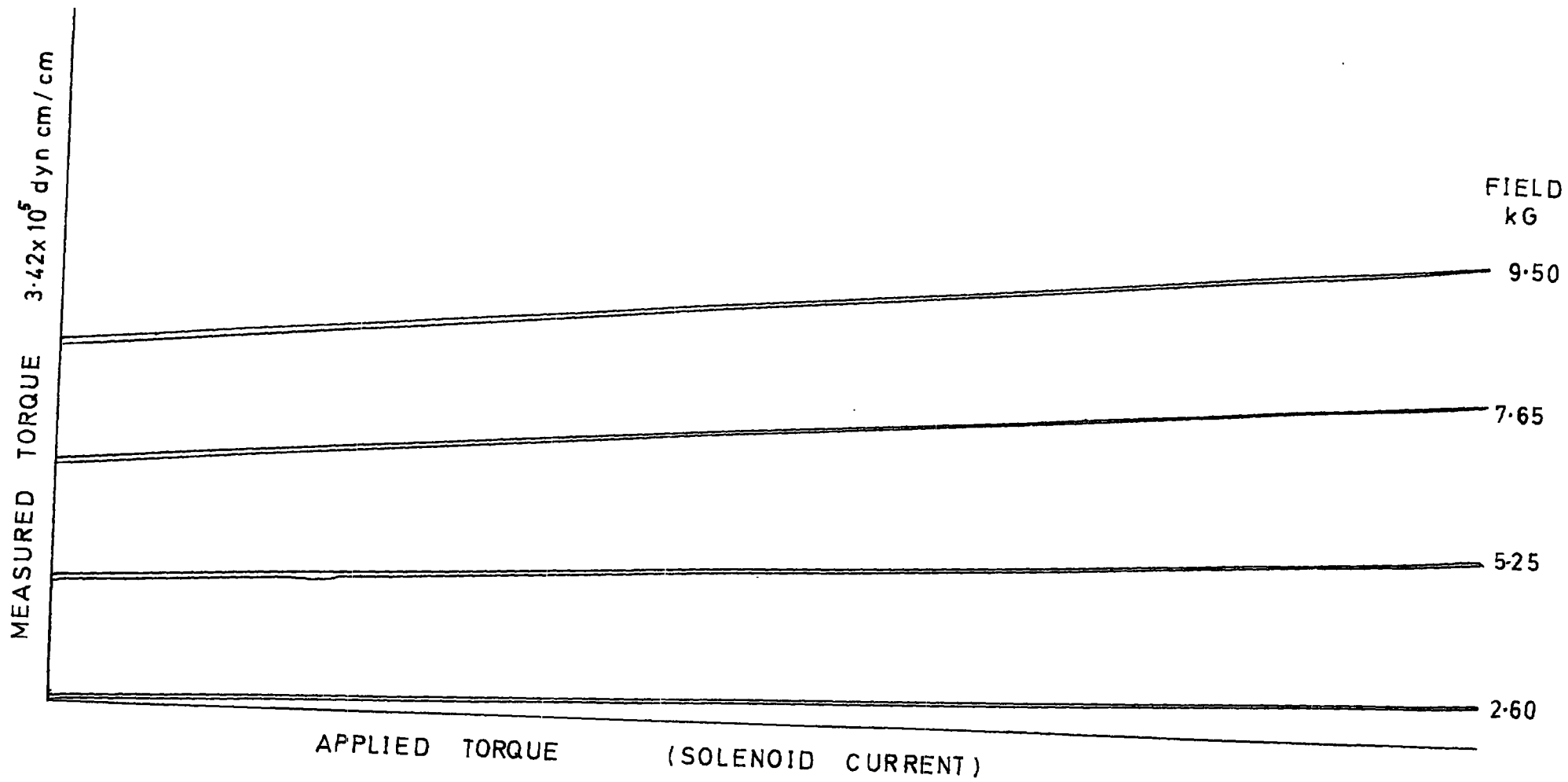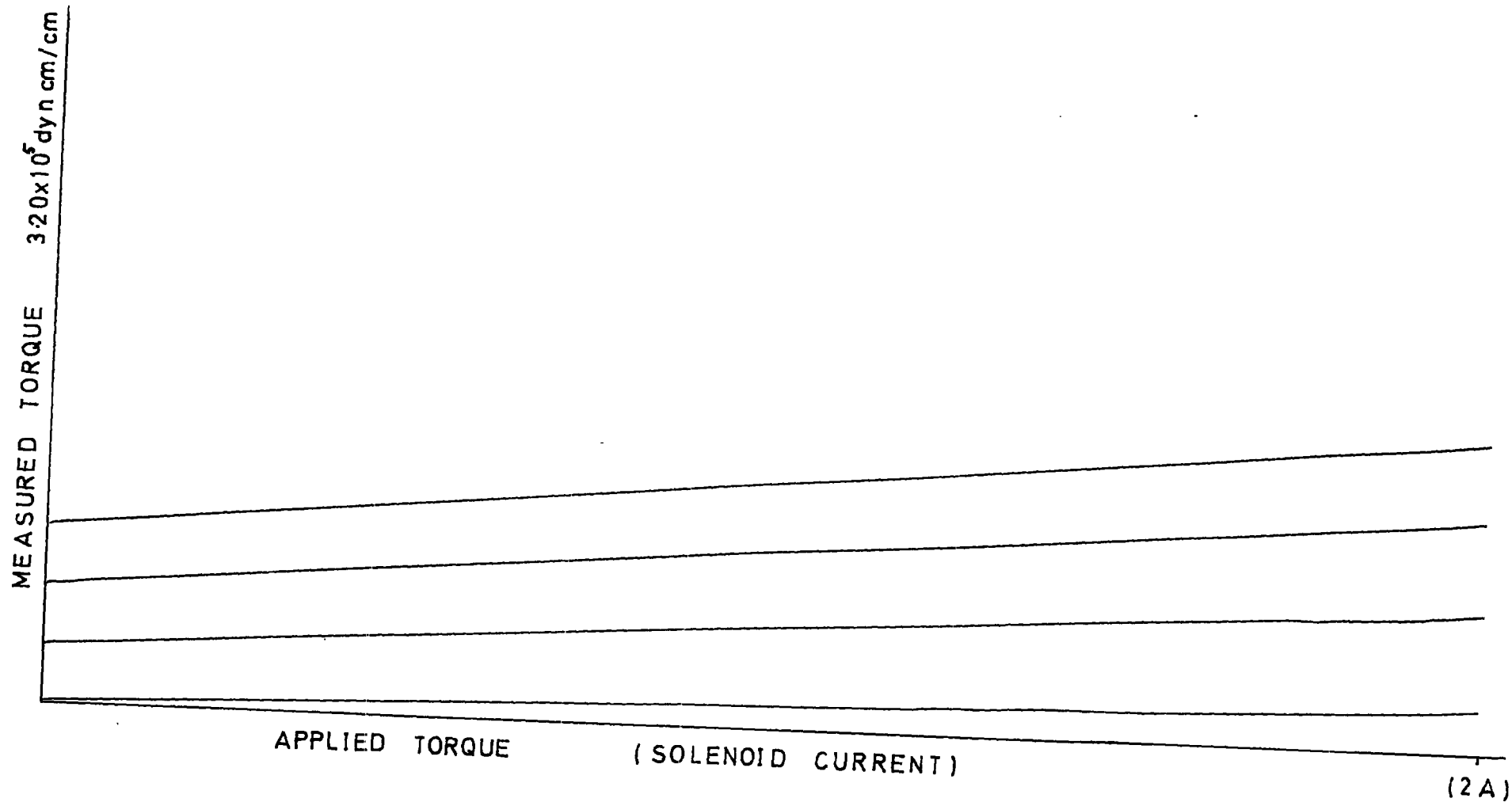
Fig. 4.10   Calibration at 120 K.

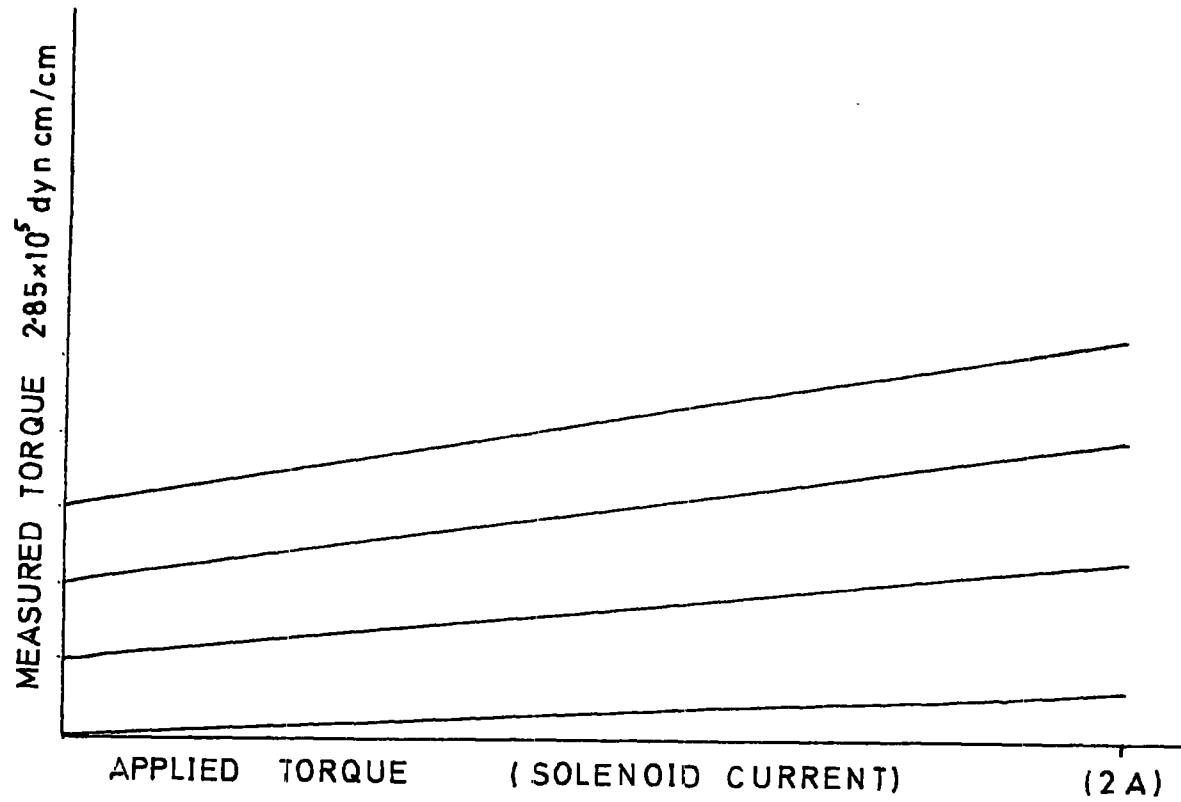Fig.4.11. Graph of applied torque versus measured torque at 140 K.

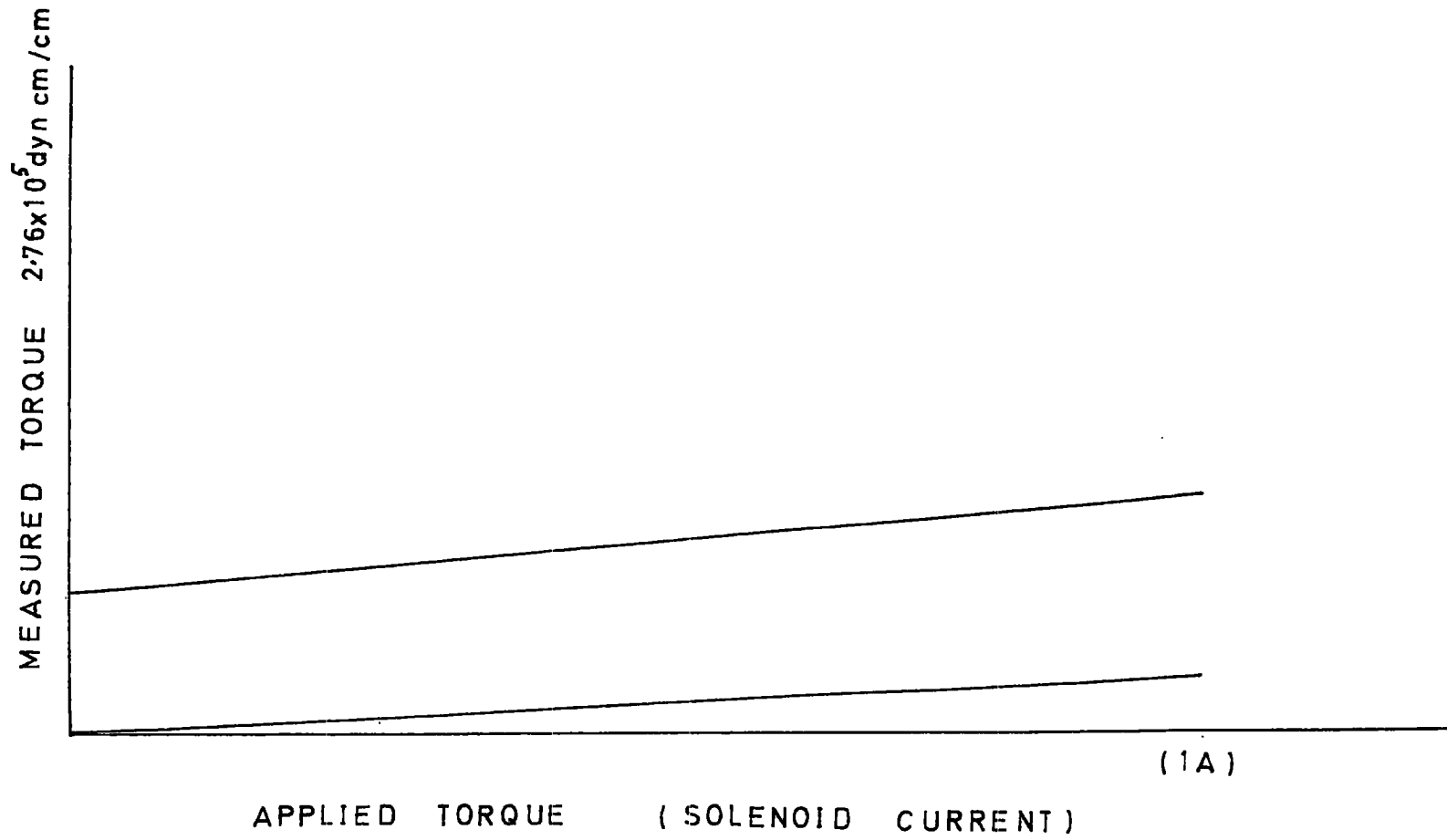Fig.4.12. Graph of applied torque against measured torque at 160 K.

Fig.4.13. Graph of applied torque against measured torque at 200 K.

Table 4.1. The amount of torque necessary to produce a $50\mu V$ output from the Wheatstone bridge at various temperatures. ($50\mu V$ is equivalent to a Y shift of 1 cm on the X - Y recorder).

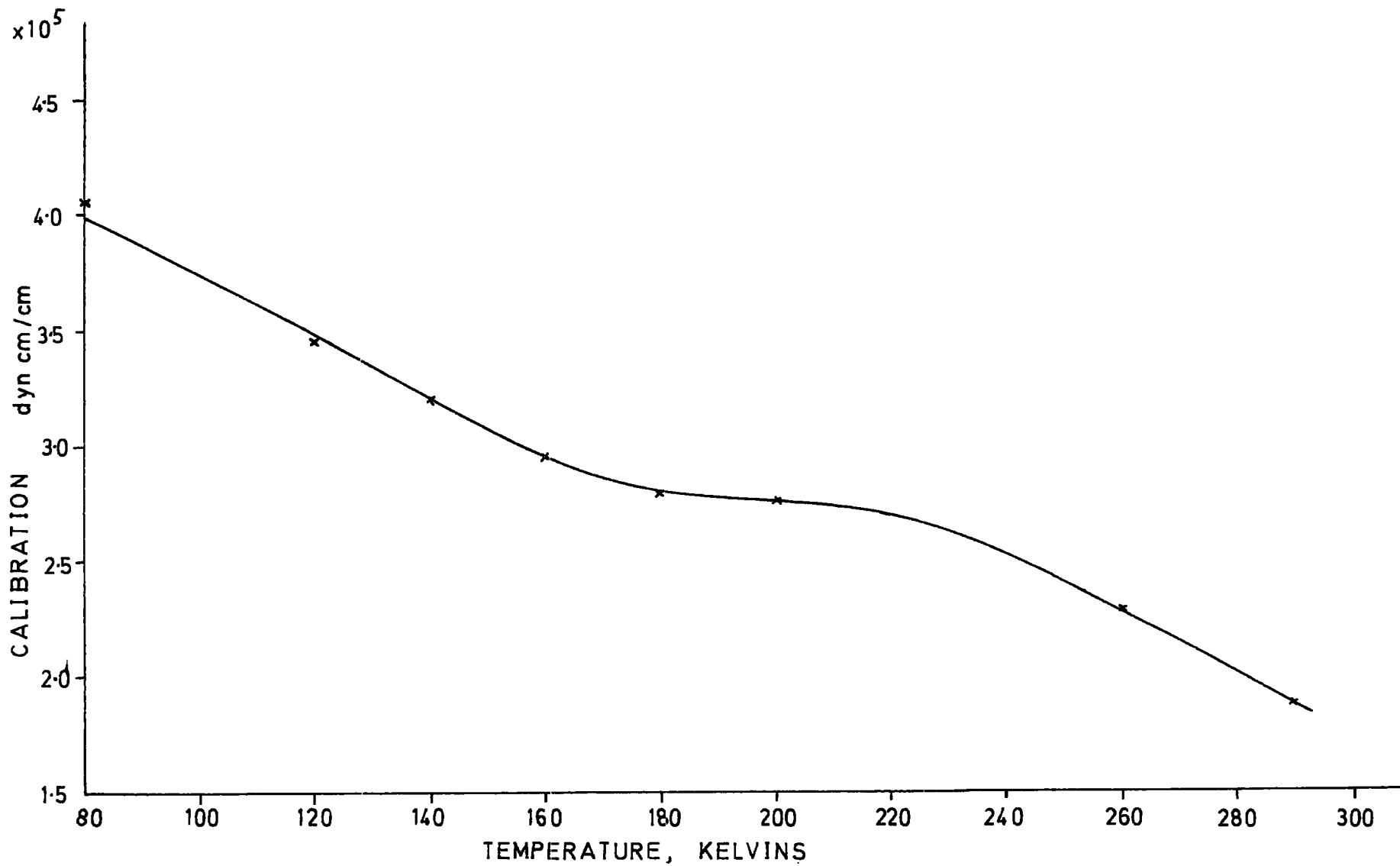| Temperature Kelvins	Calibration x 10^{-5} dyn cm per $50\mu V$.	Error x 10^{-5} dyn cm per $50\mu V$.
80	4 · 05	± 0 · 09
120	3 · 42	0 · 08
140	3 · 20	0 · 07
160	2 · 95	0 · 07
180	2 · 78	0 · 07
200	2 · 76	0 · 06
260	2 · 28	0 · 05
290	1 · 89	0 · 04

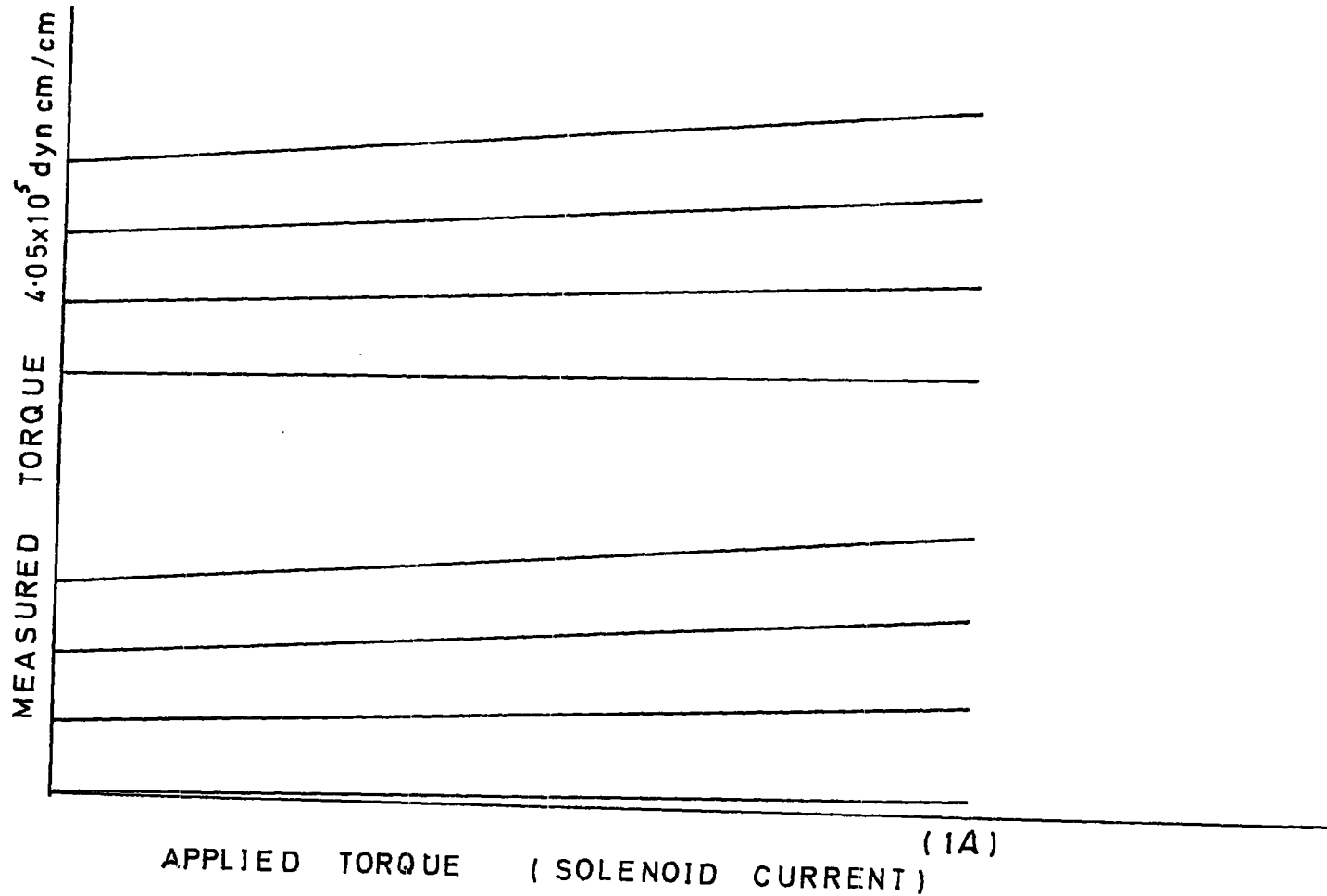Fig.4.14. Graph of torque calibration against temperature.

Fig.4.15. Graph of applied torque against measured torque at 80 K. The upper set is for identical fields with the solenoid current (and hence torque direction) reversed.

graphs indicate that a given torque applied in opposite directions will produce signals which differ in amplitude by less than 1%.

(iv) Field Dependence.

To check that the output of the bridge was not field dependent, a Hall probe was fixed close to the test solenoid and its output applied to the X terminals of the recorder, while the Wheatstone bridge was connected to the Y terminals. The field was increased slowly from zero up to 8 kG. Above 5 kG the output of the Hall probe was itself non-linear and this effect was sufficient to account entirely for the slight upward curve seen in the higher field regions of the graphs of figs. 4.16 and 4.17 . Allowing for this, the graphs indicate that the magnetometer output is definitely not field dependent at fields of up to 8 kG. Graphs were plotted at 290 K , 200 K and 100 K for various test solenoid currents. They are negligibly non-linear up to fields of 4.5 kG and after that become slightly concave upward by amounts corresponding to the higher fields for given Hall probe output.

(v)   Torque Curves.

Finally, some torque curves at various fields and temperatures are appended. Fig.4.18 shows two curves at room temperature. They were obtained from a compound Si - Fe disc created from nine discs which had been cut from a thin cold rolled silicon-iron sheet. To obtain the graphs the disc was rotated more than 360° and then back to zero. The curves show direction - reversal hysteresis, especially at maximum and minimum torques, (and there is a corresponding small angular shift in minimum and maximum torques), but the dimensions are the same for all fields further indicating the field independence of the magnetometer. There is no obvious shift in the angular positions of maxima and minima when the disc is being rotated in the same direction at different fields. The hysteresis is due to the speed with which the torque curves were taken, for the electromagnet could be run for short periods only at this stage due to difficulties with the cooling system.

The final graph, fig.4.21 is at 80 K and is a torque curve taken from the calibration solenoid in a greater time (about 90 sec). The reversal
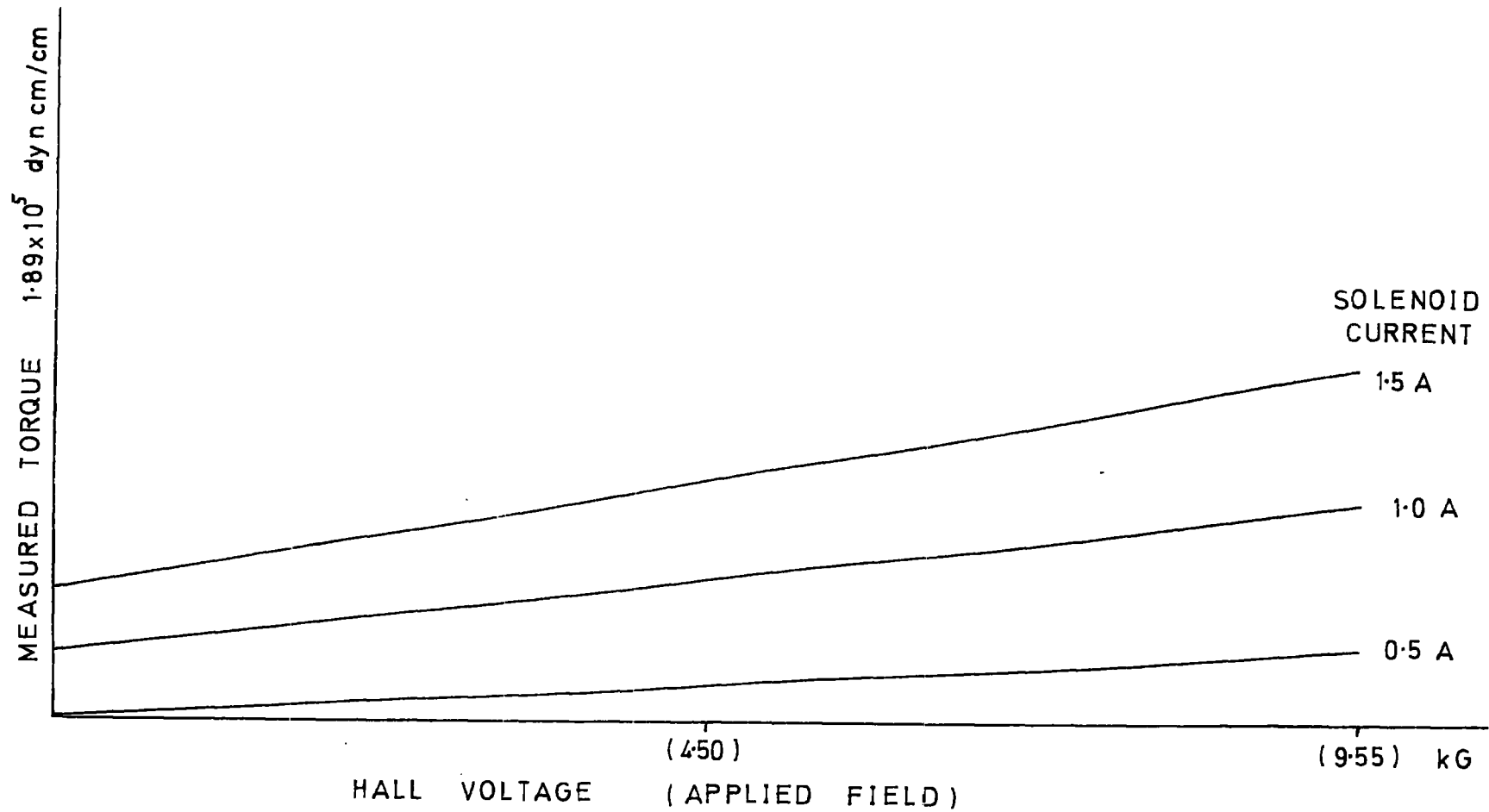
FIG. 4.16   THE GRAPH OF APPLIED FIELD AGAINST TORQUE FOR
CONSTANT SOLENOID CURRENT.

Fig.4.17. Graph of Hall probe voltage against measured torque for constant test current, taken at room temperature.

Fig.4.18. Torque curves of a compound Si-Fe disc at 290 K, in two fields.

FIG. 4.19   TORQUE CURVES OF THE COMPOUND SILICON - IRON DISC
IN TWO FIELDS AT 184K.

Fig.4.20. A torque curve of the compound silicon-iron disc at 100 K and a field of 9·70 k G.

FIG. 4.21 A TORQUE CURVE AT 80K BY THE CALIBRATION SOLENOID.

hysteresis has been nearly eliminated.

(vi) Conclusion.

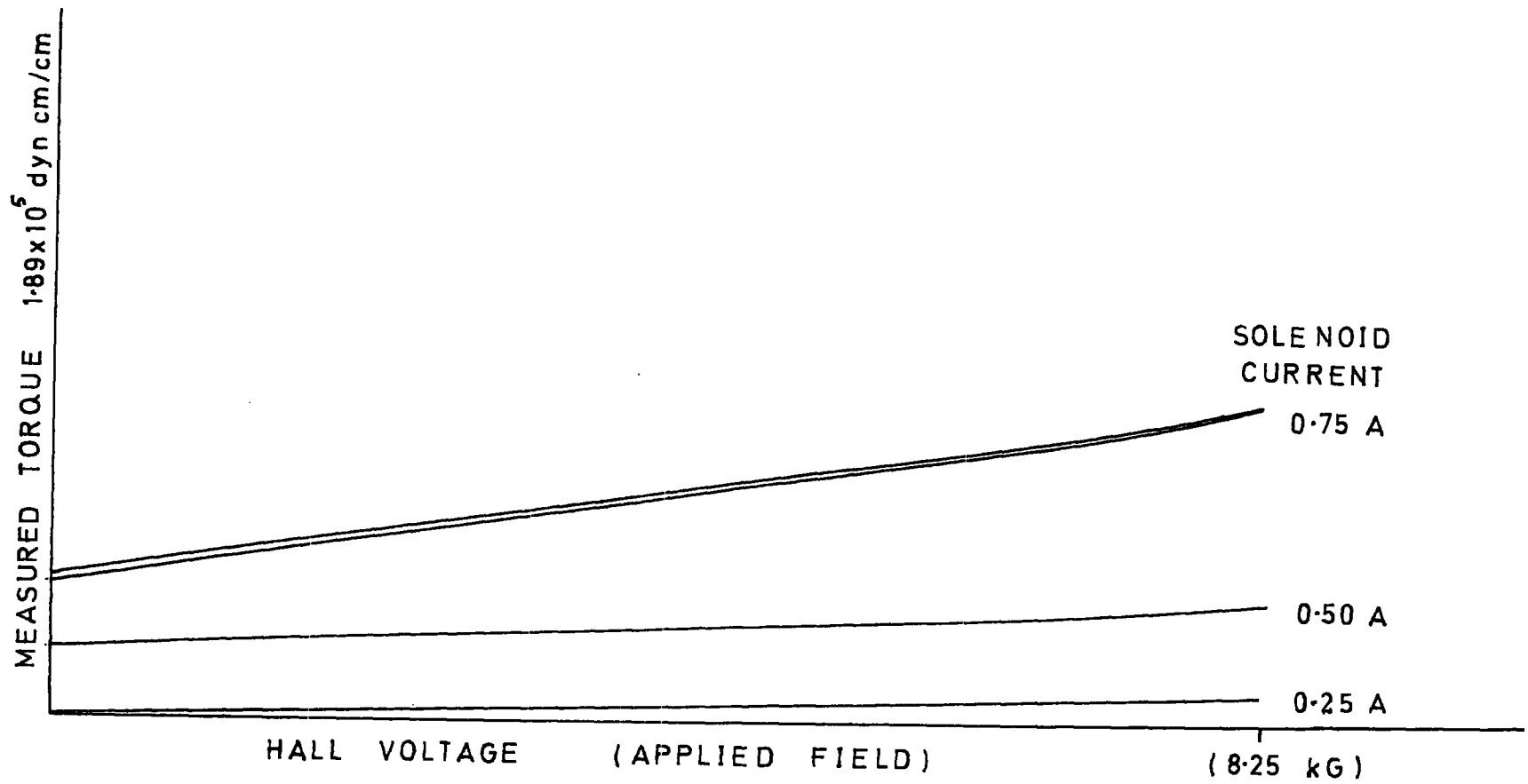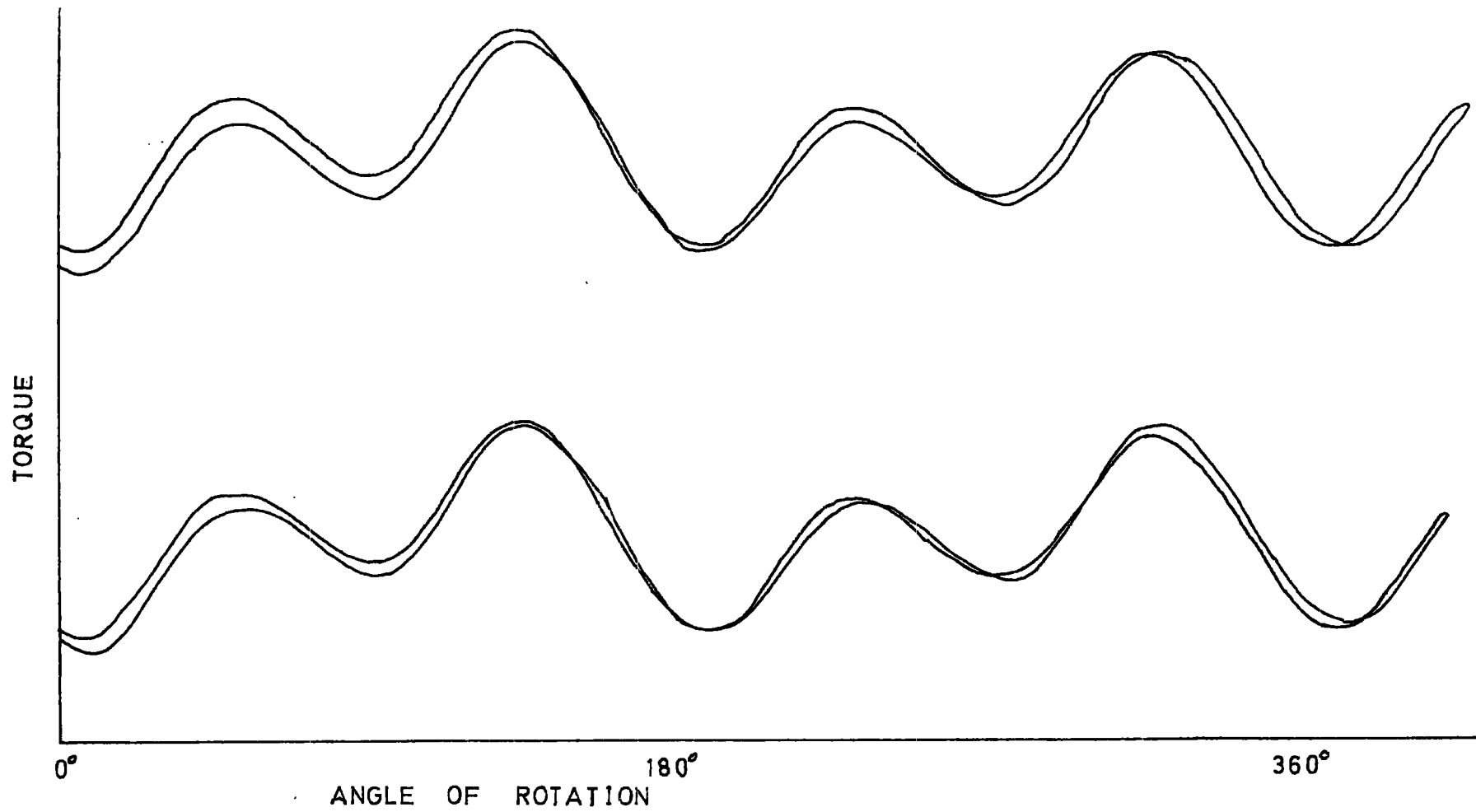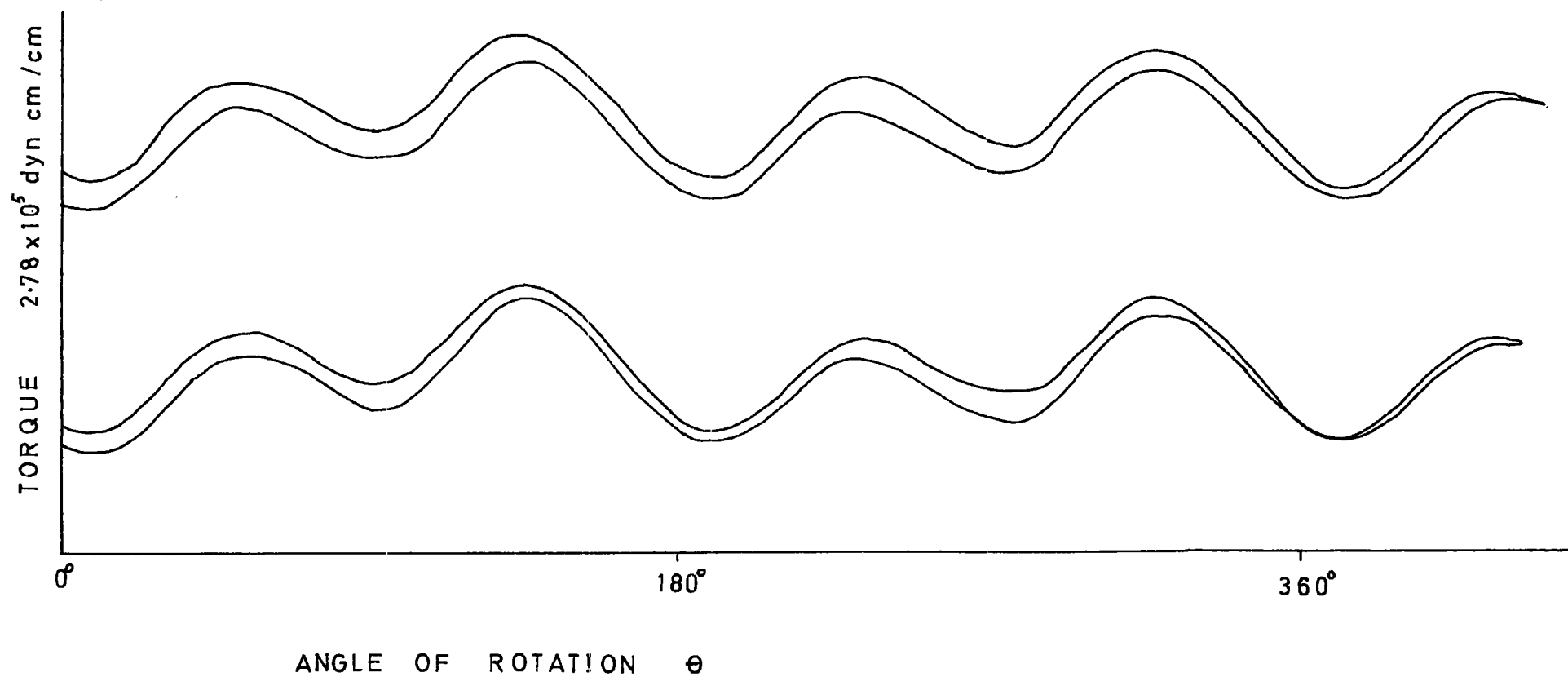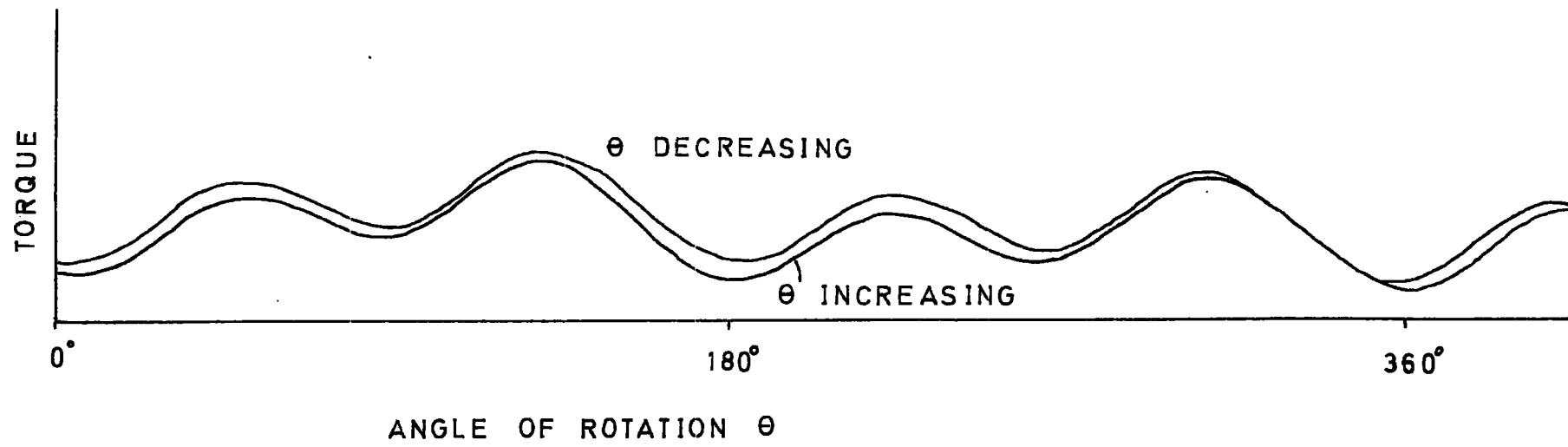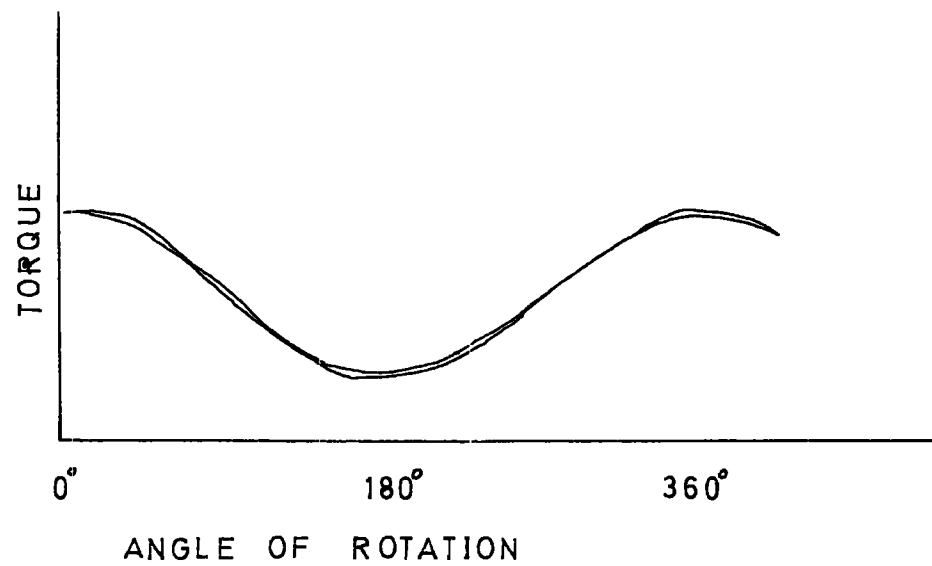In its present form the magnetometer can measure torques of up to 10^6 dyn cm at temperatures down to 80K and with an accuracy of $\pm$ 4% With the usual sizes of single crystal discs, this is sufficient to measure the highest anisotropies likely to be encountered in the rare earths, but for intermediate and low values of anisotropy at the higher temperatures, more amplification of magnetometer output will be required to produce a reasonable deflection of the recorder pen. A gain improvement of 10 - 100 times would enable anisotropy constants of as low as 10^3 erg cm^{-3} to be measured, and such a figure seems attainable on first investigations.

A Pye galvanometer amplifier, using photocell amplification, was used to pre-amplify the input to the recorder and achieved a 28 times gain without introducing significant noise or drift into the recorder output . Unfortunately the low output impedance of the preamplifier reduced the system response time significantly, and it would not be feasible to use it to produce torque curves, so a more suitable preamplifier is now under consideration.

Another benefit of being able to use low signal inputs would be the elimination of rotational hysteresis effects and the speeding up of the recording of torque results, and it is expected that low anisotropy torque curves could be produced in under a minute with negligible rotational hysteresis.

APPENDIX

Measurement of the Expansion Coefficient of Nylon 6.

A.1. Introduction.

The temperature variation of the coefficient of linear expansion of Nylon 6 was determined by the standard strain gauge technique of comparing the expansion of Nylon 6 with that of fused silica. Silica has an expansion coefficient of about 4×10^{-7} which is nearly constant in the temperature range 77K to 300K and is less than 1% of that of Nylon 6. This is smaller than other errors introduced in the experiment, so it is satisfactory to regard the expansion of silica as zero and take the calculated values for Nylon 6 as the absolute coefficient of linear expansion.

A.2. Apparatus.

(a) The Cryostat System.

A piece of fused silica and a piece of Nylon 6, each 5 m.m. x 3 m.m x 2 m.m. were cut from a larger block, degreased with acetone and washed and dried. A small area of one surface of each was coated with M-Bond 610 strain gauge cement, and a Kyowa KF-1-C3 strain gauge was bonded to each under 25lb in $^{-2}$ pressure and cured for two hours at 130° C. These gauges are of the wire type on an epoxy backing, had 119.9 Ω nominal resistance and 1 m.m. active length. The gauge factor was 2.19, and Chatterjee (ref.2) when checking the variation of gauge factor with temperature for this type of gauge (it was not specified by the manufacturer) found that the maximum variation was 5% and the mean variation 3% in the range 77K to 293K.

The gauge cement must be particularly even and thin to ensure the closest possible contact between the gauge and the surface, and reduce the dilution of strain due to the elasticity of the cement.

Details of the experimental arrangement are shown in fig.Al.

The silica and plastic were glued on their edges so that they faced each other 10 m.m. apart on a 5 m.m. thick, 15 m.m. diameter disc of tufnol, which served as a slow thermal conductor to the specimens. A copper-constantan thermo-couple was lightly glued to the tufnol between the specimens. Copper lead wires were soldered to each strain gauge, and
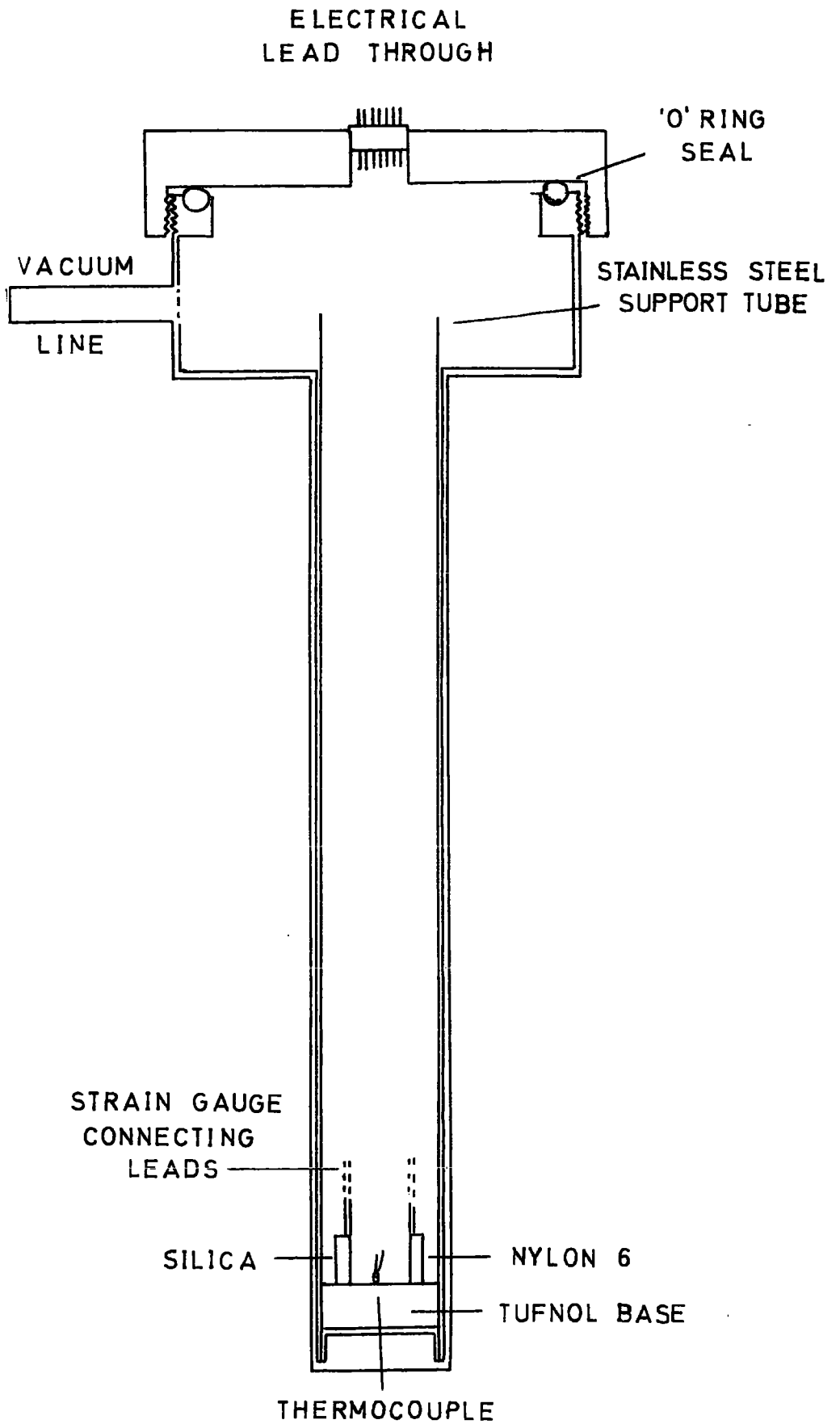
Fig.A.1. The cryostat used to determine the expansion coefficient of Nylon 6.

the disc was suspended tightly near the bottom of a thin stainless steel tube which in turn fitted firmly into the base of the cryostat.

The electrical connections were made to a lead through centred in the screw-on cap which covered the head of the cryostat. An 'O' ring completed the seal. The cryostat could be unscrewed from the cap without disturbing any electrical connections.

(b) The Wheatstone Bridge.

The active strain gauge on the plastic, and the dummy gauge on the silica, formed the lower two arms of the bridge (fig.A.2) . Each was shunted with a 100kΩ helipot. The upper arms of the bridge wefe Muirhead K-15-A, 120Ω standard resistances separated by a 1.2Ω potentiometer which was needed to balance the slight differences in the strain gauge resistances.

The null point was determined by a Pye Scalamp Galvanometer in conjunction with a Pye Galvanometer Amplif'ier. This could readily detect microvolt changes ih the bridge potential.

The power was supplied by a Farnell Cl d.c. power pack adjusted to give a 5 m A current to the strain gauges. This was well within their tolerance level, and their stability was excellent.

The maximum rate of heat that the gauges could supply to the specimens was 3 m W, and with a heat capacity of 10^{-1} JK^{-1} the specimens would be so little affected by this that there would be negligible thermal lag between specimens and thermocouple.

To minimise the effect of thermal emf's, all soldered joints at corresponding points in the bridge were placed as closely together as possible and insulated from draughts. Inasmuch as it was possible to keep the cryostat temperature steady in that time, in 15 minutes the thermal effects appeared to lead to negligible deflection of the galvanometer.

Experimental Proceedure.

The cryostat was put in a dewar of liquid nitrogen and the bridge was balanced by adjusting the apex and helipot resistances, and allowed
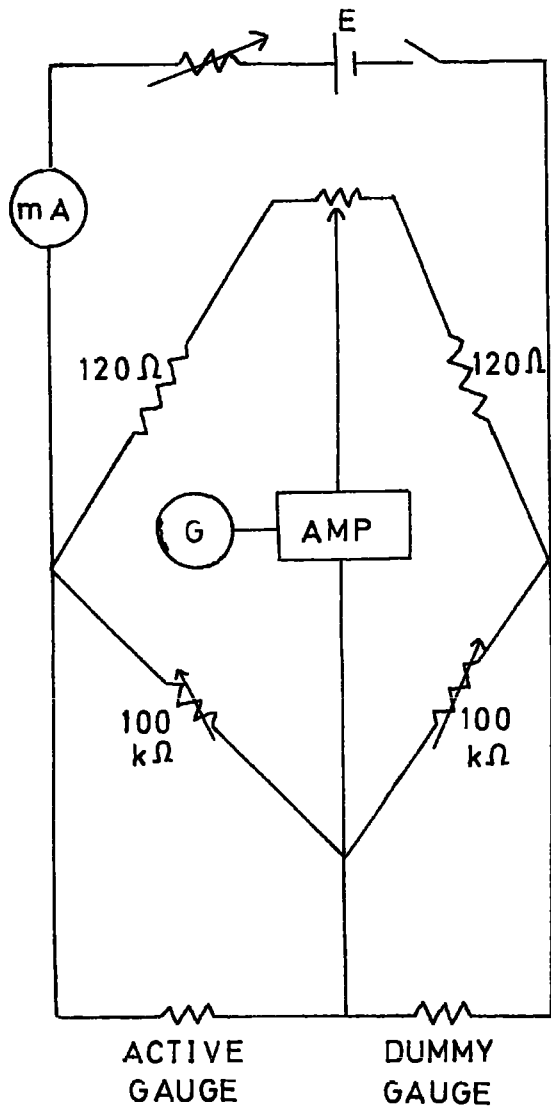
Fig. A 2. The Wheatstone bridge circuit used to determine the expansion coefficient of Nylon 6.

to stabilise for half an hour. The nitrogen was then allowed to boil

off so as to allow the specimen temperature to rise by 40K per hour.

At each 2K increase in temperature the bridge was quickly rebalanced

by adjusting one of the helipots. It was possible to do this at precise

temperatures because the galvo spot moved at a uniform rate, and with

practise it was easy to adjust the helipot at a corresponding rate, so

that the spot remained on the null point. At the correct thermocouple

reading this adjustment was halted and the helipot reading noted. The

helipot readings in conjunction with gauge factor, gauge resistance and

precise temperature change would determine the differential expansion

over that temperature.

After a 20K rise in temperature, the measuring helipot had come

near the end of its scale and had to be reset at a higher resistance;

this was compensated for by slightly adjusting the other helipot.

The temperature was determined by a copper-constantan thermocouple

with a reference junction in liquid nitrogen, the voltage being read by

digital voltmeter. The thermocouple calibration was checked at liquid

nitrogen and melting ice temperatures and the thermal e.m.f. was accurate

to better than $10\mu V$ in each case.

Several runs were made to condition the plastic to thermal cycling

and to discover the range which the helipot might cover without distort-

ing the relative conditions of the active and dummy gauges. If the

helipot resistance were too low it would reduce the current through

the corresponding gauge and lessen the sensitivity (and the errors in

determining the resistance in the helipot would be much greater). If

the helipot resistance were made too high it could increase the current

in the gauge beyond the stability level.

Results.

The average values from three runs were taken to find the mean

coefficient between each two degree interval, and the four degree

average (over a range plus and minus two degrees at each temperature)

was calculated.

If S and R are the resistances of the active gauge and helipot at some temperature, and a change in temperature of $\Delta\theta$ alters S by ΔS, then R must be altered by ΔR to maintain the balance.

If we suppose that the resistances in all other arms remain constant, then the combined resistance in this arm must remain constant, and it follows that the sensitivity is

$$\left(-\frac{\Delta R}{\Delta S}\right) = \frac{R(R+\Delta R)}{S^2} ,$$

This obviously improves at higher R.

If ΔS corresponds to a change in gauge length (and presumably in specimen length) from l_0 to l , the definition of gauge factor k is that

$$\frac{l - l_0}{l_0} = \frac{1}{k} \cdot \frac{\Delta S}{S}$$
$$= \frac{S \, \Delta R}{k R (R + \Delta R)} .$$

If α is the expansion coefficient of the material in this temperature range

$$l = l_0 (1 + \alpha \Delta\theta)$$
$$\alpha = \frac{l - l_0}{l_0} \cdot \frac{1}{\Delta\theta} \qquad \text{Equation A 1.}$$
$$\alpha = \frac{S \, \Delta R}{k R \Delta\theta (R + \Delta R)} .$$

Then α is calculated for each temperature interval $\Delta\theta$ from equation A1.

A graph of the results was plotted (fig. A 3). It shows several kinks, but the results were consistent over each run. The plastic is slightly anisotropic and the kinks probably represent some realignment of the anisotropy.

However, the most satisfactory conclusion for the magnetometer was that the strain gauges behaved consistently and regularly at all temperatures i.e. the contraction of the plastic was well within the capacity of the strain gauges.

The Four Degree Average of the Temperature Coefficient of Linear

Expansion of Nylon 6.

Temp Kelvins	2×10^6	Temp Kelvins	$\times 10^6$	Temp Kelvins	$\times 10^6$	Temp Kelvins	$\times 10^6$
84	-	138	45.4	192	55.5	246	65.1
86	47.1	140	47.1	194	55.6	248	65.4
88	49.3	142	47.8	196	56.0	250	66.3
90	49.4	144	47.5	198	57.8	252	67.0
92	50.7	146	47.1	200	59.2	254	67.5
94	49.8	148	46.0	202	59.8	256	68.5
96	48.8	150	46.4	204	58.1	258	69.7
98	46.6	152	47.0	206	56.8	260	71.4
100	44.5	154	46.7	208	56.8	262	71.7
102	43.2	156	47.9	210	56.4	264	71.3
104	42.7	158	48.4	212	55.8	266	72.2
106	41.5	160	49.7	214	57.1	268	73.1
108	42.7	162	50.2	216	57.8	270	73.9
110	43.5	164	50.6	218	58.6	272	75.3
112	43.9	166	51.3	220	59.8	274	79.2
114	41.1	168	51.9	222	61.0	276	81.5
116	37.5	170	52.0	224	60.6	278	82.6
118	37.6	172	53.0	226	59.6	280	84.9
120	40.2	174	53.1	228	60.1	282	85.3
122	42.3	176	53.0	230	60.9	284	88.4
124	41.9	178	53.2	232	61.6	286	89.7
126	42.8	180	54.0	234	62.1	288	90.1
128	43.0	182	54.2	236	62.8	290	91.0
130	43.8	184	54.7	238	62.9	292	-
132	44.0	186	55.4	240	63.1	294	-
134	44.1	188	55.7	242	63.0	296	-
136	45.1	190	55.6	244	64.1	298	-
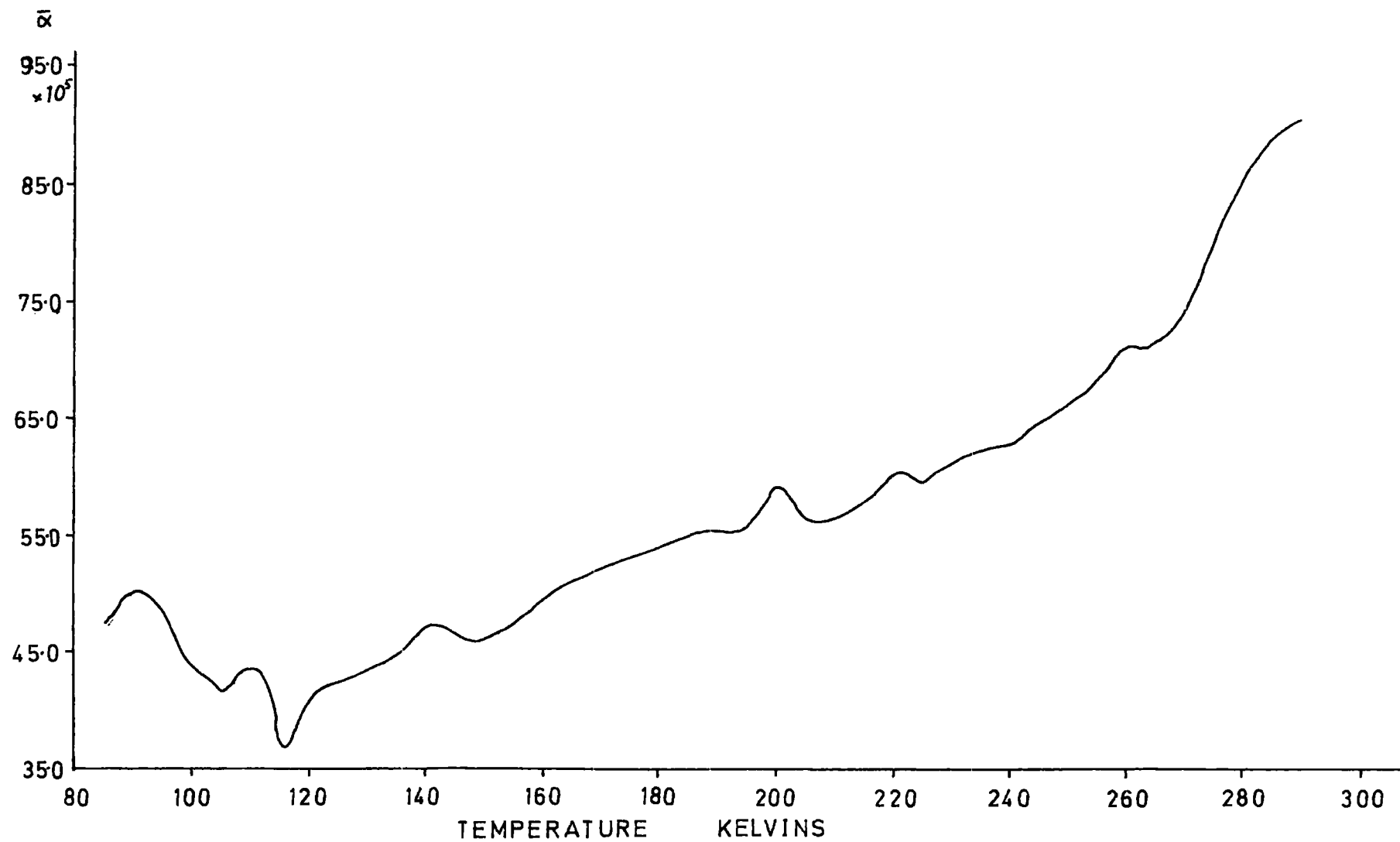
A. 3. The temperature coefficient of expansion of 'Nylon 6'.

REFERENCES.

1. S.Timoshenko; "Strength of Materials";

    D.Van Nostrand Company. Ltd., Third Ed. 1956.

2. D.Chatterjee; Magnetic Properties of Terbium – Scandium Alloys;

    Thesis, Durham University. 1972.

3. K.Honda, and S.Kaya; Sci. Rep. Tohoku, 15, 728 (1926).

4. P.Weiss; Journ.de Physique, 6, 655 (1907).

5. N.S.Akulov; Zeit.fur Phys., 52, 389 (1928).

6. P.Weiss; J.Phys. Radium, 4, 829 (1905) .

7. K.Beck; Vjschr.naturf. Ges. Zurich, Jahrg. 63 (1918) .

8. W.Sucksmith, H.H.Potter and L.Broadway; Proc.Roy.Soc. A 117, 476 (1928) .

9. P.Weiss; J.Phys. Theor.Appl., 3, 194 (1904).

10. P.Weiss; J.Phys. Theor.Appl., 4, 469 and 829 (1905).

11. P.Weiss; Arch.Sci.Phys.nat., 19, 537 (1905); 20, 213 (1905).

12. C.Guillaud; Thesis, Strasbourg. (1943)

13. W.L.Webster; Proc.Phys.Soc. (London), 42, 431 (1930) .

14. W.Heisenberg; Z.Physik, 69, 287 (1931).

15. R.M.Bozorth; Phys.Rev., 50, 1076 (1936) .

16. L.P.Tarasov and F.Bitter; Phys.Rev., 52, 353 (1937).

17. H.Schlechtweg; Ann.Physik, 5 27, 573 (1936).

18. R.M.Bozorth; "Ferromagnetism",
    pub. by D.Van Nostrand Company, Inc. (1951).

19. J.C.Maxwell; "Electricity and Magnetism" II Section 437, p.67.

    Clarendon Press, Oxford (1892).

20. J.A.Osborne; Phys.Rev., 67, 351 (1945).

21. W.Sucksmith, H.H.Potter, and L.Broadway; Proc.Roy.Soc., A 117,471 (1928).

22. K.Beck; Vjschr,naturf. Ges. Zurich, 63, 116 (1918).

23. W.L.Webster; Proc.Roy.Soc., A 109, 570 (1925).

24. K.Honda and S.Kaya; Sci.Rep. Tohoku Univ., 17, 1157 (1928) .

25. H.J.Williams; Phys.Rev. 52, 747. (1937) .

26. H.J.Williams; Rev.Sci.Instr., 8, 56 (1937).

27. O.Dahl and J.Pfaffenberger; Zeit.fur.Phys., 71, 93 (1931).

28. F.Brailsford; J.I.E.E. 83, 566 (1938).

29. R.F.Penoyer; Rev.Sci.Instr., 30, 711 (1959).

30. T.Okamura and T.Hirone; Phys.Rev., 55, 102 (1939).

31. N.S.Akulov; Zeit.fur.Phys., 67, 794 (1931).

32. R.Gans; Phys.Zeits., 33, 924 (1932).

33. R.M.Bozorth and H.J.Williams; Phys.Rev. 59, 827 (1941).

34. N.Akulov and N.Bruchatov; Ann.der Phys., 15, 741 (1932).

35. W.E.Ingerson and F.J.Beck; Rev.Sci.Instr. 9, 31 (1938).

36. D.S.Miller; Rev.Sci.Instr. 21, 605 (1950).

37. K.Tajima and S.Chikazumi; Japan. J.Appl.Phys., 6, 897 (1967).

38. C.D.Graham,Jr.; Phys.Rev. 112, 1117 (1958).

39. H.Sato and B.S.Chandrasekhar; Phys.Chem.Solids, 1, 228 (1957).

40. C.D.Graham,Jr; Phys.Soc. Japan, 17, 1310 (1962).

41. W.D.Corner, W.Roe, and K.N.R.Taylor; Proc.Phys.Soc., 80, 927 (1962).

42. P.H.Bly; Thesis, Durham University (1967).

43. M.I.Darby and K.N.R.Taylor; Proc.Int.Conf. Magnetism , Nottingham
    (1964), p.742.

44. C.D.Graham; J.Appl.Phys., 38, 1375 (1967).

45. J.J.Rhyne and A.E.Clark; J.Appl.Phys., 38, 1379 (1967).

46. R.Z.Levitin and B .K.Ponomaryov; Soviet Phys. J.E.T.P., 26, 1121 (1968).

47. M.Schieber, S.Foner, R.Docho and E.J.McNiff; J.Appl.Phys.,39,885 (1968).

48. J.J.Rhyne, S.Foner, E.S.McNiff and R.Docho; J.Appl.Phys.,39,892 (1968).

49. W.Sucksmith and J.E.Thompson; Proc.Roy.Soc,, A.225, 362 (1954).

50. J.S.Kouvel and C.D.Graham,Jr; Conference on Magnetism and Magnetic
    Materials (Boston 1956) p.85.

51. L.R.Bickford.Jr; Phys.Rev., 78, 449 (1950).

52. H.J.Williams; Phys.Rev., 52, 747 (1935).

53. G.W.Van Oosterhout; Appl.Sci.Res., B6, 101 (1956).

54. S.Foner; Rev.Sci.Instr., 27, 548 (1956).

55. S.Foner; Rev.Sci.Instr., 30, 548 (1959).

56. K.Strnat and L.Bartimay; J.Appl.Phys., 38, 1305 (1967).

57. S.Foner and E.J.McNiff,Jr; Rev.Sci.Instr., 39, 171 (1968).

58. T.R.McGuire; J.Appl.Phys., 38, 1299 (1967).

59. B.W.Mangum and D.D.Thornton; Rev.Sci.Instr., 41, 1764 (1970).

60. H.Plotkin; Quart.Progr.Rept.of the M.I.T. Research Lab.Electronics, Oct.1951, page 28.

61. D.O.Smith; Rev.Sci.Instr., 27, 261 (1956).

62. D.U.Gubser and D.E.Mapother; Rev.Sci.Instr., 40, 843 (1969).

63. B.W.Mangum and D.D.Thornton; Rev.Sci.Instr., 41, 1764 (1970).

64. P.J.Flanders and W.D.Doyle; Rev.Sci.Instr., 33, 691 (1962).

65. G.Hoffer and K.Strnat; I.E.E.E. Trans.Mag. MAG - 2, 487 (1966).

66. G.Hoffer and K.Strnat; J.Appl.Phys., 38, 1377 (1967).

67. R.S.Kaeser, E.Ambler, and J.F.Schooley; Rev.Sci.Instr., 37, 173 (1966).

68. J.E.Noakes, A.Arrott, and C.Haakana; Rev.Sci.Instr., 39, 1436 (1968).

69. D.E.Farrell; Rev.Sci.Instr., 39, 1452 (1968).

70. K.Dwight, N.Menyuk and D.Smith; J.Appl.Phys., 29, 491 (1958).

71. W.E.Ingerson and F.J.Beck; Rev.Sci.Instr., 9, 31 (1938).

72. F.B.Hagedorn; Rev.Sci.Instr. 38, 591 (1967).

73. W.R.Beam and W.T.Siegle; Rev.Sci.Instr., 36, 641 (1965).

74. P.J.Flanders; J.Appl.Phys. 38, 1293 (1967).

75. P.J.Flanders; Rev.Sci.Instr., 41, 697 (1970).

76. P.J.Flanders; I.E.E.E. Trans.Mag., MAG - 9, 94 (1973)

77. H.Gessinger, H.Kronmuller and R.Bundschuh; J.Phys. E, 3, 468 (1970).

78. K.Tajima and S.Chikazumi; J.Phys.Soc.Japan, 23, 1175 (1967).

79. H.E.Nigh, S.Legvold and F.H.Spedding; Phys.Rev., 132, 1092 (1963).

80. M.B.Salamon and D.S.Simons; Phys.Rev. B7, 229 (1973).

81. F.W.Harrison; J.Sci.Instr., 33, 5 (1956).

82. C.D.Graham,Jr; P.J.Flanders and T.Egami; A.I.P. Conf.Proc. No.10 part I, page 759 (18th Annual Conf.on Magnetism and Magnetic Materials,(1972).)

83. W.S.Byrnes and R.G. Crawford; J.Appl.Phys., 29, 493 (1958).

84. R.M.Bozorth, R.J.Gambino and A.E.Clark; J.Appl.Phys., 39, 883 (1968).

85. F.H.Spedding, R.G.Jordan and R.W.Williams, J.Chem.Phys, 51, 509 (1969).

86. R.M.Bozorth; J.Appl.Phys., 38, 1366 (1967).

87. K.P.Belov, R.Z.Levitin, S.A.Nikitin and A.V.Ped'Ko; Soviet Phys. J.E.T.P. 13, 1096 (1961).

88. K.P. Belov and A.V. Ped'Ko, Soviet Phys. J.E.T.P., $\underline{15}$, 62 (1962).

89. R.M. McClintock and R.H. Kropschot; National Bureau of Standards, unpublished data; discussed in R.B. Scott, " Cryogenic Engineering ", D. Van Nostrand Co. Inc., 1963.